UNIVERSIDAD SAN SEBASTIÁN
FACULTAD DE MEDICINA Y CIENCIA

"ROLE OF GALECTIN-8 IN MITOCHONDRIAL DYNAMICS AND ITS IMPACT IN CELL METABOLISM IN EPITHELIAL CELLS"

Thesis presented to obtain the academic degree of
Doctor in Cell Biology and Biomedicine

Tutor: Andrea Soza, PhD
Co-tutor: Claudia Oyanadel, PhD
Student: Adely Andrea De la Peña Correa

Santiago, Chile 2024

EVALUACIÓN

En Santiago, el 02 de julio de 2024 los abajo firmantes dejan constancia que la estudiante Adely de la Peña Correa del programa de Doctorado en Biología Celular y Biomedicina ha aprobado la tesis para optar al grado de Doctor en Biología Celular y Biomedicina, con una calificación de 7.0 (siete coma cero).

Tutores:

Dra. Andrea Soza

Universidad San Sebastián

Dra. Claudia Oyanadel

Universidad San Sebastián

Comisión evaluadora:

Dra. Verónica Eisner

P. Universidad Católica de Chile

Dra. Patricia Burgos

Universidad San Sebastián

Dr. Alfonso González

Universidad San Sebastián

Dr. Jaime Gutiérrez

Universidad San Sebastián

The flowers live for a couple of days, then they die, and that hurt me.
Bring me a plant instead, so it can grow into something beautiful.

F.S. Yousaf

ACKNOWLEDGE

I will always be profoundly grateful to Andrea Soza for teaching me how to do and love science. She has always encouraged me to pursue the path of science. Likewise, I would like to thank Claudia Oyanadel for the opportunity to work with her, and for all the knowledge and discussions. Additionally, I would like to thank both of you for your dedication and passion in shaping me as a scientist. Moreover, I'm deeply thankful to the members of the lab, especially to Francisca, Elisa, and Nicole, for making the lab an awesome place, for all the support, and for the laughter**.**

I would like to express my gratitude to Alfonso Gonzalez and his lab, especially to Claudio Retamal for the microscopy analysis and training in the Huygens Software, and to Mariana Labarca for the discussions and data analysis in this thesis.

I would also like to express my deep gratitude to Dr. Felix Randow for accepting me into his laboratory, allowing me to learn and grow there. Especially to Thomas Mund and Keith Boyle for guiding me during my internship, and to all the members of the lab for their warm welcome.

Finally, I would like to thank my family for always being by my side, supporting me through thick and thin, and my partner because her love and care have been a source of inspiration for me.

DECLARATION

This thesis is the result of my own work and includes nothing that is the outcome of work done in collaboration unless specified in the text. The contests have not been submitted for any other qualification at the Universidad San Sebastian or other institution.

This work was supported by funds of Agencia Nacional de Investigación y Desarrollo of Chilean Government (FONDECYT 1181907 and 1211829, ANID/BASAL grants FB210008 and ACE210009).

Adely Andrea De la Peña Correa was financed by the scholarship for students in doctoral programs of Vicerrectoría de Investigación y Doctorados of Universidad San Sebastián, Chile, and the scholarship Doctorado Nacional of Agencia Nacional de Investigación y Desarrollo of the Chilean Government (Folio n° 21221618).

Adely De la Peña Correa
Universidad San Sebastián
April 2024

TABLE OF CONTENTS

ABBREVIATIONS

ATP	Adenosine triphosphate
ANOVA	Analysis of variance
BSA	Bovine serum albumin
C-CRD	C-terminal carbohydrate recognition domain
cDNA	Complementary DNA
CRD	Carbohydrate recognition domain
DMEM	Dulbecco's Modified Eagle's medium
DMSO	Dimethyl sulfoxide
DNA	Deoxyribonucleic acid
DRP1	Dynamin-related protein 1
sNTP	Deoxyribonucleoside triphosphate
DTT	Dithiothreitol
ECL	Enhanced chemiluminescence
EDTA	Ethylenediaminetetraacetic acid
EGF	Epidermal growth factor
EGFR	Epidermal growth factor receptor
EMT	Epithelial-mesenchymal transition
FAK	Focal Adhesion Kinase
FBS	Fetal Bovine Serum
Gal	Galectin
GFP	Green fluorescent protein
GST	Glutathione S-transferase
h	Hour(s)
HRP	Horseradish peroxidase
IMM	Inner mitochondrial membrane
IPTG	Isopropyl β- d-1-thiogalactopyranoside
LB	Luria-Bertani
MFN1/2	Mitofusin 1 or 2
N-CRD	N-terminal carbohydrate recognition domain
NDP52 (CALCOCO2)	Nuclear dot protein 52 (Calcium binding and coiled-coil domain)

OMM	Outer mitochondrial membrane
ON	Over Night
OPA1	Mitochondria dynamin like GTPase
P/S	Penicilin/Streptamicin
PAGE	Polyacrylamide gel electrophoresis
PBS	Phosphate-buffered saline
PCR	Polymerase chain reaction
PEI	Polyethyleneimine
PH	Pleckstrin homology
PINK1	PTEN-induced kinase 1
PMSF	Phenylmethylsulfonyl fluoride
PVDF	Polyvinylidene difluoride
ROS	Reactive oxygen species
RT	Room Temperature
SD	Standard deviation
SDS	Sodium dodecyl sulphate
SOB	Super optimal broth
TAE	Tris-acetate-EDTA
TBST	Tris-buffered saline + Tween 20
WT	Wild type

LIST OF FIGURES

LIST OF TABLES

SUMMARY

Galectin-8 (Gal-8) belongs to a family of proteins that regulate a variety of cellular processes by interacting with β-galactosidase moieties exposed in glycoproteins and glycolipids on the cell surface and in damaged endolysosomes. Gal-8 has two carbohydrate recognition domains linked by a peptide chain and is unique among other galectins, with a high preference for α-2,3 sialic acids within its N-terminal carbohydrate recognition domain (N-CRD).

We previously demonstrated that overexpression of Gal-8 or treatment with recombinant Gal-8 activates the Focal Adhesion Kinase (FAK) - Epidermal Growth Factor Receptor (EGFR) pathway, leading to ERK activation, proliferation, migration and EMT in Madin-Darby Canine Kidney (MDCK) epithelial cells. Extensive research has established that ERK activation via the RAS-MAPK axis modulates mitochondrial dynamics, including fission, fusion, and distribution. Mitochondrial fission is carried out by the Dynamin-related/-like protein 1 (DRP1). Mitochondrial fusion is ensured by mitofusins 1 and 2 (MFN1 and MFN2) and optic atrophy 1 (OPA1), which mediate outer mitochondria membrane (OMM) and inner mitochondria membrane (IMM) fusion, respectively. Additionally, MFN2 regulates mitochondria-endoplasmic reticulum contact sites.

Activation of ERK within the RAS-MAPK axis directly promotes mitochondrial fragmentation by activating DRP1 and suppressing MFN1, leading to mitochondrial redistribution, reduction in calcium buffering, and activation of transcription factors that participate in different cellular processes such as tissue repair and cancer. Identifying molecules that can change mitochondrial dynamics is of great interest because they could modify cell metabolism, impacting wound healing, tissue regeneration, and cancer.

In this thesis, we investigate the effect of Gal-8 on mitochondrial dynamics and the participation of its carbohydrate-recognition domain in modulating these dynamics through the activation of the ERK pathway.

Our results show that recombinant Gal-8 and Gal-4 induce fragmentation, and only Gal-8 promotes the perinuclear distribution of mitochondria in MDCK depending on α-2,3 sialylated glycans. These Gal-8 mediated effects were also observed in Chinese Hamster Ovary cells (CHO) and Human Renal proximal tubule Epithelial Cells

(RPTEC). In CHO-LEC3.2.8.1 cells, which have N-glycosylation deficiency but conserve the ability to synthesize O-glycoproteins, no effect of Gal-8 was observed. Gal-8 could promote the proximity of mitochondria to the nucleus probably by MFN2 in a carbohydrate-dependent manner by recognizing α-2-3 sialylated β-galactosides, in MDCK cells

The mitochondrial fragmentation and redistribution to the perinuclear zone induced by Gal-8 required ERK and SRC activity but is independent of EGFR activation. On the other hand, DRP1 activation induced by Gal-8 depends on ERK activity in epithelial cells. We also found that Gal-8 promotes mitophagy in a carbohydrate-dependent manner in MDCK cells. Gal-8 triggers modification on the metabolic rate of MDCK cells, leading to a rise in extracellular acidification rate (ECAR) and proton leak, which is accompanied by a decrease in ATP production coupled with oxygen consumption rate (OCR).

Mitochondrial fragmentation has been associated with proliferation and EMT. Our results show that Gal-8 induces proliferation in a carbohydrate-dependent manner and EMT-dependent ERK activity.

In summary, Gal-8 is a novel regulator of mitochondrial dynamics that can impact diseases associated with mitochondrial dysfunction or physiological processes such as wound healing and tissue repair.

RESUMEN

Galectin-8 (Gal-8) pertenece a una familia de proteínas que regulan diversos procesos celulares al interactuar con β-galactosidos expuestos en glicoproteínas y glicolípidos en la superficie celular y en endolisosomas dañados. Gal-8 tiene dos dominios de reconocimiento de carbohidratos unidos por una cadena peptídica y se distingue de otros galectinas por tener una alta preferencia por ácidos siálicos α-2,3 en su dominio de reconocimiento de carbohidratos N-terminal (N-CRD).

Demostramos previamente que el tratamiento con Gal-8 recombinante activa la vía de la quinasa de adhesión focal (FAK) - receptor del factor de crecimiento epidermal (EGFR), llevando a la activación de ERK, proliferación y migración en células epiteliales de riñón de perro de la raza Madin-Darby (MDCK). Extensas investigaciones han establecido que la activación de ERK a través del eje RAS-MAPK modula la dinámica mitocondrial, incluyendo fisión, fusión y distribución. La fisión mitocondrial es realizada por la proteína similar a la dinamina 1 (DRP1). La fusión mitocondrial está garantizada por mitofusinas 1 y 2 (MFN1 y MFN2) y la proteína atrofia óptica tipo 1 (OPA1), que median la fusión de la membrana externa de la mitocondria (OMM) y la membrana interna de la mitocondria (IMM), respectivamente. Además, MFN2 regula los sitios de contacto entre mitocondrias y retículo endoplásmico.

La activación de ERK dentro del eje RAS-MAPK promueve directamente la fragmentación mitocondrial al activar DRP1 y suprimir MFN1, lo que conduce a la redistribución mitocondrial, reducción en el amortiguamiento de calcio y activación de factores de transcripción que participan en diversos procesos celulares como la reparación de tejidos y el cáncer. La identificación de moléculas que pueden alterar la dinámica mitocondrial es de gran interés porque podrían modificar el metabolismo celular, afectando la cicatrización de heridas, la regeneración de tejidos y el cáncer.
En este estudio, investigamos el efecto de Gal-8 en la dinámica mitocondrial y la participación de su dominio de reconocimiento de carbohidratos en la modulación de esta dinámica a través de la activación de la vía de ERK.

Nuestros resultados muestran que Gal-8 recombinante y Gal-4 inducen la fragmentación, y solo Gal-8 promueve la distribución perinuclear de las mitocondrias en MDCK dependiendo de los glicanos α-2,3 sialilados. Estos efectos mediados por

Gal-8 también se observaron en células de ovario de hámster chino (CHO) y en células epiteliales de túbulos renales proximales humanos (RPTEC). En células CHO-LEC3.2.8.1, que tienen deficiencia en la N-glicosilación pero conservan la capacidad de sintetizar O-glicoproteínas, no se observó ningún efecto de Gal-8. Gal-8 podría promover la proximidad de las mitocondrias al núcleo probablemente mediante MFN2 de manera dependiente de carbohidratos al reconocer β-galactósidos α-2,3 sialilados, en células MDCK.

La fragmentación mitocondrial y la redistribución a la zona perinuclear inducidas por Gal-8 requirieron la actividad de ERK y SRC pero son independientes de la activación de EGFR. Por otro lado, la activación de DRP1 inducida por Gal-8 depende de la actividad de ERK en células epiteliales. También encontramos que Gal-8 promueve la mitofagia de manera dependiente de carbohidratos en células MDCK. Gal-8 modifica la tasa metabólica de las células MDCK, reflejado en un aumento de la acidificación del medio (ECAR) y en la fuga de protones, acompañado por una disminución en la producción de ATP acoplada a la tasa de consumo de oxígeno (OCR).

La fragmentación mitocondrial se ha asociado con la proliferación y la transición epitelio-mesénquima (EMT). Nuestros resultados muestran que Gal-8 induce la proliferación de manera dependiente de carbohidratos y la actividad de EMT dependiente de ERK.

En resumen, Gal-8 es un nuevo regulador de la dinámica mitocondrial que puede tener un impacto en enfermedades asociadas con disfunción mitocondrial o en procesos fisiológicos como la cicatrización de heridas y la reparación de tejidos.

I. INTRODUCTION

1.1. Problem statement

Galectins are a family of proteins that bind carbohydrates of glycoproteins and glycolipids and modulate a broad spectrum of physiological and pathological processes (Johannes et al., 2018; Rabinovich & Croci, 2012). The family of lectins share an affinity for β-galactosides through a homologous carbohydrate recognition domain (CRD). Galectins are synthesized in the cytosol, establishing protein-protein interactions with functions in the cytoplasm and nucleus. Intracellularly, Gal-3, Gal-8, and Gal-9 constitute a protection surveillance system that detects damaged endo-lysosomes and mediates their autophagic removal, repair, and replacement (Hong et al., 2021; Hoyer et al., 2022; Jia et al., 2018, 2019; Jia et al., 2020; Thurston et al., 2012). In the extracellular space, galectins bind glycans from membrane proteins, extracellular matrix, and glycolipids, thus mediating cell signaling, cell adhesion, cell-cell interactions and endocytosis (Johannes et al., 2018).

Mitochondrial dynamics involves the fission, fusion, and distribution of mitochondria. Mitochondrial fission is carried out by the Dynamin-related/-like protein 1 (DRP1). Mitochondrial fusion is ensured by mitofusins 1 and 2 (MFN1 and MFN2) and optic atrophy 1 (OPA1), which mediate outer mitochondria membrane (OMM) and inner mitochondria membrane (IMM) fusion, respectively (Tilokani et al., 2018). Maintaining a balance of these processes allows for proper cellular metabolic function (Yapa et al., 2021). Mitochondrial dynamics can be a key mediator of cellular phenotypic change in response to stimuli due to its sensitivity to extracellular signaling and the functional changes it can impose on a cell.

Few studies show that galectins modulate mitochondrial dynamics through carbohydrate recognition (Marin-Royo et al., 2018; Wang et al., 2023). Previous studies conducted in our laboratory have shown that Gal-8 transactivates the EGFR through FAK and activates ERK in MDCK cells, leading to proliferation and EMT induction. The Ras/Raf/MEK/ERK signaling axis has been associated with mitochondrial dynamics (Kashatus et al., 2015; Prieto et al., 2016). Activating ERK promotes phosphorylation of DRP1 in Serine 616 (S616), which enhances DRP1-

mediated mitochondrial fission. In addition, ERK kinase directly phosphorylates threonine 562 (T562) of MFN1, decreasing its ability to fuse mitochondria and preventing mitochondrial fusion (Pyakurel et al., 2015). Studies suggest ERK activation may precede mitochondrial degradation (mitophagy) and induce autophagy (Huang et al., 2018).

Given these insights, we speculate that Gal-8 may serve as an extracellular signal that regulates carbohydrate-dependent mitochondrial dynamics, thereby influencing cellular functions.

1.2. Literature review

1.2.1. Mitochondria

Mitochondria are essential cellular organelles ubiquitously present in all eukaryotic cells. These are mainly organized in an interconnected tubular network that extends through the cell along the cytoskeleton (Anesti & Scorrano, 2006). In recent years, the omics era and advancements in quantitative analysis of intermediate metabolism have reshaped our understanding of mitochondria, positioning them as versatile biosynthetic and signaling organelles. Through metabokine/mitokine signaling, mito-nuclear crosstalk, and epigenomic remodeling, mitochondria exert a profound influence on cell and organism behaviors. This paradigm shift has elevated mitochondria to the forefront of biomedical research, marking them as the most extensively studied organelles. The outdated analogy of mitochondria as mere powerhouses is discarded; instead, they are recognized as living, dynamic entities actively transducing biological information involving in a variety of cellular processes, including calcium homeostasis, inflammation, reactive oxygen species (ROS) production, and apoptosis (Bergman & Ben-Shachar, 2016). Recently it has been proposed that mitochondria operate through a three-step process: mitochondria sense and respond to inputs, integrate information through dynamic interactions and produce output signals that tune the functions of other organelles, thereby systemically regulating physiology (Picard & Shirihai, 2022).

Mitochondrial dynamics involves the fission, fusion, and distribution of mitochondria, which must be balanced to maintain cellular metabolic homeostasis (Yapa et al., 2021).

1.2.1.1. Mitochondria y oxidative phosphorylation

Mitochondria play a critical role in generating metabolic energy derived from the breakdown of glucose and fatty acids, which is converted to ATP by oxidative phosphorylation (OXPHOS) (Bergman & Ben-Shachar, 2016). Mitochondria are surrounded by a double-membrane system, consisting of inner (IMM) and outer (OMM) mitochondrial membranes separated by an intermembrane space. The inner membrane forms numerous folds (cristae), extending into the organelle's interior (or matrix). The OXPHOS machinery is located in the inner mitochondrial membrane (IMM). This machinery is made up of four electron transport chain (ETC) complexes, namely complexes I to IV, that are integrated into the IMM. The ETC complexes transfer electrons from reduced substrates, such as nicotinamide adenine dinucleotide (NADH) and flavin adenine dinucleotide (FADH2) to molecular oxygen, which is the final electron acceptor in the process of oxidative phosphorylation. High-energy phosphate production is achieved by coupling electron transfer to proton translocation across the IMM, resulting in an electrochemical gradient that reflects oxygen consumption, which generates a motive force driving ATP synthesis by ATP synthase (Chen et al., 2023).

1.2.1.2. Mitochondrial fission

The master mediator of mitochondrial fission is dynamin-related protein 1 (DRP1), a GTPase that is recruited into the OMM from the cytosol by binding to mitochondrial fission factor (MFF) adaptor proteins and mitochondrial dynamics proteins of 49 and 51 kDa (MiD49/MiD51) (Palmer et al., 2011). Fission is generated after constriction by contact of the endoplasmic reticulum with the mitochondria. After this constriction, DRP1 is recruited to the mitochondria, which executes fission around the mitochondrial outer membrane, which contracts the organelle in a GTP hydrolysis process (Kalia et al., 2018). Once assembled, DRP1 is sufficient to execute membrane

constriction and cutting (Kamerkar et al., 2018). Moreover, mitochondrial fission is also regulated by numerous factors, such as the endoplasmic reticulum, contacts with actin filaments, and actin regulators (Kamerkar et al., 2018; Korobova et al., 2013; Nagashima et al., 2020; Wong et al., 2018). In addition, DRP1 activity is modulated by post-translational modifications, such as phosphorylation. There are two crucial phosphorylation sites in DRP1, Serine 616 (S616) and Serine 637 (S637). Phosphorylation in S616 stimulates DRP1 activity and increases mitochondrial fission, while phosphorylation in S637 inhibits fission (Chang & Blackstone, 2010; Cribbs & Strack, 2007).

It has also been reported that mitochondrial fission can occur independently from DRP1 (Che et al., 2015; Nemani et al., 2018). Nemani et al., observed that mitochondria can change shape when exposed to cytosolic Ca^{2+} $[Ca^{2+}]_C$, which is different from the process of mitochondrial fission (Nemani et al., 2018). $[Ca^{2+}]_C$ elevation, but not Mitochondrial Calcium Uniporter mediated Ca^{2+} uptake, appears to be essential for the process term as mitochondrial shape transition (MiST). In different cell types, MiST is mediated by the mitochondrial protein Miro1 through its EF-hand domain 1 that senses cytosolic Ca^{2+} (Nemani et al., 2018). Additionally, it has been described that EGFR can regulate mitochondrial dynamics and induce mitochondrial fission independent of DRP1 (Che et al., 2015). The authors describe that EGF induces the translocation of the EGFR from the cell membrane into the mitochondria and induces mitochondrial fission through inhibition of MFN1, without altered protein expression as well as the activation status of DRP1 (Che et al., 2015).

Fragmented mitochondria are associated with more motility, mitophagy and cell division (Wakabayashi et al., 2009) and EMT in a cancer context (Ghosh et al., 2023). Moreover, fragmented mitochondria are necessary for proliferation. During mitosis, several kinases phosphorylate the key mitochondrial factors and drive fragmentation of mitochondria to allow for their efficient distribution and inheritance to two daughter cells. Recent evidence suggests that mitochondrial fission can also actively regulate mitotic progression (Pangou & Sumara, 2021). Likewise, it has been reported that DRP1 knockdown reduces proliferation and promotes apoptosis (Zhan et al., 2016). The knockout of mouse DRP1 through genetic engineering results in embryonic lethality (Wakabayashi et al., 2009).

1.2.1.3. Mitochondrial fusion

The main components involved in mitochondrial fusion are also members of the dynamin-like GTPase family: Mitofusin 1 and 2 (MFN1/2) in the outer mitochondrial membrane (OMM) and optic atrophy 1 (OPA1) in the inner mitochondrial membrane (IMM) (Yapa et al., 2021). MFN1/2 forms heterodimers and homodimers that hydrolyze GTP to bind and fuse the outer membranes of two mitochondria (Chen et al., 2003). The fusion of internal mitochondrial membranes is based on the action of OPA1 that covers the inner mitochondrial membrane to integrate two membranes into one. Another function of OPA1 is maintaining the structural integrity of mitochondrial crests (Olichon et al., 2003).

The most efficient process of mitochondrial fusion is observed when both MFN proteins are present simultaneously in the OMM. The turnover and activity of MFNs are also precisely orchestrated by post-translational modifications. The acetylation of MFN1 at K222 or K491 inhibits the MFN1 GTPase activity (J. Y. Lee et al., 2014), likewise, the phosphorylation of MFN1 at T562 regulated by MEK/ERK cascade restricts MFN1 assembly and pro-fusion capability (Pyakurel et al., 2015). Deacetylation of MFN1 at K222 or K491 increases MFN1 activity and mitochondrial network fusion (J. Y. Lee et al., 2014). MFN2 is degraded via PRKN-mediated ubiquitination, which remodels the OMM-ER contact site and enhances mitophagy (McLelland & Fon, 2018). Under cellular stress, MFN2 is phosphorylated at Ser27 by Jun N-terminal kinase (JNK) and subsequently degraded by the proteasome. Intercepting the phosphorylation at Ser27 reduces MFN2 degradation, facilitates mitochondrial elongation, and prevents apoptosis (Leboucher et al., 2012). Additionally, genetic knockout of MFN1 and/or MFN2, destroys the mitochondrial structure and induces serious cellular defects, including smaller and more fragmented mitochondria, lower mitochondrial membrane potential, attenuated respiration activity and ATP production, which in turn suppresses cell proliferation (Pyakurel et al., 2015).

On the other hand, fusion of IMM is mainly regulated by OPA1, which is a dynamin-like GTPase inserted into the IMM by its N-terminal. There are two splicing forms of OPA1: IMM-anchored long form-Opa1 (L-OPA1) and soluble short form-Opa1 (S-OPA1). L-OPA1 is proteolytically hydrolyzed to S-OPA1 by OMA1 and YME1 Like 1 ATPase (YME1LI), and the relative levels of L-OPA1 and S-OPA1 are a key factor

in determining the viability of mitochondrial fusion (Chen et al., 2023). In addition to controlling the IMM fusion, OPA1 also orchestrates cristae integrity, mtDNA maintenance, bioenergetics, as well as respiratory chain super complex assembly, so that OPA1 directly affects mitochondrial cytochrome release and oxidative respiration efficiency (Chen et al., 2023). Early embryonic lethality is observed in double knockout or OPA1 mutant mice (Davies et al., 2007).

MFN2 is involved in various cellular functions, such as regulating contact sites between mitochondria and other organelles. It is a tethering protein in mitochondria-ER contact sites to regulate calcium homeostasis and lipid metabolism (Zaman & Shutt, 2022; Zervopoulos et al., 2022).

1.2.1.4. Mitochondrial traffic

The cytoskeleton is a structure that helps cells maintain their shape and internal organization. It also provides mechanical support that enables cells to carry out essential functions, such as spatially organizing the contents of the cell, connecting the cell physically and biochemically to the external environment, and generating coordinated forces that enable the cell to move and change shape (Fletcher & Mullins, 2010; Li et al., 2024). The eucaryotic cells must constantly reorganize the distribution of mitochondria to meet the local demands for energy, calcium, redox balance, and other mitochondrial functions. Mitochondrial localization is a result of a combination of movement along the microtubule tracks and anchoring to actin filaments (Furnish & Caino, 2020).

Mitochondrial movement from the center to distal zones is driven by microtubule-anchored kinesin. In contrast, the cytoplasmic dynein-dynactin complex orchestrates retrograde movement (distal zones to center) of mitochondria (Chen et al., 2023). The complex that connects kinesin and dynein to mitochondria is called the Miro–TRAK complex. It consists of two proteins called Miro1 and Miro2 (also known as RHOT1 and RHOT2) and two proteins called TRAK1 and TRAK2 (also known as trafficking kinesin protein 1 or 2) (Eberhardt et al., 2020; Flannery & Trushina, 2019). The mitochondrial movements on actin filaments rely on myosin motors (MYO19, MYO6, and MYO5). MYOs move along actin filaments in either anterograde or retrograde directions (Furnish & Caino, 2020).

1.2.1.5. Mitochondrial degradation – Mitophagy

During the fission-fusion cycle, the mitochondrial matrix connects and integrates neighboring regions to compensate for areas of dysfunction. This process helps in the formation of new mitochondria. If there are any malfunctioning machinery, such as electron transport chain complexes, mitochondrial fission selectively removes the affected portions and directs them to degradation through specialized autophagy pathways known as mitophagy. This process ensures the overall health and functioning of the mitochondria (Rolland et al., 2013).

Mitophagy serves in mitochondrial quality control and is carried out primarily by the PINK1-Parkin pathway (Pickles et al., 2018). The PINK1-Parkin pathway works by stabilizing the PINK1 kinase in the OMM after mitochondrial depolarization. PINK1 then phosphorylates the ubiquitin chains in OMM proteins, promoting the recruitment of ubiquitin ligase E3 Parkin. Recruitment of Parkin leads to additional ubiquitination of OMM proteins leading to subsequent recruitment of autophagy receptors and targeted removal of these depolarized mitochondria (Lazarou et al., 2015). Consequently, the ubiquitinated mitochondria are combined with LC3-positive autophagosomes by these receptors, forming autophagosomes that eliminate damaged mitochondria (Georgakopoulos et al., 2017).

Several other E3 ubiquitin ligases that can facilitate the removal of dysfunctional mitochondria have been identified. These mechanisms are independent of the PINK1-Parkin pathway and are related to mitophagy. Mitochondrial ubiquitin ligase 1 (MUL1), BCL-2 homology 3 (BH3)-containing protein NIP3-like X (NIX, also known as BNIP3L), and FUN14 domain containing 1 (FUNDC1) are among the ligases that are involved in these mechanisms (Teresak et al., 2022).

Impaired mitophagy refers to the inability of cells to effectively eliminate dysfunctional mitochondria, leading to their accumulation and disruption of mitochondrial function and cellular homeostasis (Chen et al., 2023). Defective and excessive mitophagy have been proposed to contribute to age-related neurodegenerative diseases, such as Parkinson’s and Alzheimer’s diseases, metabolic diseases, vascular complications of diabetes, myocardial injury, muscle dystrophy, and liver disease, among others. The restoration of mitophagy homeostasis

and the elimination of irreversibly damaged mitochondria could serve as potential therapies in several chronic diseases (Georgakopoulos et al., 2017).

Mitophagy is a complex process where cells eliminate damaged mitochondria and plays a role in cancer. When mitophagy is reduced, it has been linked to the development of tumors in mice, especially in the liver and pancreas. This happens when certain genes like Parkin or PINK1 are deleted (Li et al., 2018). Loss of Parkin increases proinflammatory signals, promotes genomic instability, and increases cancer cell proliferation and resistance to apoptosis (Hu et al., 2016). Interestingly, the accumulation of mitochondrial dysfunctions induced by Parkin deficiency decreases mitochondrial OXPHOS, increases ROS production and glycolysis, possibly contributing to the Warburg effect, and consequently increases tumorigenesis (Zhang et al., 2011). Furthermore, Parkin has been identified as an E3 ubiquitin ligase for HIF-1α to promote its proteasomal degradation. The downregulation of Parkin in breast cancer cells stabilizes HIF-1α and promotes metastasis (Liu et al., 2017).

Mitophagy, by removing damaged mitochondria, helps cells survive and prevents cell death (Ferro et al., 2020). In Parkin-deficient mice, melanoma growth and metastasis are suppressed, suggesting a pro-tumor role of Parkin-dependent mitophagy (Ferro et al., 2020). In addition, induction of the E3 ligase BNIP3 promotes cell migration through cytoskeleton remodeling and resistance to anoikis and invasion, suggesting a role of BNIP3-dependent mitophagy in metastasis formation (Maes et al., 2014). The pro-survival role of mitophagy has also been associated with resistance to anti-cancer treatments (Villa et al., 2017; Yan et al., 2017).

1.2.1.6. Mitochondria and metabolic reprogramming

Metabolic reprogramming is defined as the ability of cells to alter the metabolism and lead to growth and proliferation (Sciacovelli & Frezza, 2017). The metabolic reprogramming is influenced by the bioenergetic activity of mitochondria, where mitochondrial size plays a crucial role in mitochondrial function. Highly fused tubular mitochondrial networks exhibit higher ATP synthase dimerization, increased ATP synthesis, and lower degradation than fragmented mitochondria (Gomes et al., 2011). Fragmented mitochondria have mainly been associated with decreased oxidative phosphorylation activity and increased elimination efficiency through

mitophagy and intracellular mitochondrial mobility (Chen & Chan, 2017). Also, in cancer cells, more fragmented mitochondria are related to elevated rates of glycolysis, even in the presence of oxygen, allowing the use of glycolytic intermediates in anabolic metabolism to fuel cell growth and proliferation through increased synthesis of essential building blocks such as nucleotides and lipids (DeBerardinis & Chandel, 2020).

A wide variety of metabolic phenotypes are associated with mitochondrial morphologies that are highly dependent on tissue type and differentiation status. Metabolic phenotypes coordinated by mitochondria have been well described to affect cellular identity reprogramming through modulation of chromatin accessibility (Kaelin & McKnight, 2013). Mitochondria orchestrate gene expression through the synthesis of metabolites that form retrograde signals by serving as cofactors and substrates for gene expression-modifying enzymes (MacKenzie et al., 2007). Among them, acetyl-CoA (J. V. Lee et al., 2014), synthesized in the cytoplasm from mitochondrial-derived citrate, is the substrate for the acetylation of histones, DNA, and cytosolic enzymes. Alterations in levels of reactive oxygen species synthesized within mitochondria can both directly modify enzymes such as p38 MAPK and DUSP6 and activate antioxidant programs such as the NRF2 pathway that modulate gene expression through direct binding of ROS-sensitive transcription factors (Xue et al., 2020). Additionally, mitochondrial content affects the mitochondrial capacity to buffer cytosolic calcium, which modulates the activity of calcium-sensitive cellular signaling such as that mediated by Calcineurin (Guha et al., 2014). This exemplifies how incoming signals alter mitochondrial function and how mitochondria affect the signaling strength of pathways sensitive to mitochondrial outputs. Also, retrograde signaling networks can form significant interactions in which one mitochondrial metabolite may influence the activation of another mitochondrial retrograde signaling program (Shi & Tu, 2015).

Changes in the dynamics of mitochondria can directly impact mitochondrial and cellular function. This can lead to changes in the metabolic rate of cells based on their demands and improve the turnover of mitochondria (Ma et al., 2020). Mitochondrial dysfunction caused by MFN deficiency or GTPase activity decline manifests as metabolic dysfunction, leading to various pathological conditions through elevated ROS levels, mtDNA depletion, decreased ATP synthesis, and OXPHOS suppression. Alternatively, the fusion of mitochondria counteracts metabolic insults primarily by

enhancing OXPHOS and ATP generation and preventing mitochondria against mitophagy. However, dysfunctional mitochondria and cellular dysfunction occur when the balance between mitochondrial dynamics and function is lost (Xiao et al., 2022).

1.2.1.7. Mitochondria and perinuclear distribution

Mitochondria can appear in three patterns in the cells: homogeneous/random, aggregated/fused, or perinuclear. It has been reported that mitochondria with high ATP production localize to the periphery of cells instead of the perinuclear position. It has also been described in various cell types that mitochondria tend to be distributed around the nucleus. However, the functional implication of perinuclear mitochondrial distribution is not clear (Collins et al., 2002). The following functions have been attributed to the perinuclear distribution of mitochondria:

1. Mitochondria that assemble near the nucleus could favor the transport of macromolecules across the nuclear pores and the transport of mitochondrial proteins to the mitochondria (Naik et al., 2019). Such a perinuclear distribution might also buffer the nucleus during Ca^{2+} fluctuations in the cytoplasm (Park et al., 2001).

2. Mitochondria regulate second messenger concentrations, like ROS, with localized movement. Under hypoxia, endothelial cells show retrograde mitochondrial movement towards the nucleus, influenced by microtubules and dynein. This clustering induces ROS accumulation in the nucleus, impacting VEGF expression. Although HIF-1α levels are unaffected, perinuclear mitochondrial clustering crucially modifies the VEGF promoter, shaping transcriptional responses to hypoxia (Al-Mehdi et al., 2012).

3. Mitochondria around the nucleus maintain lower O_2 levels compared to the mitochondria distributed random in the cytosol. Pharmacological and genetic interventions impacting mitochondrial respiration alter nuclear O_2 levels, affecting cellular processes and gene expression. These insights highlight the dynamic regulation of nuclear O_2 by mitochondrial activity, potentially influencing oxidative stress and age-related phenomena (Mori et al., 2023).

1.2.2. Protein glycosylation and cell function

The glycan structures found in cells and tissues, known as the glycome, store vital biological information that significantly contributes to the reprogramming of cellular fate and function (Dube & Bertozzi, 2005; Ohtsubo & Marth, 2006; Reily et al., 2019). The diversity and spatiotemporal regulation of glycans within glycoconjugates depend on the synchronized activity of glycan-modifying enzymes. Glycan remodeling is regulated by both intracellular and environmental signals, including metabolic stress, oxygen and nutrient availability, growth factors and cytokines (Ohtsubo & Marth, 2006). Aberrant glycosylation has been associated with the dysregulation of numerous cellular processes, including cellular communication, proliferation, differentiation, and survival (Ohtsubo & Marth, 2006). Changes in mitochondrial dynamics can alter the glycosylation patterns on cell surfaces, by altering the substrate availability for N- and O- glycosylation (Chiaradonna et al., 2018).

1.2.2.1. Galectins

The glycan code is decodified by a group of proteins called galectins. Galectins are carbohydrate-binding proteins involved in the regulation of a variety of cellular processes interacting with glycoproteins and glycolipids bearing β-galactoside moieties (Barake et al., 2020; Johannes et al., 2018; Rabinovich & Croci, 2012). Galectins are found both in the cytosolic compartment and extracellularly due to unconventional secretion, as they lack a signal peptide for the classical exocytic secretory route (Barake et al., 2020; Johannes et al., 2018).

Sixteen galectins have been described in animals, classified into three groups according to their structure and number of CRDs (Cummings, 2009). The prototypical galectins (Gal-1, -2, -5, -7, -10, -11, -13, -14, -15, and -16) contain a single CRD and a short N-terminal sequence allowing dimerization. The tandem-repeat galectins (Gal-4, -6, -8, -9 and -12) contain two different CRDs separated by a linker peptide within a single polypeptide molecule. Only galectin-3 belongs to the chimeric galectin type bearing a single CRD and a large amino-terminal non-lectin domain that contributes to self-aggregation (Cummings, 2009; Johannes et al., 2018).

In the cytosol, galectins recognize host glycans in damaged organelles and promote their reparation or removal and replacement in response to diverse stimuli (Hong et al., 2021; Hoyer et al., 2022; Jia et al., 2018, 2019; Jia et al., 2020; Thurston et al., 2012). Galectins have also been found to establish direct protein-protein interaction (Vladoiu et al., 2014), with carbohydrate-independent functions in diverse cellular processes, including mRNA splicing and stabilization, cell proliferation, apoptosis, and cell cycle progression (Coppin et al., 2020).

In the extracellular space, galectins bind glycans from cell surface membrane proteins, extracellular matrix, and glycolipids, thus mediating cell signaling, cell adhesion and cell-cell interactions (Barake et al., 2020; Cummings, 2009). Galectins also modulate intracellular trafficking of cell surface proteins (Johannes et al., 2018). In contrast to the classic concept of one ligand one receptor, galectins interact with many glycoproteins simultaneously, thus exerting a more global regulation on cells (Barake et al., 2020).

1.2.2.2. Galectins and mitochondria

Until now, only Gal-3 has been associated with changes in mitochondrial dynamics (Coppin et al., 2020; Marin-Royo et al., 2018). Coppin et al., reported that intracellular Gal-3 regulates mitochondrial bioenergetics and ER stress response in cancer cells (Coppin et al., 2020). Wang et al. reported that extracellular Gal-3 downregulates genes of the respiratory chain complex and inhibits mitochondrial biogenesis (Wang et al., 2023). Also, Gal-3 inhibition by citrus pectin partially prevent mitochondrial damage induced by lipotoxicity in a model of high-fat diet in rats (Wang et al., 2023).

1.2.2.3. Galectin-8

Gal-8 is one of the most widely expressed galectin in human tissues and in cancerous cells. Gal-8 belongs to the tandem repeat group. Its N-terminal CRD (N-CRD) has a high affinity for terminal α-2,3-sialic acid, which gives it unique functional properties (Cagnoni et al., 2020). Otherwise, the C-terminal CRD has an affinity for non-sialylated oligosaccharides, such as polylactosamine and glycans of blood

antigens A and B (Elola et al., 2014). Notably, both binding pockets of the CRD have 8 crucial amino acids that recognize the glycosylation. The N-terminal CRD of Gal-8 recognizes glycoproteins and glycolipids that contain α-2,3-sialic acid by amino acid R69. Otherwise, the C-terminal domain of Gal-8 recognizes non-sialylated oligosaccharides by the amino acid R275 (Hirabayashi et al., 2002) (Figure 1). Additionally, there are three isoforms of the Gal-8 protein in humans, known as Gal-8S (small), Gal-8M (medium), and Gal-8L (long). Among these isoforms, Gal-8M is the most studied (Cagnoni et al., 2020), which was used in this thesis.

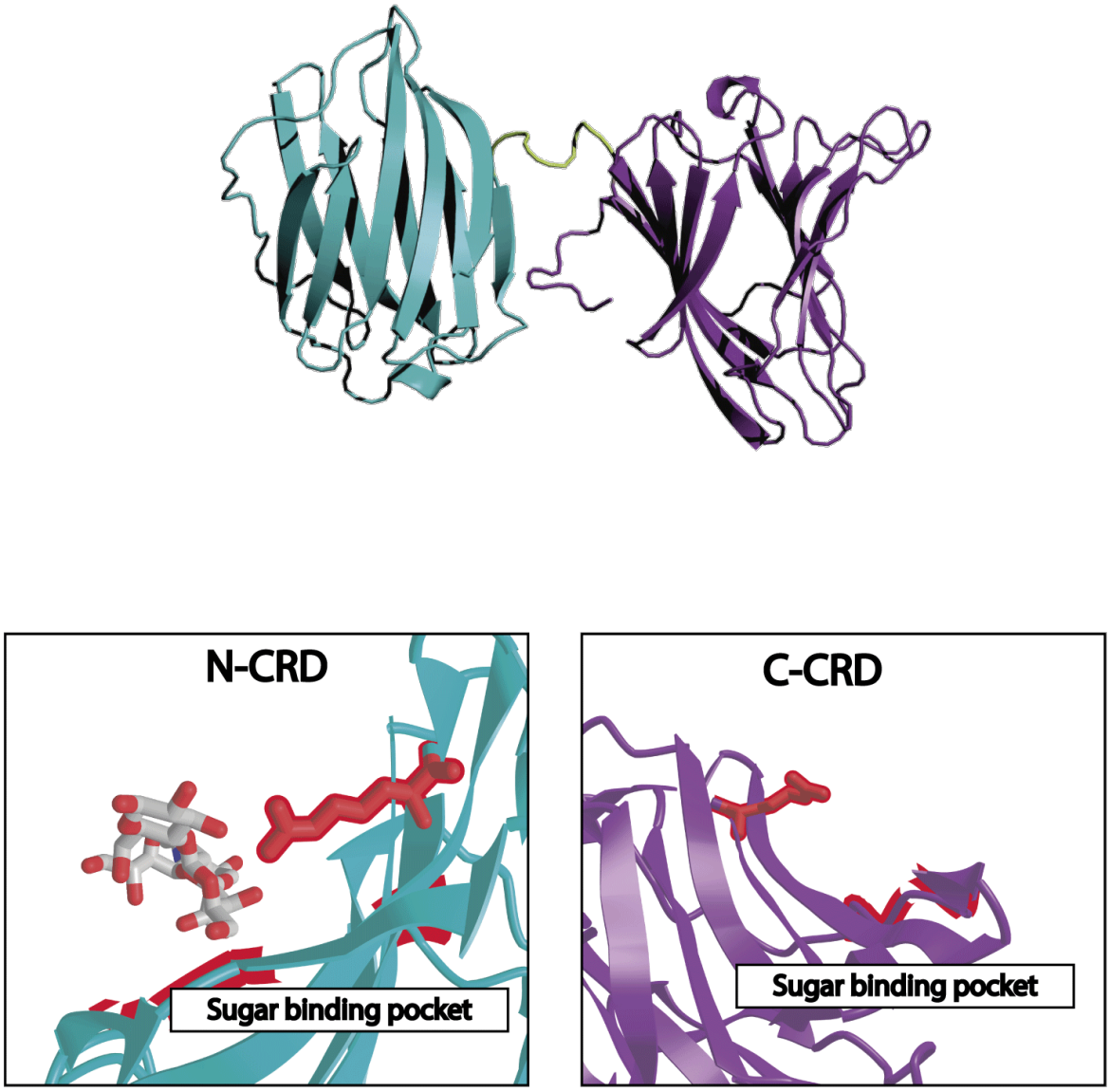

Figure 1. Structure of Gal-8 and the sugar binding pocket.

Gal-8 belongs to the Lectin family. In particular, the tandem repeat-type galectins that have two CRDs connected by a linker peptide. The N-terminal domain of Gal-8, colored as cyan, has a high affinity for sialic acid at position α-2,3, which gives Gal-8 its distinctive characteristic. The C-terminal domain has an affinity for N-acetyllactosamine, colored as purple. Both terminals have 8 amino acids essential for the binding pocket, where the major affinity of the N- terminal is provided by the amino acid R69, and for the C- terminal, the amino acid R275.

Intracellularly, Gal-8 has been described to have an important role in recognizing carbohydrates exposed in damaged endomembranous and targeting them to autophagy degradation. This is achieved by recruiting the autophagy receptor nuclear domain 10 protein 52 (NDP52) (Thurston et al., 2012). This mechanism of clearing damaged endomembrane acts as a protective system against the infection of certain bacteria and the spread of pathogenic protein aggregates (Jia et al., 2019; Thurston et al., 2012).

Extracellularly, Gal-8 has diverse functions in various cell types and tissues. Gal-8 promotes the maturation of B cells into plasma cells and improves antigen presentation in B lymphocytes (Obino et al., 2018). In T cells, Gal-8 regulates the synapses and, after T cell activation, induces apoptosis through β1 integrins (Prato et al., 2020). In human platelets, Gal-8 promotes spreading, fibrinogen binding and elevations of intracellular calcium levels (Romaniuk et al., 2010). In the brain, Gal-8 has an immunomodulatory role in ameliorating autoimmune encephalomyelitis by modulating the balance of helper T cell polarization and T regulatory cells (Pardo et al., 2017). Also, Gal-8 is neuroprotective against several damaging agents in vitro and in vivo, acting through β1 integrins (Pardo et al., 2017). Gal-8 could be relevant in inflammatory processes as a potent immunosuppressive agent since, in the brain, Gal-8 acts as an anti-inflammatory and a neuroprotective factor. However, it can be neutralized by blocking autoantibodies (anti-Gal-8) in inflammatory conditions and autoimmunity (Pardo et al., 2017).

Likewise, Gal-8 has been reported as a fibrogenic stimulator exerting its function through the β1-Integrin/FAK pathway in human gingival fibroblasts (Smith et al., 2020). Otherwise, extracellularly Gal-8 treatment was associated with the accumulation of phosphorylated myosin light chain and the formation of stress fibers inhibited by the Rho inhibitor in the trabecular meshwork (Diskin et al., 2012).

Gal-8 is a widely expressed galectin in human carcinomas (Elola et al., 2014). It has been associated with an unfavorable prognosis in various types of cancer (Gentilini et al., 2017; Reticker-Flynn et al., 2012). Gal-8 can contribute to cancer progression and metastasis by regulating the production of immunoregulatory cytokines, thereby facilitating the recruitment of cancer cells to metastatic sites (Prato et al., 2020; Shatz-Azoulay et al., 2020). Gal-8 promotes tumorigenesis by stimulating angiogenesis and integrin-mediated cell adhesion during metastasis (Reticker-Flynn

et al., 2012). Recent studies from our laboratory demonstrate that overexpressing Gal-8 in non-neoplastic MDCK cells transactivates EGFR, via FAK, in sub confluent cells, promoting ERK activation, migration, proliferation and EMT in a carbohydrate-dependent manner (Oyanadel et al., 2018).

ERK, a key player in mitochondrial dynamics during tumor progression, enhances DRP1-mediated mitochondrial fission and inhibits fusion by phosphorylating DRP1 and MFN1 (Kashatus et al., 2015; Prieto et al., 2016; Pyakurel et al., 2015). Activation of ERK is also linked to autophagy and mitophagy initiation (Huang et al., 2018). Therefore, in this thesis, we studied the role of Gal-8 in mitochondrial dynamics in nontumoral epithelial cells and its impact on cellular metabolism.

PROJECT AIMS

1.3. Hypothesis

“Galectin-8 changes mitochondrial dynamics through its carbohydrate recognition domain and promotes metabolic reprogramming in epithelial cells”

1.4. General aims

To evaluate the carbohydrate-dependent effects of Gal-8 on mitochondrial dynamics mediated by ERK and DRP1 signaling and their implications on metabolic reprogramming in epithelial cells.

1.5. Specific aims

1 – To analyze the role of Gal-8 on fragmentation and distribution of mitochondria through carbohydrates recognition, ERK activation and DRP1 in epithelial cells.

1.a) To determine the effect of Gal-8 on fragmentation and distribution of mitochondria.
1.b) To analyze the dependency of the carbohydrate recognition of Gal-8 on fragmentation and distribution of mitochondria.
1.c) To evaluate the implication of ERK activation in Gal-8-driven mitochondrial fragmentation and distribution.
1.d) To investigate the role of DRP1 in Gal-8-induced mitochondrial fragmentation and distribution.

2 – To analyze the role of Gal-8 in metabolic reprograming in epithelial cells through carbohydrate dependence.

2.a) To analyze the effect of Gal-8 on mitophagy and its dependence on carbohydrates.
2.b) To evaluate the implications of Gal-8 on oxygen consumption rate (OCR) and extracellular acidification rate (ECAR).
2.c) To analyze the effect of Gal-8 on proliferation and EMT markers in epithelial cells.

II. MATERIALS AND METHODS

2.1 Reagents

- Bovine serum albumin (BSA) powder, glycerol, glycine and methanol were purchased from Fisher Scientific, HEPES, Tris-HCL, Trizma base and glutathione – from Sigma, Tween 20 and triton X-100 – from VWR, dithiothreitol (DTT) – from Melford, distilled water – from Life Technologies.
- Fetal bovine serum (FBS) was obtained from Labtech.
- Protease inhibitors leupeptin, aprotinin, benzamide and phenylmethylsulphonyl fluoride (PMSF) were from Sigma.
- Selection agents were obtained from Melford (amplicilin), Life Technologies (puromycin, blasticidin S HCl), Merck (kanamycin).
- Primers (describe below) were order from Sigma.
- Inhibitors: Tyrphostin AG1478 (CAS 175178-82-2 Santa Cruz), PD98059 (513001 - Merck) and PP2 (P0042 – Sigma-Aldrich)

2.2 Antibodies

The following antibodies were used for Western blots.

Antibody	Source	Application
DRP1	Cell Signaling	WB 1:2000
pS616 DRP1	Cell Signaling	WB 1:2000
ERK	Cell Signaling	WB 1:2000
pThr202/Tyr204 ERK	Cell Signaling	WB 1:2000
MFN1	Cell Signaling	WB 1:2000
MFN2	Cell Signaling	WB 1:2000
Snail	Cell Signaling	WB 1:2000
ZO-1	Cell Signaling	WB 1:2000
GAPDH	ThermoFisher	WB 1:5000
NDP52	Cell Signaling	WB 1:2000
LC3	Cell Signaling	WB 1:2000
e-Cadherin	Cell Signaling	WB 1:2000

N-Cadherin	Cell Signaling	WB 1:2000
Vimentin	Cell Signaling	WB 1:2000
HRP-conjugated secondary antibodies	Dako	WB 1:5000

Table 2.1. Antibodies used in this work. WB – Western blot.

2.3 Primers

Primers used for amplification of open reading frames.

ID	Gene	Sequence	D	RE
trx414	galectin 8	ACATGTCCATGATGTTGTCCTTAAACAACC	F	PciI
trx414	galectin 8	GCGGCCGCCTACCAGCTCCTTACTTCCAGTAAGTG	R	NotI

Table 2.2 Primers used for amplification of the indicated genes. All primers are show in the 5' to 3' orientation. ID – identification name, D – direction, F – Forward, R – reverse, RE – restriction enzyme site.

Primers used for site-directed mutagenesis.

Mutation	Gene	ID	Sequence	D
R69H	galectin 8	MPW334	ATGAAAGGCCACATCGGC GGC AGGTTTCATGCTGCTGCC	R
		MPM335	GGCAGCAGCATGAAACCT GCC GCCGATGTGGCCTTTCAT	F
R275H	galectin 8	MPW332	AAATGCTTTAATATTCAG ATG TGGGTTCAAGTGTAGAGC	R
		MPW333	GCTCTACACTTGAACCCA CAT CTGAATATTAAAGCATTT	F

Table 2.3. Primers used to generate point mutations in the indicates genes. The nucleotide changes to generate point mutations are shown in lowercase. All primers are show in the 5' to 3' orientation. ID – identification name, D – direction, F – Forward, R – reverse.

Primers used for sequencing.

Vector	ID	D	Sequence
M6P	FLX190	F	TAGACGGCATCGCAGCTTGGA
	FLX561	R	ACGCACACCGGCCTTATTCCA
pEMT30	pGEX-5	F	CTGGCAAGCCAGTTTGG
	pET-RP	R	CTAGTTATTGCTCAGCGG

Table 2.4. Primers used for sequencing of the indicated vectors. All primers are show in the 5' to 3' orientation. ID – identification name, D – direction, F – Forward, R – reverse.

2.4 Plasmids

- M6P plasmids were used to produce recombinant MLV for protein expression in MDCK and RPTEC cells.
- pETM30 vector was used to produce recombinant proteins tagged with His-GST in *E*. coli.

Plasmids used in this project are summarized in table 2.5 -2.6.

Plasmids with IDs containing letters ADP were created by me (Adely De la Peña), TH – by Dr. Thomas Mund.

Plasmids used for retroviral transduction or transfection of cells.

ID	Name	Resistance
TH-GG10	M6blast-MT-GFP	Blasticidin
TH-GA4	M6Pblast-Keima-FIS1	Blasticidin
TH-GC6	pNF-κB-MetLuc2-reporter	-

Table 2.5. Plasmids used for retroviral transduction of cells.

Plasmids used for protein expression in E. coli

ID	Name
ADP01	pETM30-galectin-8
ADP02	pETM30-galectin-8-R69H
ADP03	pETM30-galectin-8-R275H
ADP05	pETM30-galectin-8-R69H-R275H
ADP06	pETM30-galectin-1
ADP07	pETM30-galectin-2
ADP08	pETM30-galectin-3
ADP09	pETM30-galectin-4
ADP10	pETM30-galectin-7
ADP11	pETM30-galectin-10

Table 2.6. Plasmids used for protein expression in E. coli.

2.5 Bacterial strains

- Escherichia coli (E. coli) strain MC1061 was used for plasmid production.
- Escherichia coli (E. coli) strain BL21 was used for protein expression.

2.6 Eukaryotic cell lines

- HEK293ET, an epithelial cell line derived from the human embryonic kidney, was obtained from the European Collection of Cell Culture and used for virus production.
- MDCK, an epithelial cell line derived from dog kidney, was obtained from the European Collection of Cell Culture. It was used for the experiment assays.
- RPTEC, a primary renal proximal tubule epithelial cell, was obtained Sigma-Aldrich. It was used for the experiment assays.
- CHO-K1, an epithelial cell line derived from the ovary of the Chinese hamster, was obtained from the European Collection of Cell Culture. It was used for the experiment assays.

- CHO-LEC3.2.8.1 is an epithelial cell line derived from the ovary of the Chinese hamster, which lacks mature glycans (Patnaik & Stanley, 2006). These mutant cells have been isolated by selection for resistance to the cytotoxicity of plant lectins. This cell was used for the experiment assays.

2.7. Molecular cloning

2.7.1. Polymerase Chain Reaction (PCR)

PCR was used for amplification of required genes from cDNA libraries or plasmids constructs, and assembly PCR was used to introduce point mutations into DNA sequences. Primers pairs complementary to the 21 – 27 nucleotides at 5' and 3' end of a gene (forward and reverse) were designed to amplify required genes by PCR. The primers contained the appropriate DNA restriction enzyme sites to facilitate cloning of the amplified genes into plasmid vectors. Mutagenic primers pairs of 34 – 46 nucleotides containing the desired nucleotide changes and complementary to 12 – 20 nucleotides flanking the mutation site were designed for assembly PCR. Two PCR reactions were performed to introduce the desired nucleotide changes into a gene of interest. The first PCR round included amplifications from wild type DNA using external forward and reverse wild type primers combined with mutagenic primers of the opposite direction. The PCR products generated in the first PCR rounded were solved in 1.5% NuSieve GTG low melting temperature agarose (Lonza) gels, supplemented with SYBR safe (Life Technology) for visualization of DNA, run at 90 V for 30 minutes in TAE buffer (40 mM Tris (pH 7.6), 20 mM acetic acid, 1 mM EDTA). PCR products were excised from the gel and purified using QIAquick Gel Extraction kit (Qiagen) according to manufacturer's instructions. The purified fragments obtained from the first round of PCR were used as DNA template to amplify the full-length mutated gene with the external forward and reverse wild type primers KOD Hot Start Polymerase kit (Millipore) was used for PCR reactions, performed in a Veriti Thermal Cycle (applied Biosystems). A 50 ul PCR reaction mix contained 5 ul of 10X KOD Hot Start Polymerase Buffer, 5 ul of 2mM deoxyribonucleoside triphosphate (dNTPs), 3 ul of 25mM Mg SO4, 2.5 ul of dimethyl sulfoxide (DMSO, Fisher Scientific), 0.5 ul of 10X KOD Hot Start Polymerase, 1.5 ul of 10 uM of forward and reverse primer and DNA

(50 ng of plasmid or 1.5 mmol of cDNA library). A standard PCR program included the following steps: initial denaturation (95°C, 2 minutes), followed by 20- 35 cycles of denaturation (95°C, 20 seconds), primer annealing (56-60°C, 20 seconds) and extension (70°C, 20 seconds per kilobase of amplification product), and final extension (70°C, 10 minutes) (Thurston et al., 2016).

2.7.2. Digestion of DNA with restriction enzyme

DNA restriction enzymes (New England BioLabs) were used to digest plasmids or PCR products, containing the appropriate restriction enzyme recognition sites, and create the desired ends. A 20 ul digestion reaction mix consisted of 2 ul of appropriate NEBuffer (New England BioLabs), 0.2 – 0.5 ul DNA restriction enzyme (s) and 0.5 – 1 ug of DNA, diluted in distilled water. The digestion reaction mixes were incubated at 37°C for 1 – 2 hours, mixed with loading buffer (30% glycerol, 10 mM EDTA, 0.05% Orange G (Sigma)) and resolved in 1.5% NuSieve GTG low melting temperature agarose (Lonza) gels, supplemented with SYBR Safe (Life Technologies) for visualization of DNA, run at 90V for 30 - 40 minutes in TAE buffer (40 mM Tris (pH 7.6), 20 mM acetic acid, 1 mM EDTA). Bands containing the desired DNA fragments, visualized using a blue light transilluminator, were excised from the gel and incubated at 70°C for 5 – 10 minutes to ensure melting of agarose directly before adding the DNA fragments into the ligation mix (Ravenhill et al., 2019).

2.7.3. Ligation of DNA fragments

Plasmid constructs were created by ligating the insert DNA fragments with the dephosphorylated by 10% alkaline phosphate (Roche) plasmid vector, both digested with the appropriate DNA restriction enzymes. A ligation mix consisted of 28 ul of distilled water, 2 ul of BSA (New England BioLabs), 5 ul of 10X T4 ligase buffer (New England BioLabs), 5 ul of ligation additives (1 mM ATP, 10 mM DTT), 0.3 ul of T4 ligase (New England BioLabs), 2 ul of digested and de-phosphorylated vector and either 4 ul of digested insert DNA fragment (positive) or 4 ul of distilled water (negative, to ensure efficient de-phosphorylation of the vector). Ligation mixes were incubated at

room temperature for 2 hours or longer before using them for transformation of competent E. coli (Ravenhill et al., 2019).

2.7.4. Transformation of competent E. coli

To obtain bacteria expressing a plasmid construct of interest, 50-200 ng of plasmid or 5 ul of ligation mix were added to 50 ul of chemically competent E. coli strain MC1061. Bacteria were incubated with the plasmid or ligation mix on ice for 30 minutes, followed by heat shock at 37°C for 5 minutes and plating on agar plates containing the appropriate antibiotic (100 ug/ml of ampicillin or 50 ug/ml of kanamycin). In case of transformation with a plasmid carrying kanamycin resistance, bacteria were grown in 1 ml of SOB (Super Optimal Broth) at 37°C for 1 hour with shaking before plating (Ravenhill et al., 2019).

2.7.5. Plasmid purification and verification

Colonies of transformed E. coli were grown in a 2 ml of LB medium, containing the appropriate antibiotic, at 37°C with shaking for 10 - 15 hours. QIAprep Spin Miniprep Kit (Qiagen) was used for plasmid purification according to the manufactirer's instructions. The appropriate DNA restriction enzymes were used for analysis of isolated plasmid DNA. The products of restriction digests (performed as describe above) were mixed with loading buffer (30% glycerol, 10 mM EDTA, 0.05% Orange G (Sigma) and resolved in 1% agarose (Biogene) gels, supplemented with SYBR Safe (Life Technology) for visualization of DNA, run at 90V for 30 – 40 minutes in TAE buffer (40 mM Tris (pH 7.6), 20 mM acetic acid, 1 mM EDTA). Plasmid constructs were verified by sequencing using GATC service (Ravenhill et al., 2019).

2.8. Eukaryotic cell culture and manipulation

2.8.1. Eukaryotic cell culture

Cells were grown in DMEM (Dulbecco's Modified Eagle Medium; Thermo Fisher) containing 10% SFB (Fetal Bovine Serum), in addition to antibiotics P/S

(penicillin 100 U/ml and streptomycin 100 mg/ml) at 37°C and 5% CO_2. RPTEC cells were growth in MEM-α (Minimum Essential Medium; Thermo Fisher) supplemented with RPTEC complete supplement (Sigma-Aldrich), P/S (penicillin 100 U/ml and streptomycin 100 mg/ml) and Glutamine 2mM at 37°C and 5% CO_2 (Oyanadel et al., 2018).

2.8.2. DNA transfection

HEK293ET cells were seeded in 6-well plated at $1x10^5$ cells per well in DMEM supplemented with 10% FBS (Fetal Bovine Serum). A transfection mix contained 0.15M NaCl, 500 ng of plasmid and 0.1 mg/ml of PEI (Polyethyleneimine, Polysciences) and was incubated for 10 minutes at room temperature before adding to the cells (Ravenhill et al., 2019).

2.8.3. Virus production

Retroviruses-containing supernatants were produced in HEK293ET cells following transfection with 500 ng of a proviral plasmid and plasmids encoding the viral capsid VSV-G (150 ng) and retroviral gag/pol (350 ng), using PEI as described above. The virus-containing supernatants were collected after 48 hours of incubation at 37°C, centrifugated at 8000 rpm for 3 minutes at room temperature and stored at -20°C if necessary (Ravenhill et al., 2019).

2.8.4. Viral transduction

MDCK or RPTEC cells expressing the required proteins were obtained by viral transduction. Viral supernatants, titrated in 500 ul of DMEM containing 10% FBS and 80 ug/ml of polybrene (hexadimethrine bromide; Sigma), were added to MDCK or RPTEC cells, seeded at $5x10^4$ cells per well in 24-well in 6 well plate 12-18 hours prior to transduction. The cells were centrifugated at 1800 rpm for 2 hours at 25°C. Cells transduced with the drug-resistant retroviruses were selected in DMEM medium containing 10 ug/ml of blasticidin S HCl 48 hours after transduction (Ravenhill et al., 2019).

2.9. Protein detection, interaction, and analysis

2.9.1. Sample preparation

To detect protein expression in cells, cells were lysed in lysis buffer (20 mM Tris-HCl (pH = 7.4), 150 mM NaCl, 10% glycerol, 1 mM EDTA, 0.5% Triton X-100) for 30 minutes at 4°C, followed by centrifugation at 14000 rpm for 10 minutes at 4°C. The supernatants were mixed with 4X loading buffer (40 mM Tris-HCl (pH = 6.8), 8% SDS, 40% glycerol, 100 mM DTT, 0.15% bromophenol blue) and incubated at 95°C for 5 minutes (Oyanadel et al., 2018).

2.9.2. SDS Polyacrylamide gel electrophoresis (SDS-PAGE)

NuPAGE 4-12% Bis-Tris pre-cast gels (Life Technologies) were used for SDS-PAGE of protein samples according to manufacturer's instructions. Gels were run in MES SDS Running buffer (Formedium) at 180 V for 1 hour. Precision Plus Protein prestained Standards (BioRad) were incubated to facilitate estimation of molecular weights of proteins in the subsequent applications. Gels were further processed for Coomassie Blue staining or Western blot (Ravenhill et al., 2019).

2.9.3. Coomassie blue staining

Gels were incubated in 15 – 20 ml of Instant Blue (Abcam), a Coomassie based staining solution, for 30 – 90 minutes to visualize proteins separated by SDS-PAG. Following the incubation, the gels were extensively washed in water until the background staining was removed.

2.9.4. Western blot

Western blot, also referred as protein immunoblot, was used for detection of specific proteins in samples. After the separation of proteins by SDS-PAGE, gels were blotted onto methanol-activated and pre-equilibrated Immobilon-P PVDF membranes (Milipore) for 1 hour at 30 V. Wet transfer method, during which the gels and the PVDF

membranes were sandwiched between sponge and filter paper, clamped together, and submerged in transfer buffer (Life Technologies), was used. Following the transfer, the membranes were blocked in 5% non-fat dried milk in TBST (100 mM Tris-HCl (pH 7.4), 150 mM NaCl, 0.1% Tween 20) for 1 hour at room temperature on orbital shaker. After the blocking the membranes were incubated with primary antibodies, diluted in 2% BSA in TBST, at 4°C overnight on orbital shaker. Then the membranes were washed three times with TBST for a total time of 45 minutes and incubated with the appropriate HRP-conjugated secondary antibodies, diluted in 5% non-fat dried milk in TBST, for 1 hour at room temperature on orbital shaker. Three washes with TBST for a total time of 45 minutes followed the incubation with secondary antibodies. The proteins were visualized using ECL (Enchanced Chemiluminescence) detection reagents (GE Healthcare) according to manufacturer's instructions. Following a 1-minute incubation with the ECL mix the membranes were placed into an iBright 1500 (Invitrogen) (Oyanadel et al., 2018).

2.9.5. Protein expression in bacteria

pETM30 vector was used for expression of proteins, fused to His-GST in *E. coli* strain BL21. Following transfection with plasmid constructs encoding proteins of interest (as describe above), bacteria were grown in 2 ml of kanamycin-containing 2x YT medium overnight at 37°C shaking at 200 rpm. Then bacterial cultures were diluted 1:1000 of kanamycin-containing 2x YT medium, grown for 3 – 3.5 hours at 37°C shaking at 200 rpm until the cultures reached an OD_{600} of 0.6-0.8 and supplemented with 0.1 mM IPTG (Isopropyl β-D-1thiogalactopyranoside). Bacteria were incubated with IPTG for 12-16 hours at 16°C shaking at 200 rpm before harvesting by centrifugation at 4200 rpm for 30 minutes at 4°C. The pellet was frozen at first at liquid nitrogen, and then stored at -80°C (Ravenhill et al., 2019).

2.9.6. Protein purification

The pellets of the point 2.9.5. were resuspended in 25 ml of bacteria lysis buffer (20 mM Tris-HCl (pH 7.4), 150 mM NaCl, 1 mM DTT, 1 tablet of complete EDTA-free Protease inhibitor cocktail (Roche) per 50 ml, 20 ug/ml DNaseI (Sigma) for 60 minutes

at 4°C in a beaker with a magnetic stirrer. Once thoroughly resuspended was filter with a cell strainer 70 uM (Falcon). The bacteria were lysis using EmulsiFlex C3 (Avestin). Bacteria lysates were centrifuged at 20000 rpm for 30 minutes at 4°C, and the supernatants (cleared lysate) were added to a column of GST-Sepharose (GE Healthcare) for 2 hours at 4°C shaking. The GST-Sepharose was collected and centrifugated 3 minutes at 2000 rpm. The supernatant was washed with glutathione buffer (20 mM Tris-HCl (pH 7.4), 150 mM NaCl, 1 mM DTT, 20 mM Glutathione (pH 8.0)) three time for 20-40 minutes at RT, and then incubated with TEV protease (1%) O/N at 4°C shaking. The protein was incubated in a binding resin Ni-NTA magnetic agarose beads in 10mM of Imidazole for 2 hours at 4°C shaking. Then centrifugated for 3 minutes at 2000 rpm. Protein expression was confirmed by SDS-PAGE followed by Coomassie Blue staining (Figure 2) (Ravenhill et al., 2019).

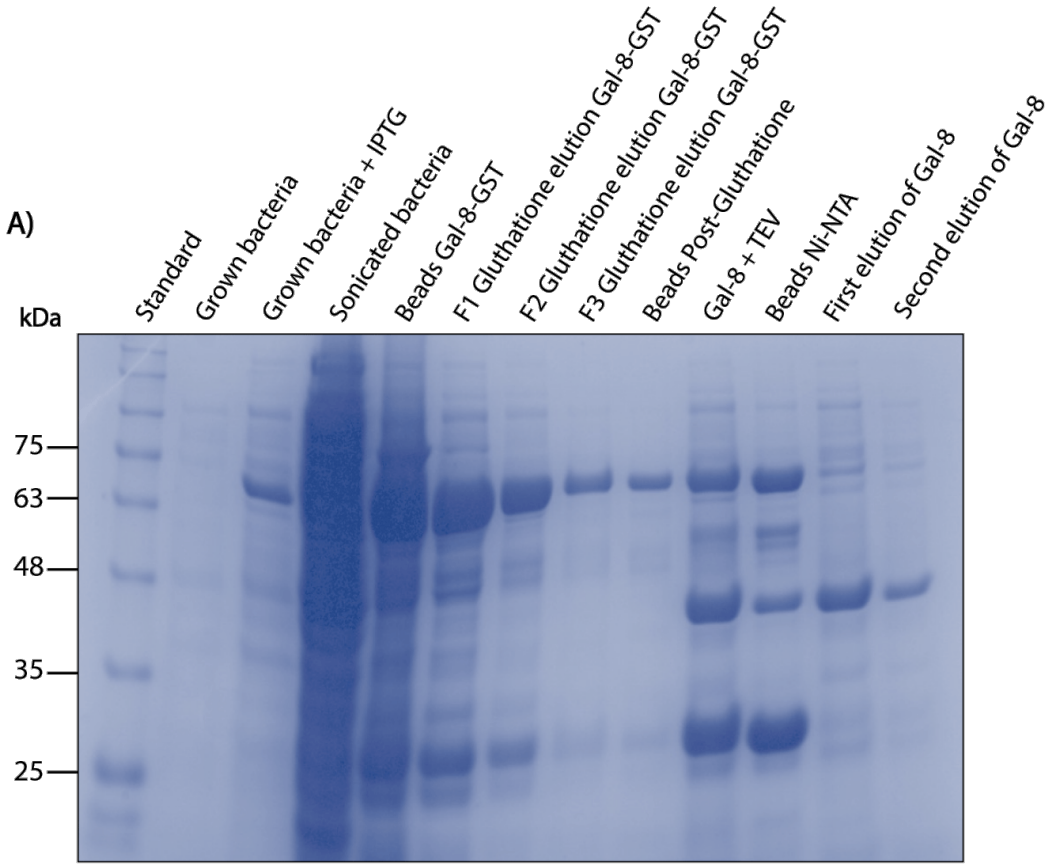

Figure 2. Purification of Galectins.

pETM30 vector was used for expression of proteins, fused to His-GST in *E. coli* strain BL21. The lysates bacteria were added to a Glutathione-Superflow Resin columns, and then incubated with TEV protease. The supernatant was incubated with resin Ni-NTA magnetic agarose beads to remove the TEV protease and the GST-Sepharose. Then, the resulting purification fractions were analyzed by SDS-PAGE. A) A purification example of Gal-8.

2.9.7. Immunofluorescence microscopy

Cells grown on glass coverslips were fixed using 4% paraformaldehyde (in PBS) for 30 minutes at room temperature, washed four time with PBS. For mitochondria staining, prior to cell fixation, cells were treated with MitoTracker CMTMRos (500 ng) for 30 minutes and then fixed. Then, the covers were washed with distillated water with Hoechst for stain the nucleus. The coverslips were mounted on glass slides using ProLong Gold or FluoromonG antifade reagent and let dry for 24 hours before analysis on the microscope (Oyanadel et al., 2018; Ravenhill et al., 2019). Two types of microscopes were used:

1. Confocal microscopy SP8 was used to analyze the fission and distribution patterns of the mitochondria and for live cell imaging where cells were placed in the plate of the microscope in an environment at 37°C with 5% CO_2. This equipment was used in collaboration with Dr. Claudio Retamal (CEBICEM) and at the MRC Laboratory of Molecular Biology in collaboration with Dr. Felix Randow. For each image the scale bar = 10µm.

2. Super-resolution microscopy (Structured Illumination Microscopy - SIM) was used to analyze the proximity between mitochondria and the nucleus. This equipment was used in collaboration with Dr. Felix Randow at the MRC Laboratory of Molecular Biology in Cambridge. For each image the scale bar = 10µm.

2.10. Proliferation assay

2.10.1. Crystal violet assay

$1x10^5$ MDCK cells were seeded triplicate for each condition. The next day, the medium was replaced with a medium without serum, and the cells were treatment with Gal-8, Gal-8-R69H, Gal-8-R275H or Gal-8-R69H-R275H (50 µg/ml) for 72 hours. Colonies were fixed using PFA 4%, followed by staining with crystal violet, washing, air-drying, and pictures were taken in a phase contrast microscopy at 40–400X magnification. After acquiring the images, the stained cells are lysed with 100 µL of a

solution of 0.1 M Na_2HPO_4 pH 7.4 and 50% ethanol, incubating for 10 min. And it is measured in an Elisa reader at an absorbance of 570 nm (Oyanadel et al., 2018).

2.10.2. Trypan blue cell counting

$1x10^5$ MDCK cells were plated in triplicate for each condition. The next day the medium was replaced with a medium without serum, and the cells were treatment with Gal-8, Gal-8 R69H, Gal-8-R275H or Gal-8-R69H-R275H (50 µg/ml) for 72 hours. Next, the number of cells were counted using Trypan blue and an Automated Cell Counters (Oyanadel et al., 2018).

2.11. Seahorse XFp assay

Live cell analyses of oxygen consumption rate (OCR) and extracellular acidification rate (ECAR) were measured with the Seahorse XFp system (Agilent) in collaboration with MRC Laboratory of Molecular Biology with Dr. Harvey McMahon.

Cell characterization was performed on MDCK cells according to the manufacturer's protocol. Cells were plated at 20.000 cells per well and allowed to seed 6 hours, then the cells were treatment with vehicle or Gal-8 (50 µg/ml) 24 hours in a cell culture incubator at 37°C with an XFp cartridge hydrating overnight in a nonCO_2 incubator at 37°C. On the day of the analysis, assay media provided by Agilent was prepared similar to culture media (25 mM glucose, 1 mM sodium pyruvate, and 4 mM L-glutamine) and pH was adjusted to 7.4. The XFp miniplate was washed one with the medium and a final volume of 180 ml assay media was added to cells. Then, the XFp miniplate was allowed to equilibrate in a nonCO2 incubator at 37°C for 60 min prior to assay initiation. XFp cartridge loaded as follows for cell mito stress test assay: Port A on the XFp cartridge was designated for treatment containing oligomycin (ATP-Synthase inhibitor) at 100 µM, port B with 100 µM FCCP (mitochondrial membrane depolarizer), and port C with a mixture of 50 µM of each rotenone (complex I inhibitor) and antimycin A (complex III inhibitor) (stock concentration). Furthermore, XFp cartridge loaded as follows for ATP real-time rate assay: oligomycin (ATP- Synthase inhibitor) at 150 µM, port B with a mixture of 50 µM of each rotenone (complex I inhibitor) and antimycin A (complex III inhibitor) (stock well concentration). Aside from

a normalized plating protocol, each run is normalized to control basal ECAR or OCR to account for between-run variation (Anderson et al., 2018). Figures represent parameters calculated using normalized percentage values. All calculations were made within each individual well. n=3 independent experiments, with 3 replicates each.

2.12. Transmission electron microscopy

To evaluate mitochondrial ultrastructure, pellets of 8×10^5 of RPTEC cells treated with or without Gal-8 were fixed with glutaraldehyde 2.5%. Images of ultra-thin sections were acquired in a transmission electron microscope TALOS F200C G2 system (Thermo Scientific), equipped with a Ceta 16M CMOS camera at 200kV, at the Advanced Microscopy Facility UMA-UC, Pontificia Universidad Católica de Chile.

2.13. Software analysis

Huygens software was used to process and deconvolute the images obtained in confocal and super-resolution microscopy and quantify the number, length, surface area, and distance between objects. The training in software analysis was in collaboration with Dr. Claudio Retamal at the CEBICEM and with Dr. Jerome Boulanger at the MRC Laboratory of Molecular Biology. ImageJ was used to measure immunoblots. All data analysis was performed in GraphPad Prism 8. Results were plotted with mean ± standard deviation (SD). Statistical significance of data comparison was performed depending on each experiment: to compared between two samples T Student or to compared more than two samples ANOVA with a posterior Tukey to define the difference between each sample. The values of $P<0.05$ (*), $P<0.01$ (**), $P<0.001$ (***) were considered statistically significant and are indicated in each figure, when there was no statistical difference, they were indicated as ns (Not significant).

III. RESULTS

3.1. Gal-8 induces mitochondrial fragmentation and redistribution of mitochondria to the perinuclear zone.

Various stimuli have been observed to impact mitochondrial dynamics, influencing cellular functions such as proliferation or differentiation. Although several studies have shown that galectins can modify various cellular functions both intracellularly and extracellularly, it has not yet been detailed how they affect mitochondrial dynamics and metabolism at the extracellular level.

To investigate whether Gal-8 induces mitochondrial fragmentation, MDCK cells were exposed to 50 µg/ml of Gal-8 for 24 hours, or to CCCP, a protonophore and chemical inhibitor of oxidative phosphorylation (Kotova & Antonenko, 2022). Then the mitochondria were labeled with MitoTracker CMTMRos. The images were captured using a confocal microscope in Z-stack to make a surface rendering 3D reconstruction of mitochondria using Huygens software, which allows the analysis of the length and the surface of mitochondria (Figure 3A). Our findings show that Gal-8 triggers a decrease in both length and surface area, similar to CCCP, a well-known inducer of mitochondrial fragmentation (Figure 3B). In addition, treatment with Gal-8 and CCCP leads to an increase in the number of mitochondria, as shown in Figure 3C.

To investigate whether Gal-8 induces mitochondrial fragmentation in other epithelial cells a similar analysis was done in epithelial Chinese Hamster Ovary cells - CHO cells (Figure 4A) and Human Renal Proximal Tubule Epithelial Cells - RPTEC cells (Figure 4B). Similar results were obtained in length and surface, showing that Gal-8 promotes mitochondrial fragmentation (Figure 4C). Also, Gal-8 treatment increases the number of mitochondria in CHO and RPTEC cells (Figure 4E). Moreover, electron microscopy was performed to evaluate mitochondrial integrity in RPTEC cells treated with or without Gal-8 (Figure 4F). The image shows that the mitochondria have intact mitochondrial cristae in both cases, as indicated by the yellow arrows.

Additionally, MDCK cells were treated with Galectin-1, -2, -3, -4, -7, -8 or -10 (50 µg/ml) for 24 hours to determine if any of them could lead to mitochondrial fragmentation (Figure 5A). After 24 hours of treatment, only Gal-4 and Gal-8 reduce

the length and surface area of mitochondria in MDCK cells, while other galectins (-1, -2, -3, -7, and -10) do not have this effect (Figure 5B).

These results indicate that Gal-4 and Gal-8 can promote mitochondrial fragmentation in epithelial cells after 24 hours of treatment.

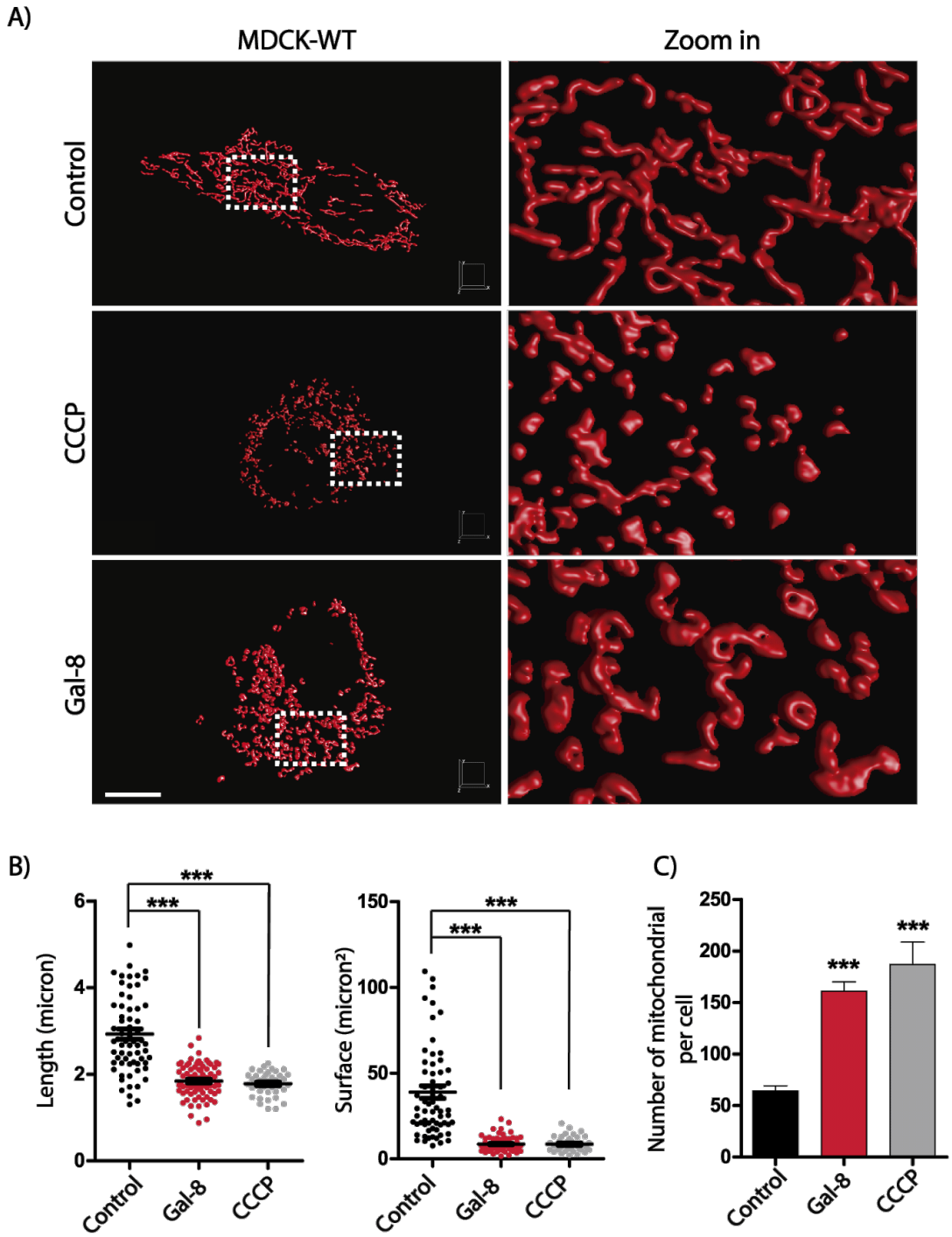

Figure 3. Gal-8 induces mitochondrial fragmentation in MDCK cells.

MDCK cells were treated with Gal-8 (50 µg/ml) or CCCP (10 µM) for 24 hours. Mitochondria were labeled with MitoTracker CMTMRos. A) The images were captured using a confocal microscope in Z-stack to make a surface rendering 3D reconstruction of mitochondria using Huygens software, which allows the analysis of the length and the surface of mitochondria. B) Graphs showing the length and surface of mitochondria quantified by Huygens Software. C) Graph shows the number of mitochondria quantified by Huygens Software (Means ± s.d., n=3, 25 cells per experiment, One-Way ANOVA with a posterior Tukey, ***p<0.001). Scale bar = 10µm.

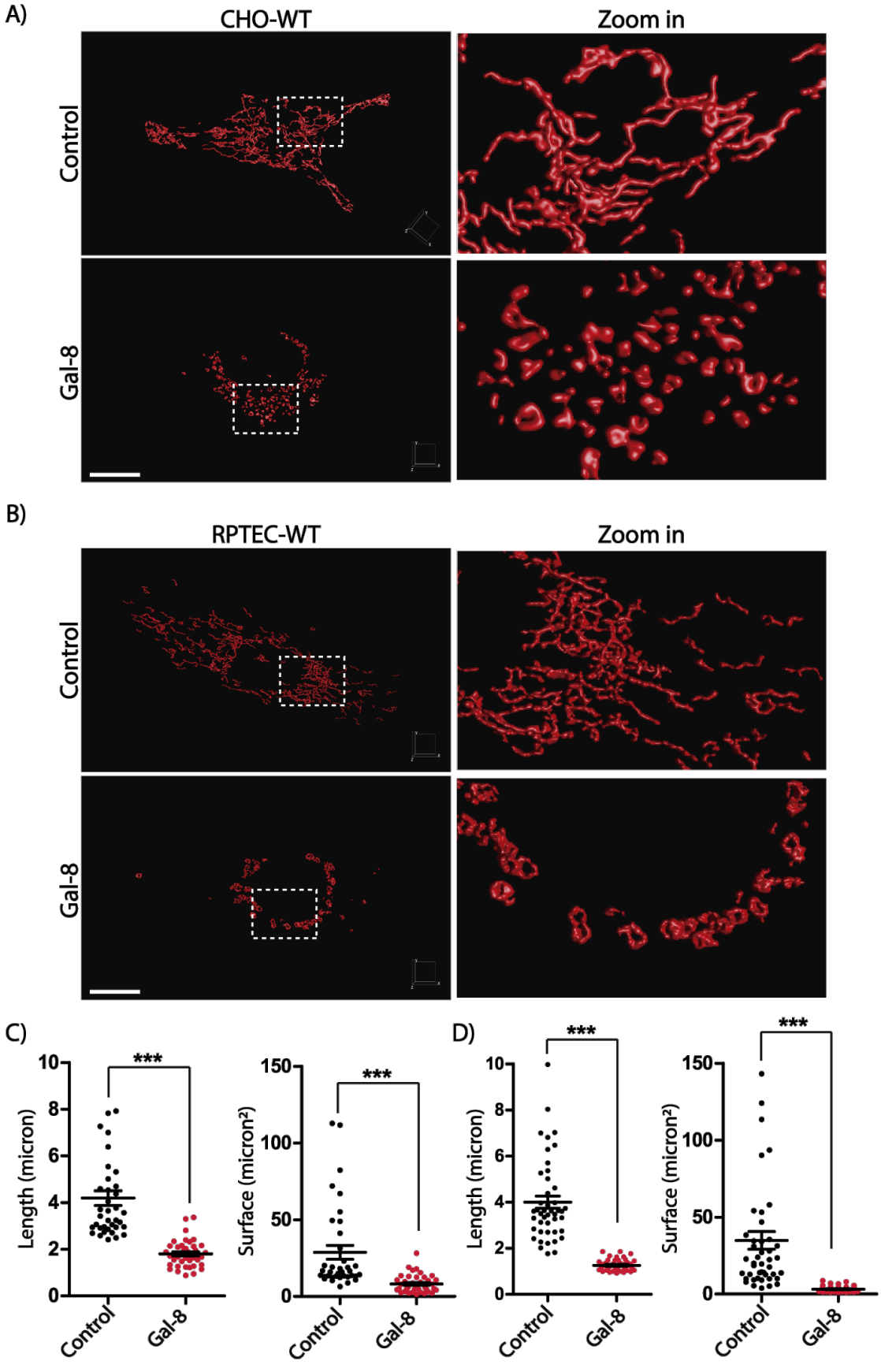
A)
CHO-WT
Zoom in
Control
Gal-8
B)
RPTEC-WT
Zoom in
Control
Gal-8
C)
D)
Length (micron)
Surface (micron²)
***
Control
Gal-8

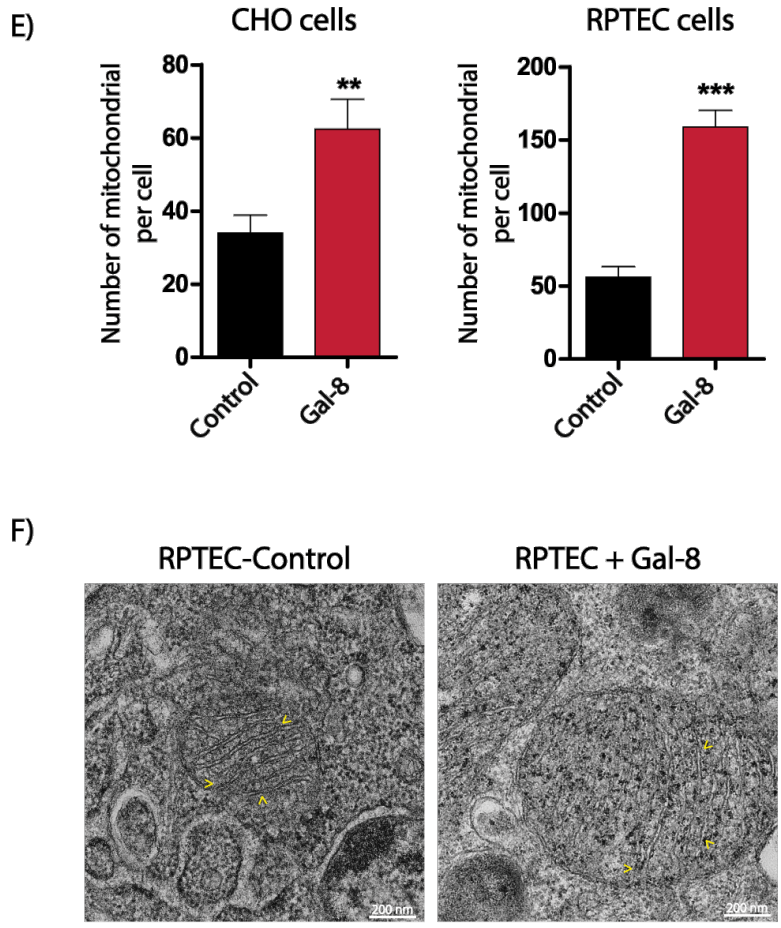

Figure 4. Gal-8 induces mitochondrial fragmentation in CHO and RPTEC cells. 3D Confocal microscopy showing MitoTracker CMTMRos stained mitochondria. Huygens Software rendering of mitochondria of CHO A) and RPTEC B) cells that were treated with Gal-8 (50 µg/ml) for 24h. Graphs showing the length and surface of mitochondria of CHO C) and RPTEC D) cells quantified by Huygens Software. E) Graphs show the number of mitochondria from CHO and RPTEC cells quantified by Huygens Software. F) Electron microscopy of RPTEC cells (Means ± s.d., n=3, 15 cells per experiment, T Student, **p < 0.01, ***p<0.001). Scale bar = 10µm.

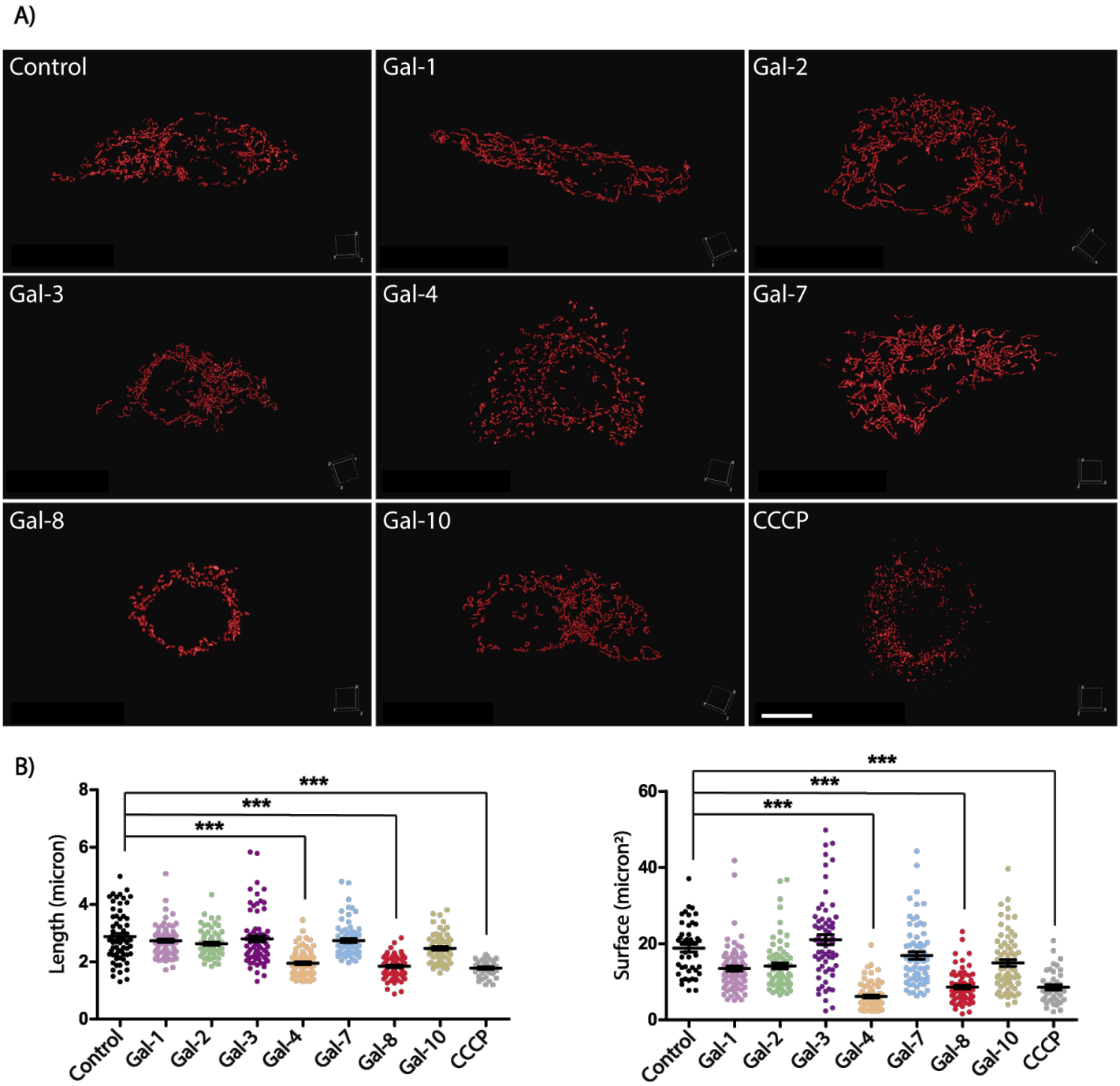

Figure 5. Gal-4 induces mitochondrial fragmentation similar to Gal-8.

MDCK cells were treated with Gal-1, -2, -3, -4, -7, -8 or -10 (50 µg/ml) for 24 hours or CCCP (10 µM). Mitochondria were labeled with MitoTracker CMTMRos. A) The images were captured using a confocal microscope in Z-stack to make a surface rendering 3D reconstruction of mitochondria using Huygens software, which allows the analysis of the length and the surface of mitochondria. B) Graphs showing the length and surface of mitochondria quantified by Huygens Software. (Means ± s.d., n=3, 25 cells per experiment, One-Way ANOVA with a posterior Tukey, ***p<0.001). Scale bar = 10µm.

To evaluate the distribution pattern of mitochondria, MDCK, CHO and RPTEC epithelial cells were treated with Gal-8 (50 µg/ml), or CCCP (10 µM) for 24 hours. Mitochondria were then labeled with MitoTracker CMTMRos, and the nucleus with Hoechst. The images were captured in confocal microscopy in Z-Stack and were reconstructed using Huygens Software (Figure 6A, C, E). The distribution of mitochondria throughout the cell was measured using Huygens software. To do this, the nuclei were delimited and the distance from the limit of the nucleus to the surface of each mitochondria was measured. Data are shown as the frequency distribution of mitochondria at distance to the nucleus per µm (Figure 6B left panel). Otherwise, to measure the perinuclear distribution of mitochondria, the mitochondria surrounding the nucleus were delimited within a radius of 5 µm (Figure 6B right panel). MDCK (Figure 6B), CHO (Figure 6D) and RPTEC (Figure 6F) cells exhibit a relocation of mitochondria towards the perinuclear zone after being treated with Gal-8 (50 µg/ml) for 24 hours. Otherwise, when MDCK cells were exposed to Gal-1, -2, -3, -4, -7 or -10 (50 µg/ml) for 24 hours, there were no changes observed in the distribution pattern of mitochondria (Figure 7A-B).

These results indicate that only Gal-8, among other galectins, induces changes in the distribution pattern of mitochondria towards the perinuclear zone.

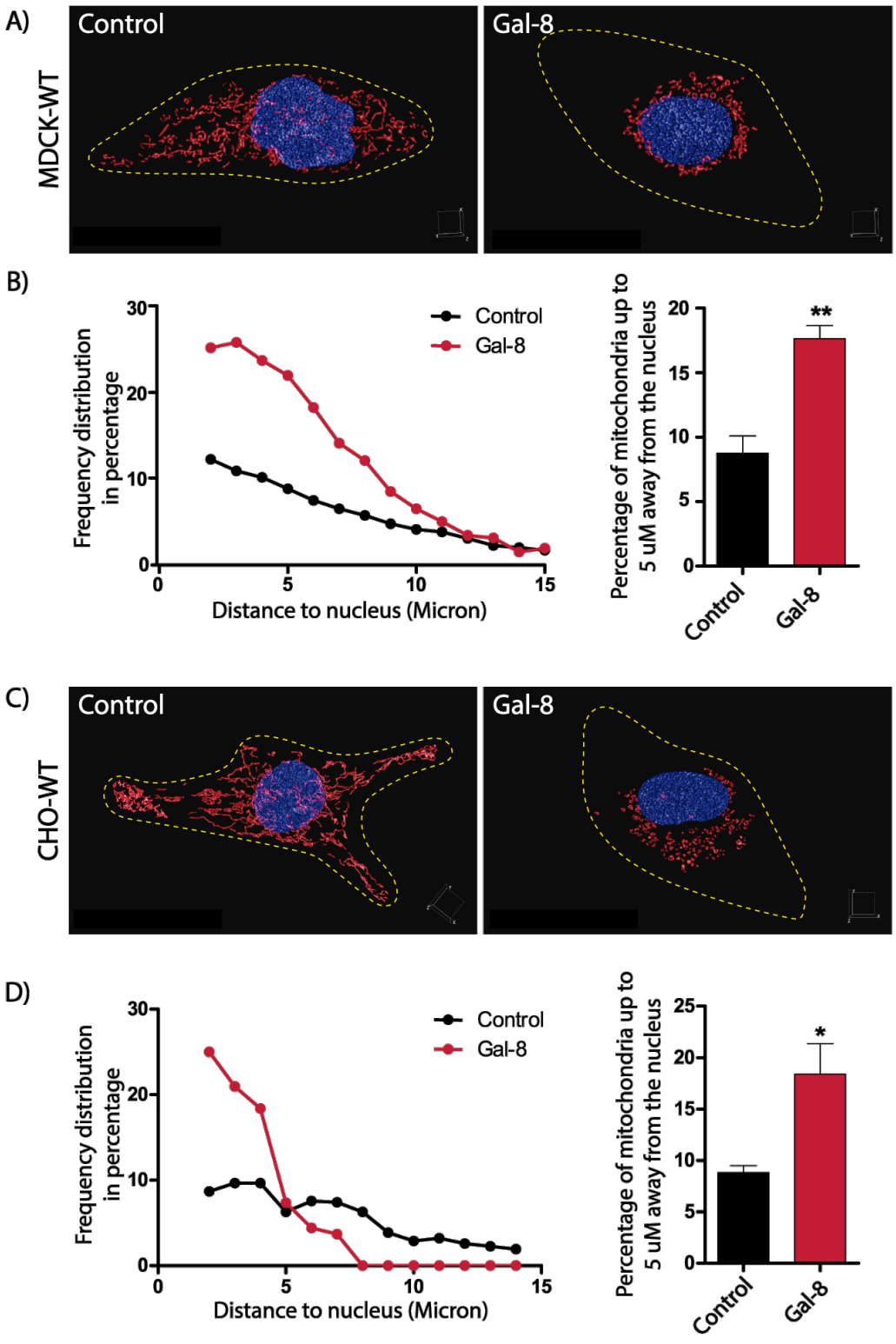
A)
MDCK-WT
Control
Gal-8
B)
Frequency distribution in percentage
Distance to nucleus (Micron)
Control
Gal-8
Percentage of mitochondria up to 5 uM away from the nucleus
**
C)
CHO-WT
Control
Gal-8
D)
Frequency distribution in percentage
Distance to nucleus (Micron)
Control
Gal-8
Percentage of mitochondria up to 5 uM away from the nucleus
*

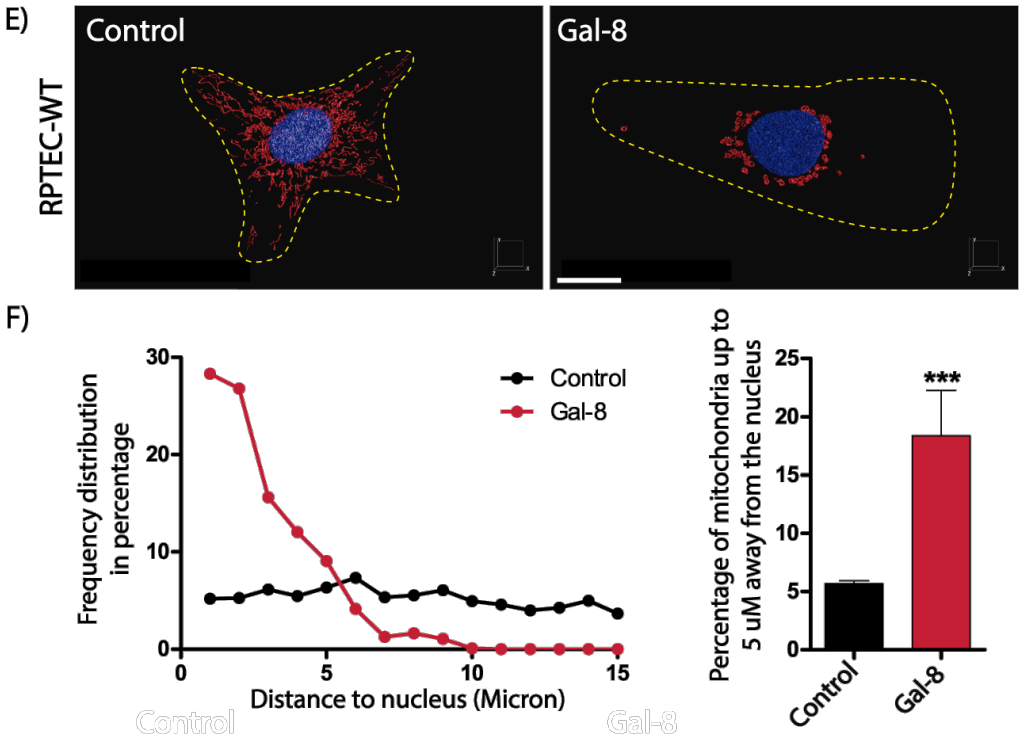

Figure 6. Gal-8 induces redistribution of the mitochondria to the perinuclear zone in epithelial cells.

MDCK A), CHO C) and RPTEC E) cells were treated with Gal-8 (50 µg/ml) for 24 hours. Mitochondria were labeled with MitoTracker CMTMRos, and the nucleus with Hoechst. The images were captured using a confocal microscope in Z-stack to make a surface rendering 3D reconstruction of mitochondria using Huygens software, which allows the analysis of the distribution of mitochondria. Frequency distribution of the distance of mitochondria to the nucleus in MDCK B), CHO D) and RPTEC F) cells quantified by Huygens Software (Means ± s.d., n=3, 15 cells per experiment, T Student, *p<0.05, **p < 0.01, ***p<0.001). Scale bar = 10µm.

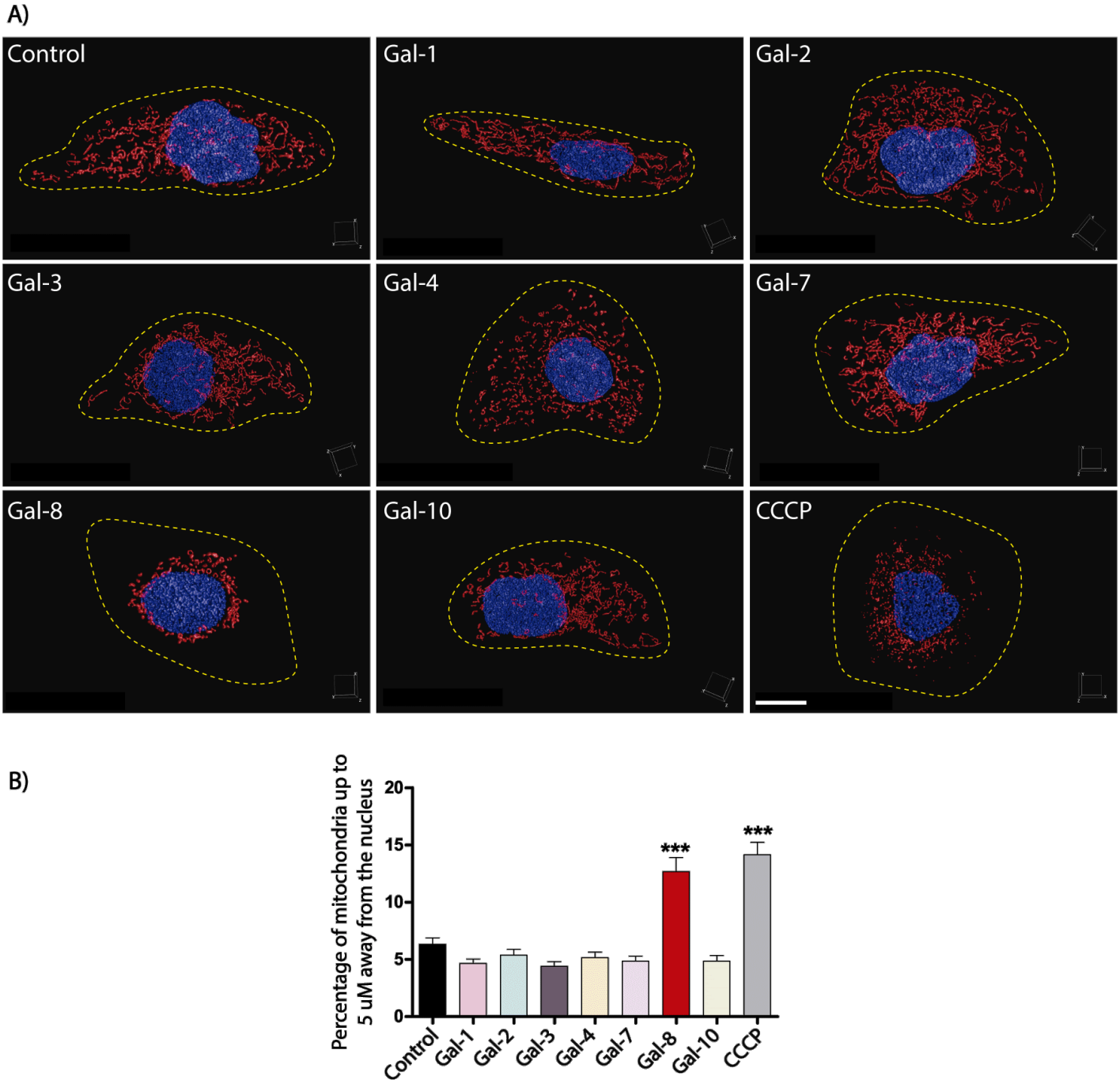

Figure 7. Redistribution of mitochondria to the perinuclear zone is only induced by Gal-8 in MDCK cells.

MDCK cells were treated with Gal-1, -2, -3, -4, -7, -8 or -10 (50 µg/ml) for 24 hours or CCCP (10 µM). Mitochondria were labeled with MitoTracker CMTMRos, and the nucleus with Hoechst. A) The images were captured using a confocal microscope in Z-stack to make a surface rendering 3D reconstruction of mitochondria using Huygens software, which allows the analysis of the distribution of mitochondria. B) Frequency distribution of the distance of mitochondria to the nucleus quantified by Huygens Software (Means ± s.d., n=3, 25 cells per experiment, One-Way ANOVA with a posterior Tukey, ***p<0.001). Scale bar = 10µm.

Otherwise, to analyze the kinetic of the fragmentation and distribution of mitochondria driven by Gal-8, MDCK cells were treated with Gal-8 (50 µg/ml) for 15 minutes or 4 hours and labeled with MitoTracker CMTMRos, and the nucleus with Hoechst (Figure 8). Then, the images were captured in a confocal microscope in a Z-stack and reconstructed using Huygens Software (Figure 8A). MDCK cells treated with Gal-8 for 15 minutes showed a fragmentation of mitochondria, although there are no changes in the distribution patterns of mitochondria (Figure 8B-C). Furthermore, MDCK cells treated with Gal-8 for 4 hours did not show fragmentation or changes in the distribution patterns of mitochondria (Figure 8B-C).

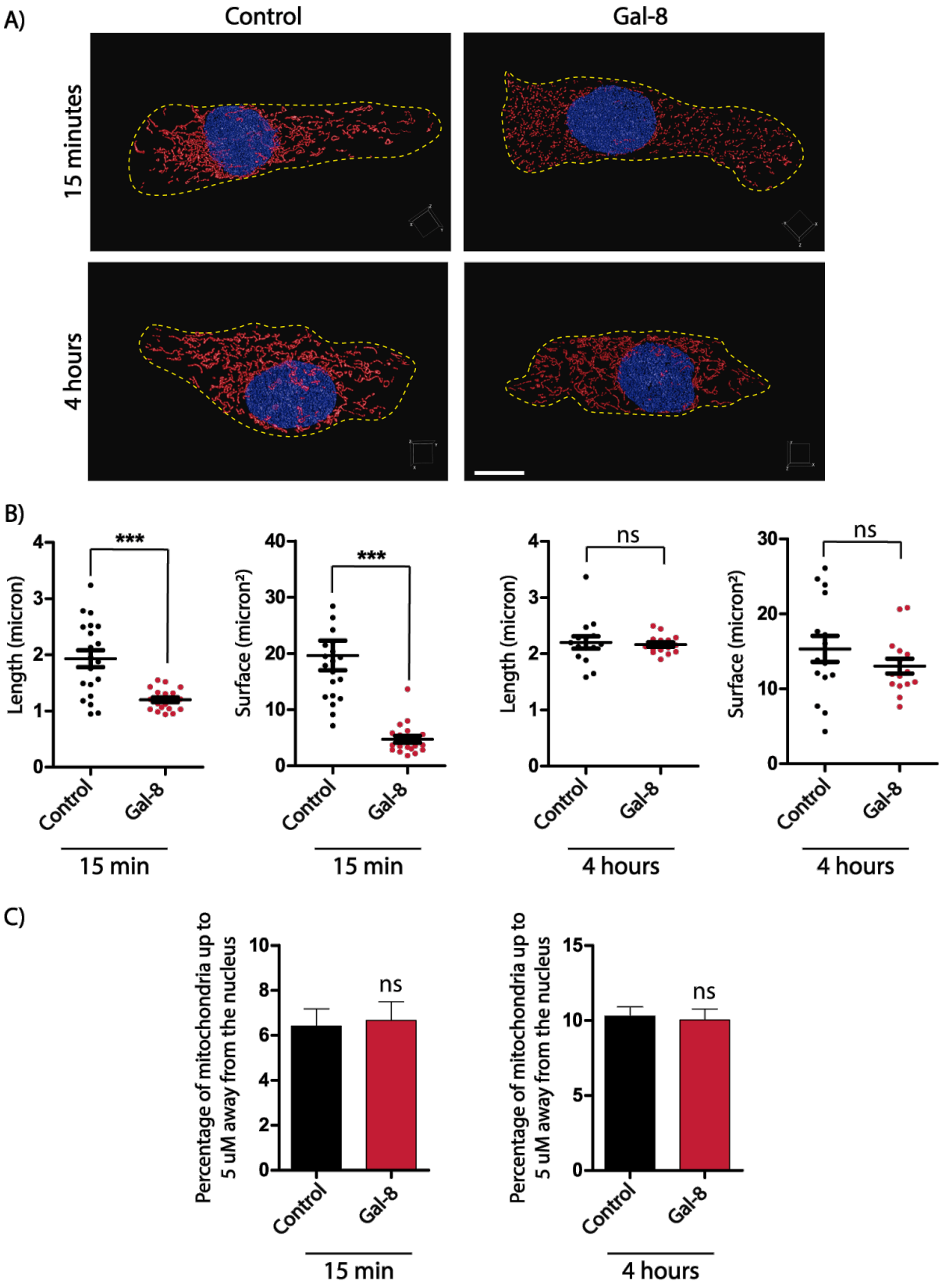
A)
Control
Gal-8
15 minutes
4 hours
B)
Length (micron)
***
Control
Gal-8
15 min
Surface (micron²)
***
Control
Gal-8
15 min
Length (micron)
ns
Control
Gal-8
4 hours
Surface (micron²)
ns
Control
Gal-8
4 hours
C)
Percentage of mitochondria up to 5 uM away from the nucleus
ns
Control
Gal-8
15 min
Percentage of mitochondria up to 5 uM away from the nucleus
ns
Control
Gal-8
4 hours

Figure 8. Kinetics of fragmentation and distribution of mitochondria.

MDCK cells were treated with Gal-8 (50 µg/ml) for 15 minutes or 4 hours. Mitochondria were labeled with MitoTracker CMTMRos and Hoechst. A) The images were captured using a confocal microscope in Z-stack to make a surface rendering 3D reconstruction of mitochondria using Huygens software. B) Graphs showing the length and surface of mitochondria quantified by Huygens Software. C) Frequency distribution of the distance of mitochondria to the nucleus quantified by Huygens Software (Means ± s.d., n=3, 5 cells per experiment, T Student, ***$p<0.001$). Scale bar = 10µm.

3.2. Gal-8 promotes mitochondrial fragmentation and redistribution of mitochondria to the perinuclear zone involving carbohydrate recognition.

Gal-8 is a tandem repeat galectin, with its N-terminal CRD exhibiting a strong preference affinity for sialylated β-galactosides, particularly sialylated glycans at the α-2,3 position, providing Gal-8 with unique functional properties. On the other hand, the C-terminal CRD displays an affinity for non-sialylated oligosaccharides (Elola et al., 2014). Carbohydrate binding mutations, including Gal-8-R69H and Gal-8-R275H, have been documented in the literature (Hirabayashi et al., 2002). In particular, full-length Gal-8 lacking the carbohydrate-binding activity of N-terminal CRD (Gal-8-R69H) hinders the interaction with sialylated β-galactosides, while inactivation of the C-terminal domain (Gal-8-R275H) interferes with the interaction with polylactosamines galactosides (Hirabayashi et al., 2002).

To investigate whether the interaction between Gal-8 and carbohydrates is responsible for the mitochondrial fragmentation and redistribution in epithelial cells, Gal-8-R69H or Gal-8-R275H, or double mutated Gal-8-R69H- R275H were used. First, the binding affinity of each mutant was tested using the mutant proteins fused to GST. MDCK cells were treated with 50 µg/ml of each galectin for 30 minutes. Afterwards, the cells were labeled with a fluorescent antibody against GST and the binding of each galectin to the cell was measured by flow cytometry (Figure 9A). As expected, the recombinant Gal-8 with mutations in the CRD showed less affinity to the cell surface than the wild-type recombinant Gal-8.

Then, to explore if the carbohydrate recognition of Gal-8 is necessary to trigger mitochondrial fragmentation and change the distribution patterns of mitochondria, MDCK cells were treated with 50 µg/ml of Gal-8, Gal-8-R69H, Gal-8-R275H, Gal-8-R69H-R275H or CCCP for 24 hours. After this time, mitochondria were labeled with the MitoTracker CMTMRos to analyze the cells by confocal microscopy (Figure 9B). Mitochondria fragmentation analyzed by length and surface (Figure 9C) and perinuclear distribution (Figure 9D) were not observed in MDCK cells treated with Gal-8-R69H or the double Gal-8-R69H-R275H mutants. In contrast, MDCK cells treated with the Gal-8-R275H mutant show a similar effect as Gal-8 (Figure 9C-D).

These results indicate that Gal-8 promotes mitochondrial fragmentation and perinuclear distribution through its N-terminal domain, which interacts with sialylated glycans in α-2,3 position.

Furthermore, CHO cells were used to analyze the contribution of glycoconjugates on the cell surface. CHO-LEC3.2.8.1 cells are Chinese hamster ovary cells that have N-glycosylation deficiency but conserve the ability to synthesize O-glycoproteins (Stanley, 1989). CHO and CHO-LEC3.2.8.1 cells were treated with 50 µg/ml of Gal-8 for 24 hours, and then mitochondria were labeled with MitoTracker CMTMRos to analyze the cells by confocal microscopy (Figure 10). In the control condition, CHO cells display a tubular and homogenous distribution of mitochondria; nevertheless, CHO-LEC3.8.2.1 shows more fragmented mitochondria without change in the distribution patterns of mitochondria (Figure 10B-C). When the cells were treated with 50 µg/ml of Gal-8, CHO cells displayed more fragmented mitochondria with a perinuclear distribution of mitochondria. However, CHO-LEC3.8.2.1 did not trigger a perinuclear distribution of mitochondria, and mitochondria are fragmented per se (Figure 10B-C).

Furthermore, to determine the contribution of glycoconjugates on the cell surface, CHO (Figure 11) and CHO-LEC3.2.8.1 (Figure 12) cells were treated with 50 µg/ml of Gal-8, Gal-8-R69H, or Gal-8-R275H for 24 hours, and then mitochondria were labeled with MitoTracker CMTMRos to analyze the cells by confocal microscopy. Gal-8 and Gal8-R275H mutant, but not Gal8-R69H mutant, induces mitochondrial fragmentation and redistribution of mitochondria to the perinuclear zone in CHO cells (Figure 11B-C). In contrast, in CHO-LEC3.2.8.1 cells, none of the treatments with Gal-8 or mutants affected mitochondrial fragmentation or changes in the distribution patterns of mitochondria (Figure 12B-C).

These findings suggest that Gal-8 induces the fragmentation of mitochondria and their subsequent redistribution to the perinuclear zone by recognizing N-glycoproteins that contain α-2-3 sialylated β-galactosides.

A)

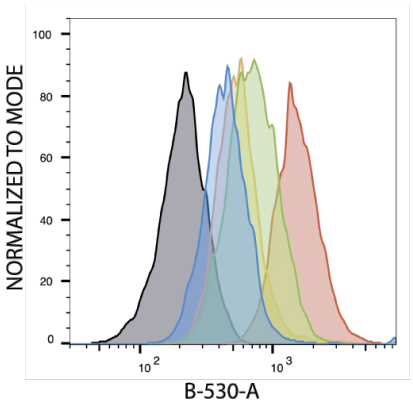

	Sample name
	GST-Control
	GST-Gal-8
	GST-Gal-8-R69H
	GST-Gal-8-R275H
	GST-Gal-8-R69H-R275H

B)

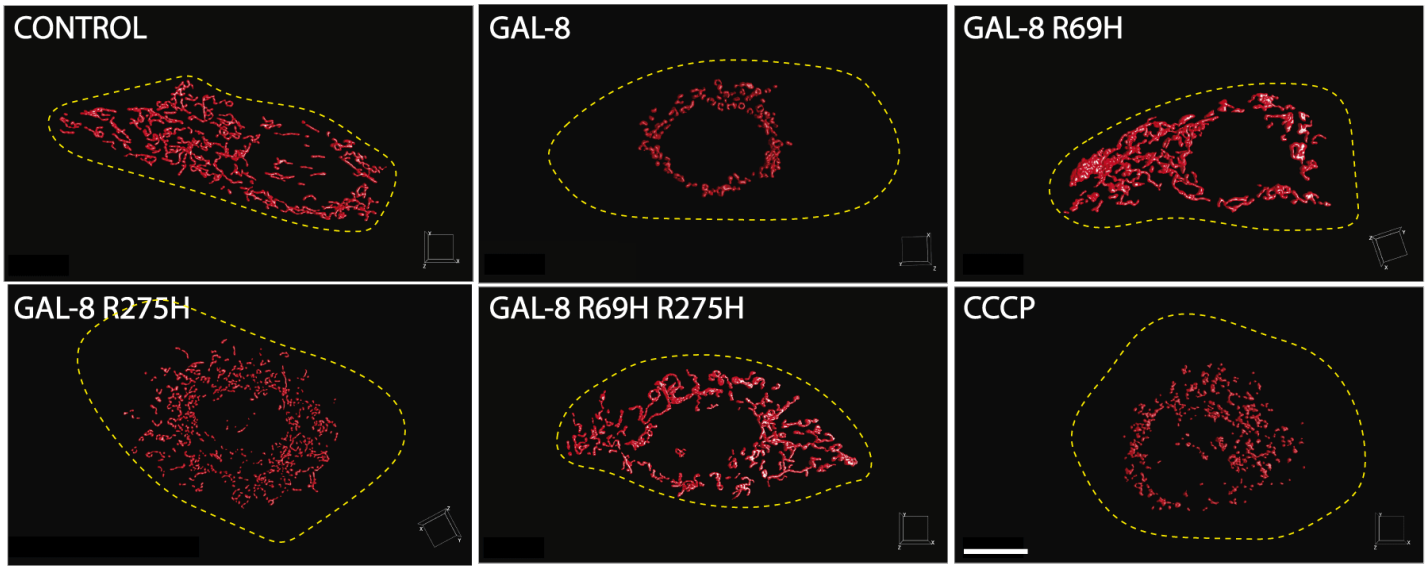

C)

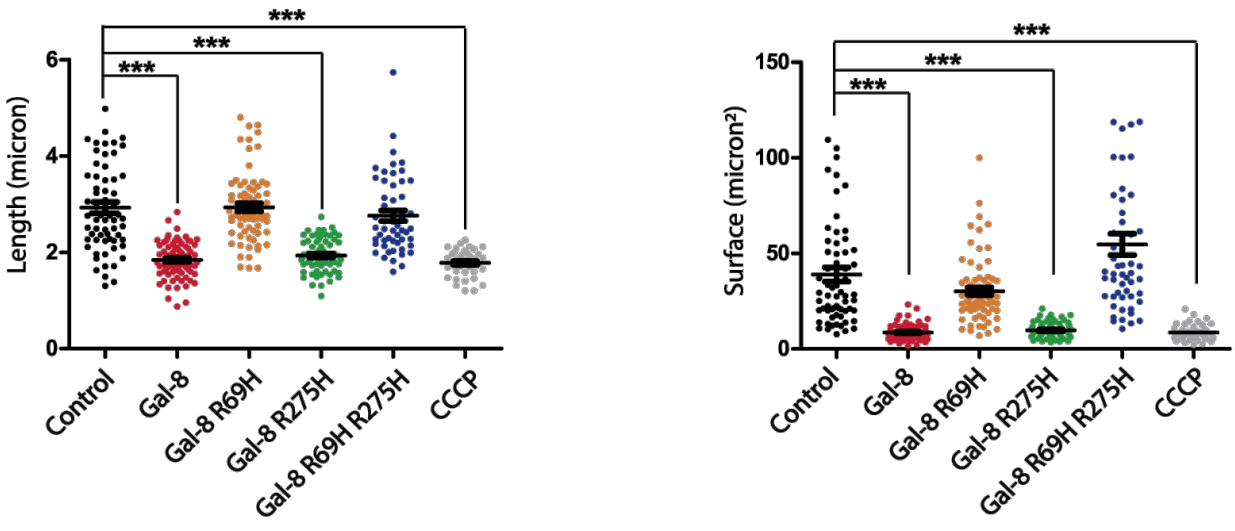

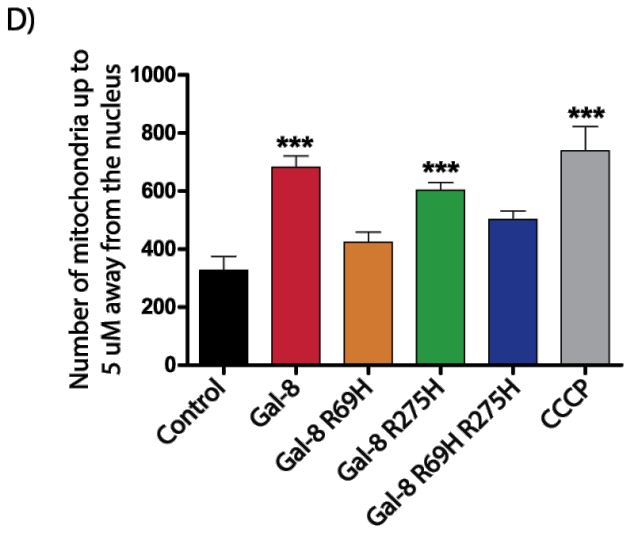

Figure 9. Gal-8 induces mitochondrial fragmentation and redistribution of mitochondria in a carbohydrate-dependent manner in MDCK cells.

Three Gal-8 mutants with mutations in the sugar-binding domain were tested: Gal-8-R69H, Gal-8-R275H, and Gal-8-R69H-R275H, which had a double mutation. A) The binding of each mutant to MDCK cells was measured by flow cytometry, using the Gal-8 mutants fused to GST. B) MDCK cells were treated with the Gal-8, Gal-8-R69H, Gal-8-R275H, Gal-8-R69H-R275H (50 µg/ml), or CCCP (10 µM) for 24 hours. Mitochondria were labeled with MitoTracker CMTMRos. Images were captured using a Z-stack confocal microscope to perform a 3D reconstruction of the surface of mitochondria using Huygens software, which allows analysis of mitochondrial length, surface area, and distribution. C) Graphs showing mitochondrial length and surface quantification. D) Frequency distribution of the distance of mitochondria to the nucleus (Means ± s.d., n=3, 25 cells per experiment, One-Way ANOVA with a posterior Tukey, ***$p<0.001$). Scale bar = 10µm.

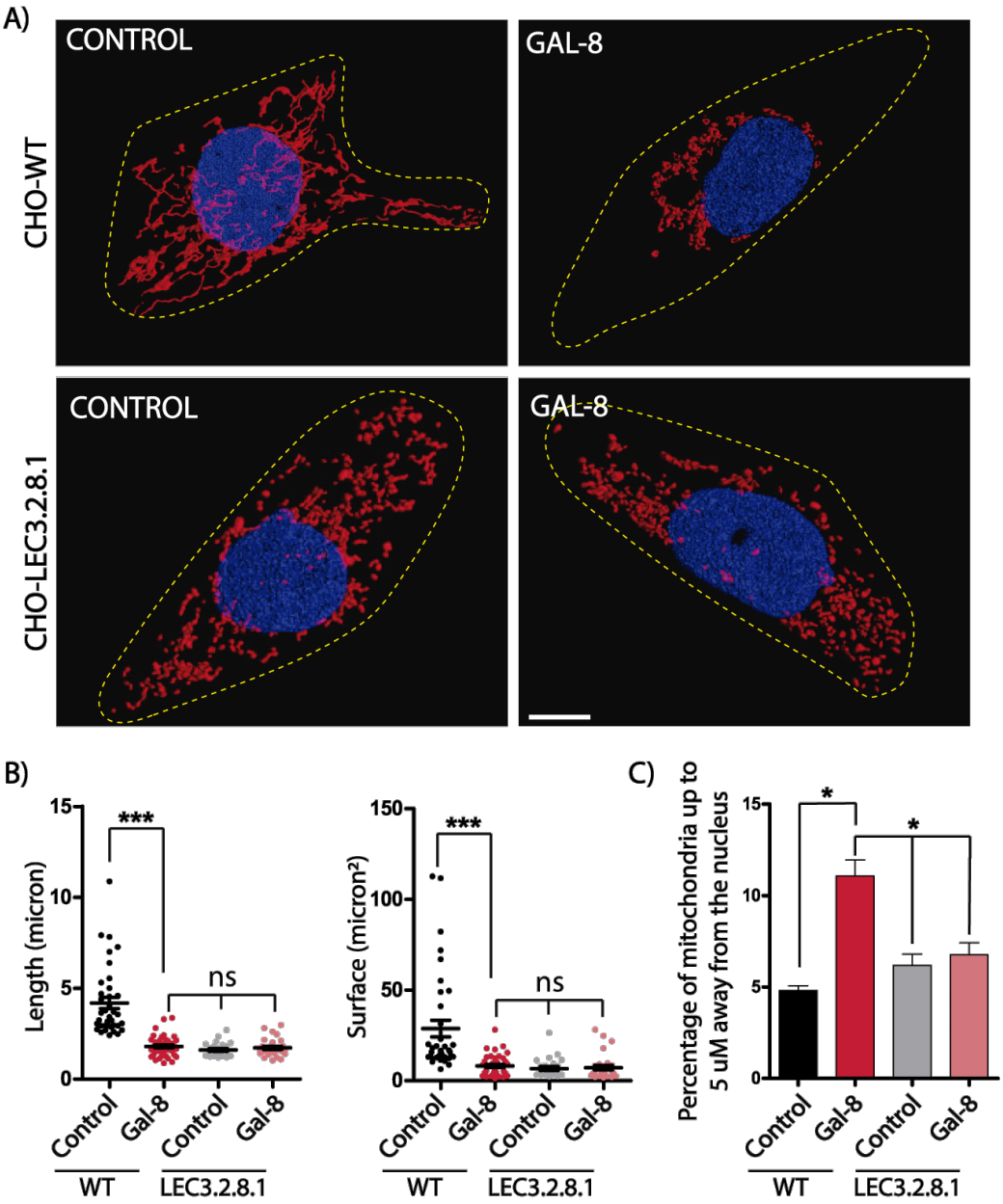

Figure 10. Perinuclear distribution of mitochondrial induces by Gal-8 dependent on surface N-glycan glycoconjugate.

CHO-WT and CHO-LEC3.2.8.1 cells were treated with Gal-8 (50 µg/ml) for 24 hours. Mitochondria were labeled with MitoTracker CMTMRos and Hoechst. A) The images were captured using a confocal microscope in Z-stack to make a surface rendering 3D reconstruction of mitochondria using Huygens software. B) Graphs showing the length and surface of mitochondria quantified by Huygens Software. C) Frequency distribution of the distance of mitochondria to the nucleus quantified by Huygens Software (Means ± s.d., n=3, 25 cells per experiment, One-Way ANOVA with a posterior Tukey, *p<0.05, ***p<0.001). Scale bar = 10µm.

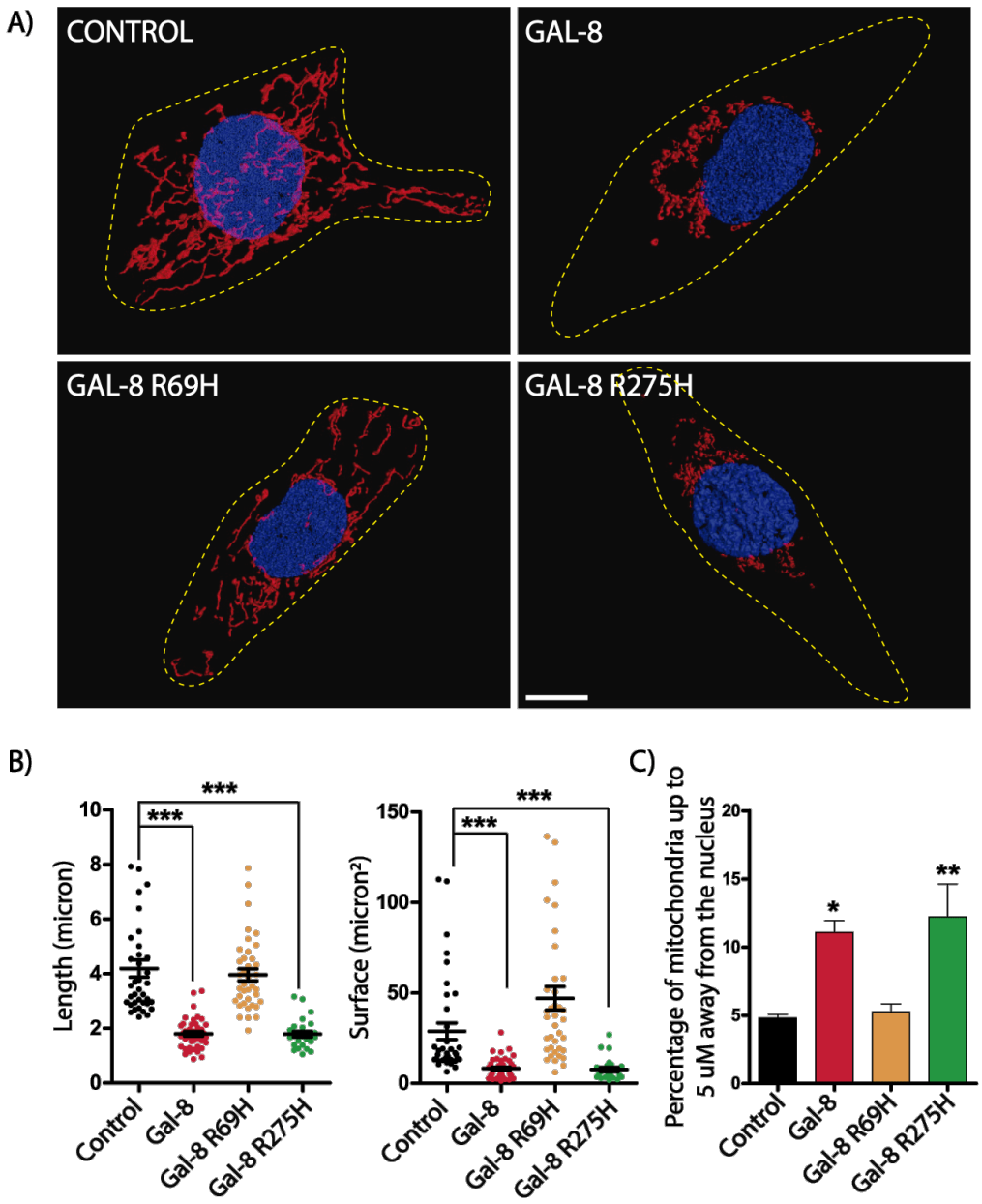

Figure 11. Gal-8 induces fragmentation and perinuclear distribution of mitochondria in a carbohydrate recognition-dependent manner in CHO cells. Confocal 3D microscopy showing MitoTracker CMTMRos stained mitochondria and Hoechst-stained nucleus in fixed CHO cells that were treated with Gal-8, Gal-8-R69H, Gal-8-R275H (50 µg/ml) for 24 hours A) Huygens Software 3D surface rendering reconstruction of mitochondria in CHO cells. B) Graphs showing the length and surface of mitochondria quantified by Huygens Software. C) Frequency distribution of the distance of mitochondria to the nucleus quantified by Huygens Software. (Means ± s.d., n=3, 15 cells per experiment, One-Way ANOVA with a posterior Tukey, *p<0.05, **p < 0.01, ***p<0.001). Scale bar = 10µm.

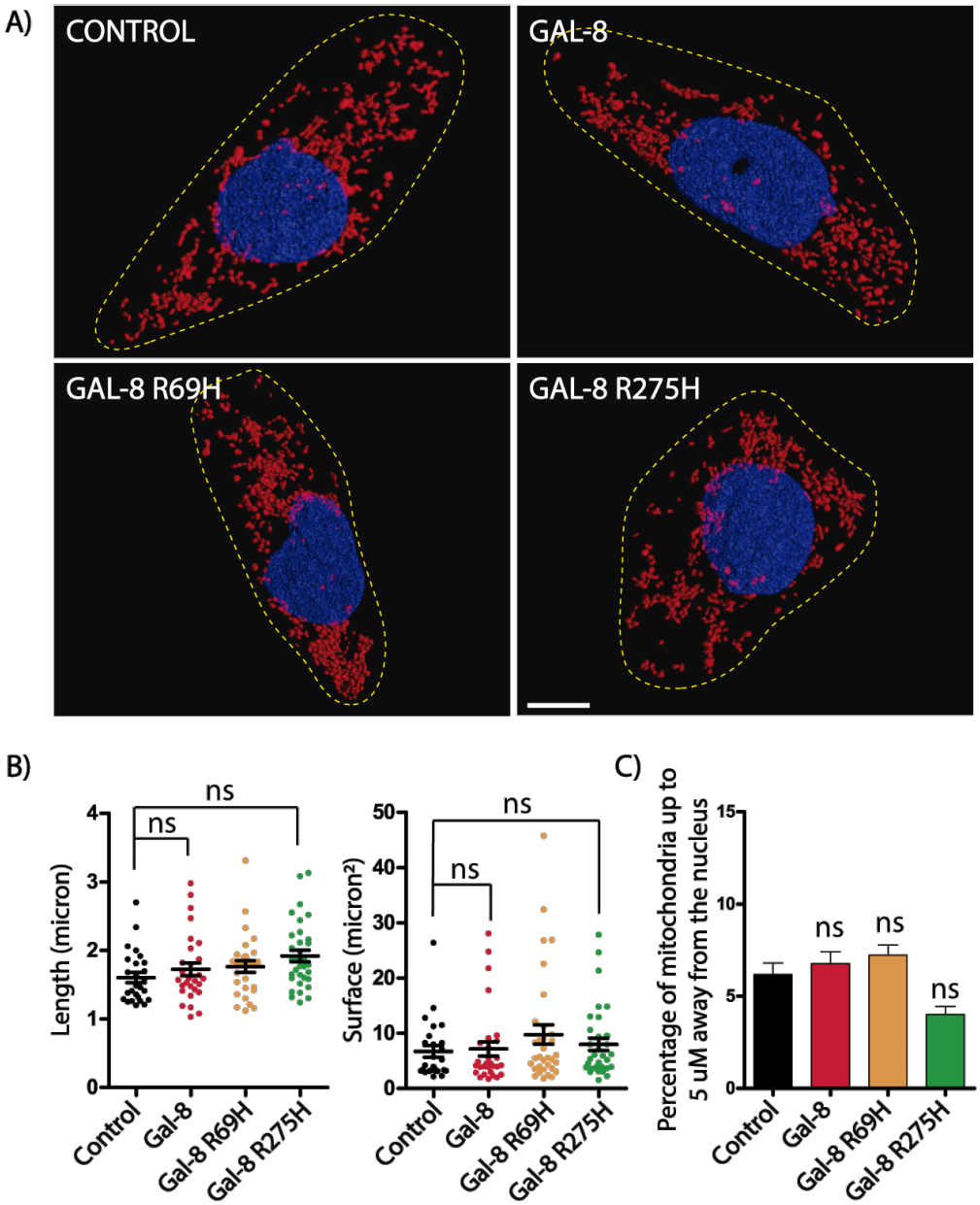

Figure 12. Gal-8 induces perinuclear mitochondrial distribution depending on surface glycosylation patterns of α-2-3 sialylated N-glycans.

Confocal microscopy in Z-Stack showing MitoTracker CMTMRos stained mitochondria and Hoechst-stained nucleus in fixed CHO-LEC3.2.8.1 cells that were treated with Gal-8, Gal-8-R69H, Gal-8-R275H (50 µg/ml) for 24 hours. A) Huygens Software 3D surface rendering reconstruction of mitochondria in CHO-LEC3.2.8.1 cells. B) Graphs showing the length and surface of mitochondria quantified by Huygens Software. C) Frequency distribution of the distance of mitochondria to the nucleus quantified by Huygens Software. (Means ± s.d., n=3, 15 cells per experiment, One-Way ANOVA with a posterior Tukey). Scale bar = 10µm.

The perinuclear localization induced by Gal-8 suggests a potential mitochondria-nucleus contact that could have functional consequences. Stable mitochondria-nucleus contact sites have not been described. In 2020, Desai and their collaborators reported that signals from the mitochondria to the nucleus, known as retrograde signals, were facilitated by the proximity between mitochondria-nucleus (Desai et al., 2013) through the MFN2 protein (Zervopoulos et al., 2022).

To a preliminary exploration if Gal-8 promotes MFN2 mitochondria-nucleus proximity we used super-resolution microscopy (Structured Illumination Microscopy - SIM). For this purpose, MDCK cells were transduced with mt-GFP to label mitochondria and transfected with mCherry-MFN2. MDCK-mt-GFP-mCherry-MFN2 cells were then treated with 50 µg/ml of Gal-8 or Gal-8 mutants for 24 hours, and the nucleus was stained with Hoechst and fixed. The images were captured in a Z-stack in Structured Illumination Microscopy – SIM with allow a resolution of 120 nm per pixel (figure 13A). Gal-8 and Gal-8-R275H treated cells show MFN2 in the proximity between mitochondria and the nucleus. This effect was not observed when cells were incubated with Gal-8-R69H or Gal-8-R69H-R275H (Figure 13B). Furthermore, to assess the impact of Gal-8 on mitochondrial fusion proteins, were measured the levels of MFN1 and MFN2 by immunoblot after 4 or 24 hours of Gal-8 treatment (50 µg/ml) in MDCK cells (Figure 14A-B). The quantifications of the immunoblots showed an increase in MFN2 protein levels after 24 hours of Gal-8 treatment (Figure 14B).

These results suggest that Gal-8 could promote the proximity of mitochondria to the nucleus probably by MFN2 in a carbohydrate-dependent manner by recognizing α-2-3 sialylated β-galactosides, in MDCK cells

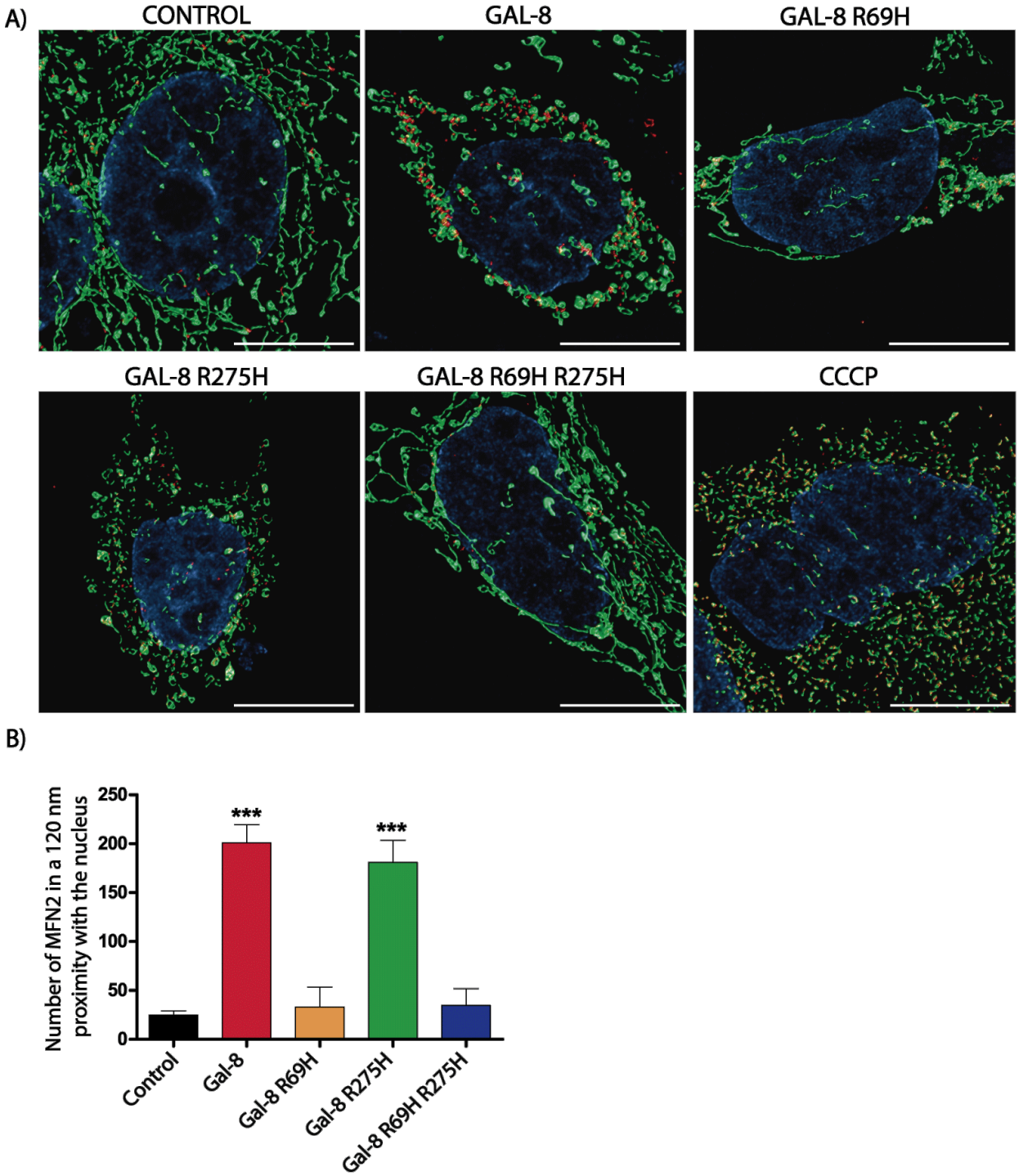

Figure 13. Super-resolution microscopy of mitochondria-nucleus contact sites. Super-resolution microscopy (Structured Illumination Microscopy - SIM) in Z-Stack showing mCherry-MFN2, mt-GFP-Mitochondria and Hoechst-stained nucleus in fixed MDCK cells that were treated with Gal-8, Gal-8-R69H, Gal-8-R275H, Gal-8-R69H-R275H (50 µg/ml) or CCCP (10 µM) for 24h. A) 3D surface rendering reconstruction of cells using Huygens software. B) Graphs showing the numbers of MFN2 in a proximity of 120 nm to the nucleus quantified using the Huygens Software (Means ± s.d., n=3, 25 cells per experiment, One-Way ANOVA with a posterior Tukey, ***$p<0.001$). Scale bar = 10µm.

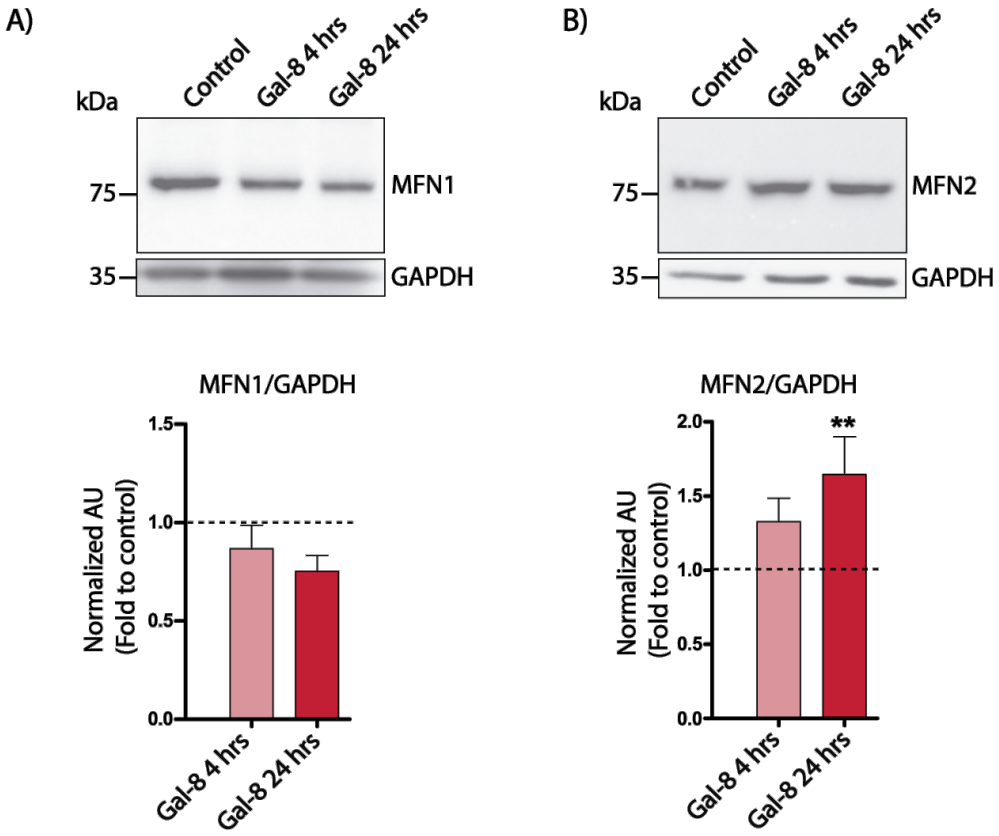

Figure 14. Gal-8 increases MFN2 protein levels.

Immunoblots show the levels of MFN1 A) and MFN2 B) of MDCK cells treated with 50 µg/ml of Gal-8 for 4h and 24h. The graphs represent the quantification of MFN1/GAPDH A) and MFN2/GAPDH B) (Means ± s.d. n=3 three independent experiments, One-Way ANOVA with a posterior Tukey, **p < 0.01).

3.3. Mitochondrial fragmentation and redistribution to the perinuclear zone induced by Gal-8 depend on ERK activity,

Our laboratory has published that overexpressing Gal-8 in MDCK cells, leads to the binding of Gal-8 to integrin. This interaction transactivates the EGFR via FAK, which in turn promotes the activation of ERK (Oyanadel et al., 2018). To investigate whether the activation of EGFR/ERK pathway by Gal-8 is involved in the fragmentation and redistribution of mitochondria to the perinuclear zone, MDCK cells (Figure 15) and RPTEC cells (Figure 16) were pretreated for 30 min with MEK inhibitor PD98059 (25 μM), SRC inhibitor PP2 (10 μM) or EGFR inhibitor AG1478 (0,1 μM), and then incubated with 50 μg/ml of Gal-8 for 24 hours. The mitochondria were then labeled with MitoTracker CMTMRos and the nucleus with Hoechst. The images were taken in a confocal microscope in Z-Stack to reconstruct the mitochondria (Figure 15A and Figure 16A). Quantitative analysis has shown that Gal-8 reduces the length and surface of mitochondria in both MDCK (Figure 15B) and RPTEC cells (Figure 16B). This process depends on ERK and SRC activity but not on the tyrosine kinase activity of EGFR. Similarly, the perinuclear redistribution of mitochondria triggered by Gal-8 also requires ERK and SRC activity without the involvement of the tyrosine kinase activity of EGFR in both cell types (Figure 15C and Figure 16C).

These results suggest that the mitochondrial fragmentation and redistribution to the perinuclear zone induced by Gal-8 required ERK and SRC activity but is independent of the tyrosine kinase activity of EGFR.

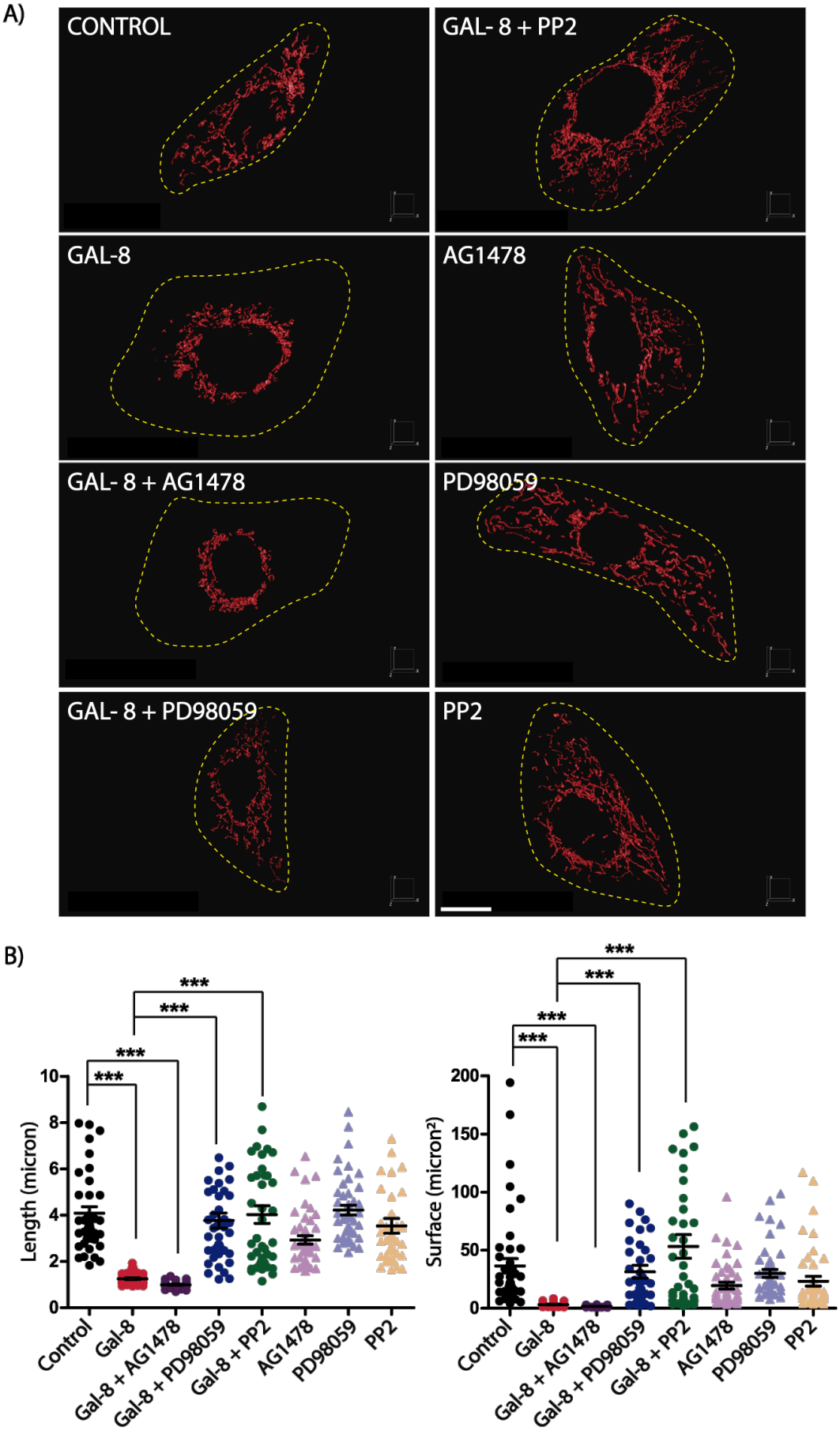
A)
CONTROL
GAL- 8 + PP2
GAL-8
AG1478
GAL- 8 + AG1478
PD98059
GAL- 8 + PD98059
PP2
B)
Length (micron)
Surface (micron²)
***
Control
Gal-8
Gal-8 + AG1478
Gal-8 + PD98059
Gal-8 + PP2
AG1478
PD98059
PP2

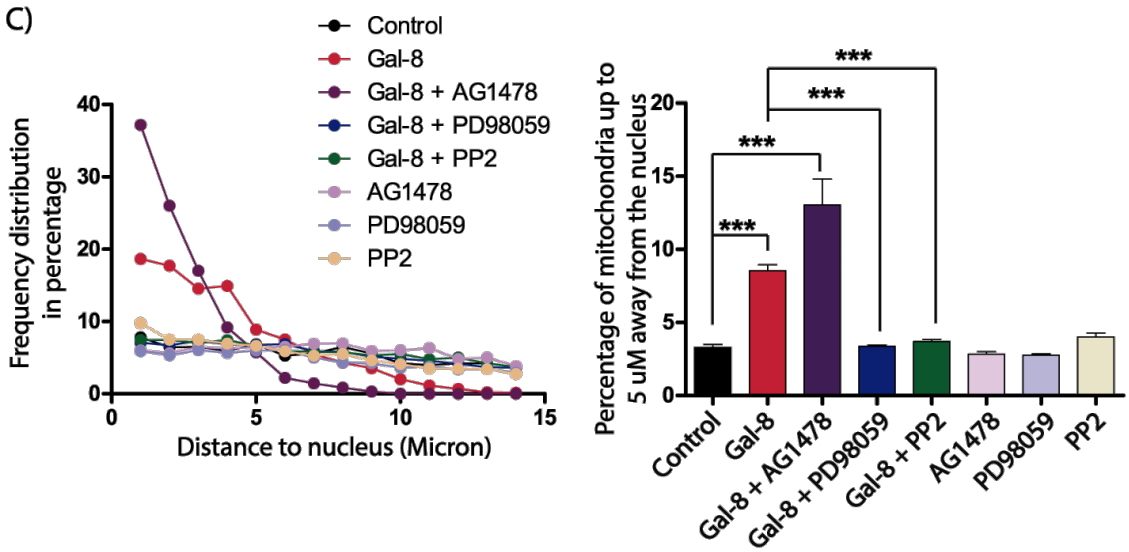

Figure 15. Fragmentation and redistribution of mitochondria to the perinuclear zone induced by Gal-8 depend on ERK and SRC activity, but no on tyrosine kinase activity of EGFR in MDCK cells.

Confocal 3D microscopy showing MitoTracker CMTMRos stained mitochondria and Hoechst-stained nucleus in fixed MDCK cells that were treated with Gal-8 (50 µg/ml) in the presence or absence of the MEK inhibitor PD98059 (25 µM), SRC inhibitor PP2 (10 µM) or EGFR inhibitor AG1478 (0,1 µM) for 24h. A) Huygens Software 3D surface rendering reconstruction of mitochondria in MDCK cells. B) Length and surface of mitochondria quantified by Huygens Software. C) Frequency distribution of the distance of mitochondria to the nucleus quantified by Huygens Software (Means ± s.d. n=3, 15 cells per experiment, One-Way ANOVA with a posterior Tukey, ***p<0.001). Scale bar = 10µm.

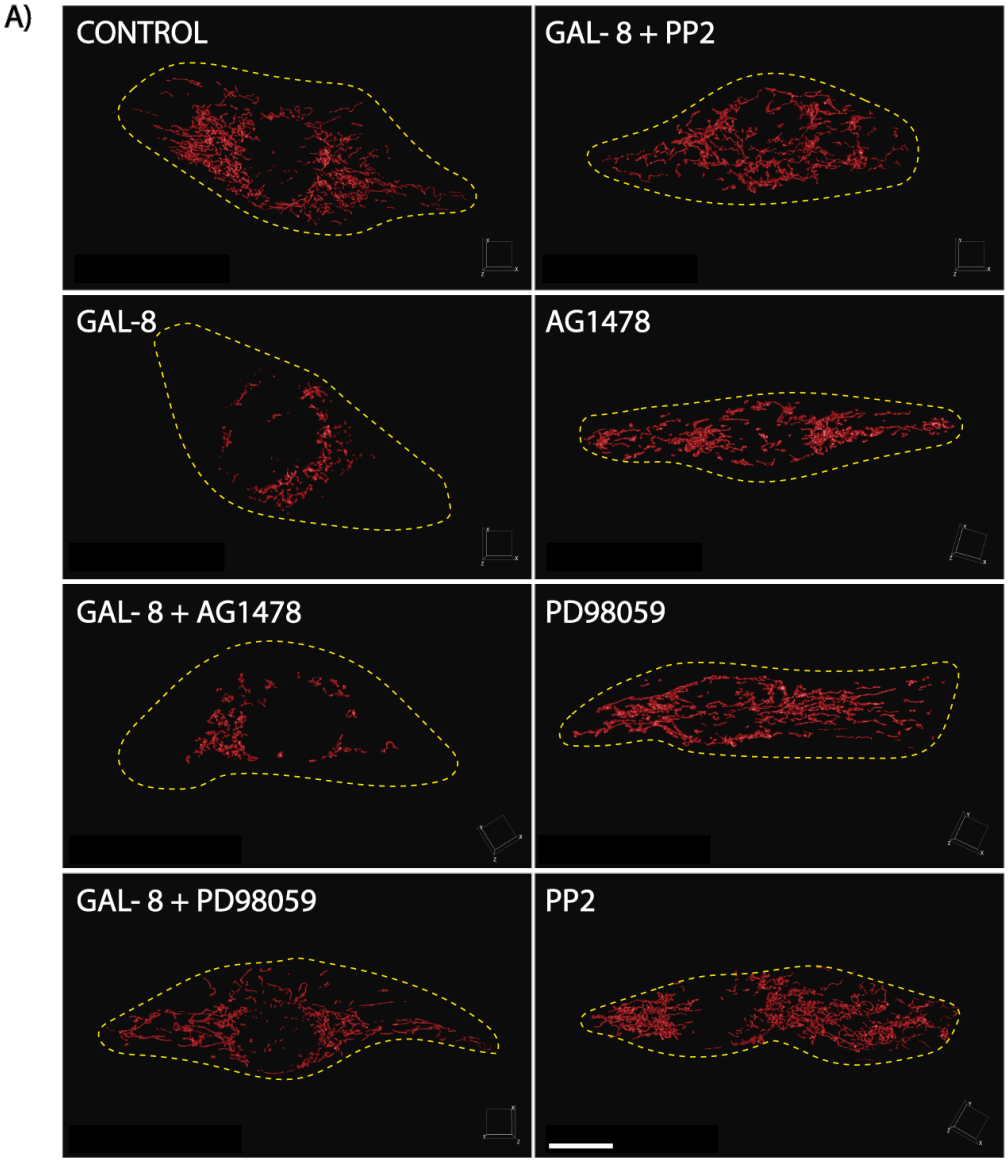
A)
CONTROL
GAL- 8 + PP2
GAL-8
AG1478
GAL- 8 + AG1478
PD98059
GAL- 8 + PD98059
PP2

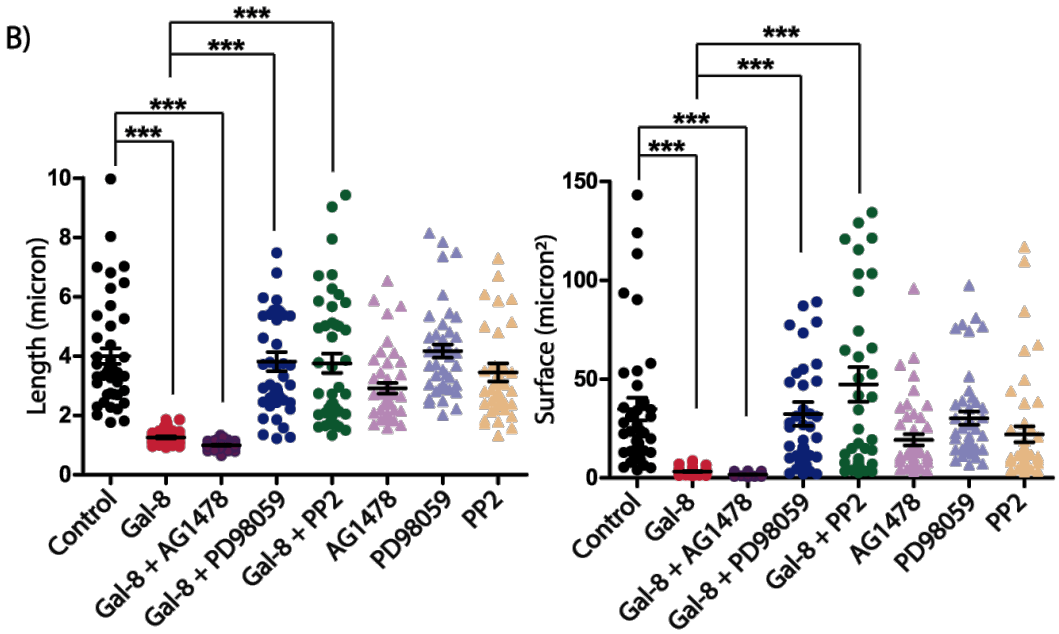
B)
Length (micron)
Surface (micron²)
***
Control
Gal-8
Gal-8 + AG1478
Gal-8 + PD98059
Gal-8 + PP2
AG1478
PD98059
PP2

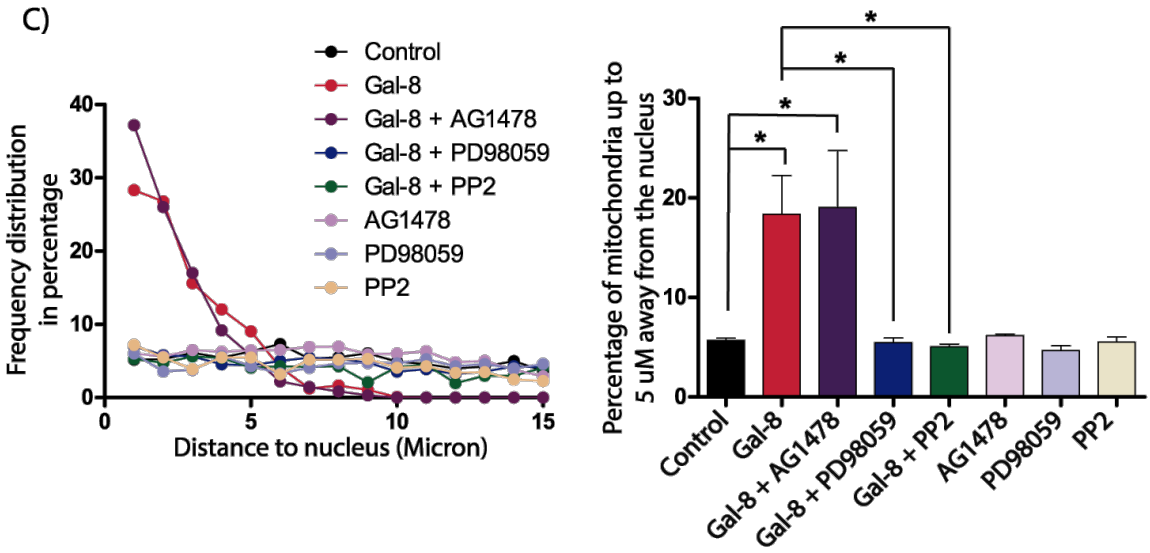

Figure 16. Fragmentation and redistribution of mitochondria to the perinuclear zone induced by Gal-8 depend on ERK and SRC activity, but no on tyrosine kinase activity of EGFR in RPTEC cells.

Confocal microscopy in Z-Stack showing MitoTracker CMTMRos stained mitochondria and Hoechst-stained nucleus in fixed RPTEC cells that were treated with Gal-8 (50 µg/ml) in the presence or absence of the MEK inhibitor PD98059 (25 µM), SRC inhibitor PP2 (10 µM) or EGFR inhibitor AG1478 (0,1 µM) for 24h. A) Huygens Software 3D surface rendering reconstruction of mitochondria in RPTEC cells. B) Length and surface of mitochondria quantified by Huygens Software. C) Frequency distribution of the distance of mitochondria to the nucleus quantified by Huygens Software (Means ± s.d. n=3, 15 cells per experiment, One-Way ANOVA with a posterior Tukey, *p<0.05, ***p<0.001). Scale bar = 10µm.

3.4. Fragmentation and redistribution of mitochondria to the perinuclear zone induced by Gal-8 depend on DRP1.

Phosphorylation of DRP1 is the most studied regulation mechanism for mitochondrial shape (Zerihun et al., 2023). It has been reported that ERK directly phosphorylates DRP1 at S616 leading to mitochondrial fragmentation (Kashatus et al., 2015). Additionally, ERK kinase has been shown to phosphorylate T562 of MFN1, decreasing its ability to tether mitochondria together and preventing mitochondrial fusion, leading to mitochondrial fragmentation (Pyakurel et al., 2015). To investigate whether the activation of the EGFR/ERK pathway by Gal-8 induces phosphorylation of DRP1 at S616 (pDRP1), leading to changes in mitochondrial fragmentation and distribution patterns, MDCK cells were treated with 50 µg/ml of Gal-8 for 1, 2, 4, 8 or 24 hours. The protein levels of pDRP, DRP1, pERK and ERK were analyzed by immunoblot (Figure 17A-B). Quantitative analysis of the immunoblots demonstrated an increase in pDRP1 levels after 24 hours. In contrast, phosphorylated pERK exhibited sustained activation starting at 4 hours following Gal-8 treatment. These effects were accompanied by no change in the total level of ERK or DRP1 proteins over time (Figure 17B). Similar experiments were done in RPTEC cells showing that 50 µg/ml of Gal-8 for 24 hours resulted in increased levels of DRP1 and pERK (Figure 17C-D), however, pDRP1 was not detected in RPTEC cells (Data not shown). To determine whether the EGFR/ERK signaling pathway plays a role in DRP1 activation, RPTEC cells were pre-treated for 30 minutes with EGFR inhibitor AG1478 (0,1 µM) or ERK inhibitor PD98059 (25 µM), and then treated with 50 µg/ml of Gal-8 for 24 hours (Figure 17E-F). DRP1 and pERK levels increased with Gal-8 in an ERK-dependent but EGFR tyrosine kinase activity-independent manner, as shown by immunoblot analysis (Figure 17E-F).

These results suggest that Gal-8 promotes DRP1 activation via ERK-dependent pathway in epithelial cells.

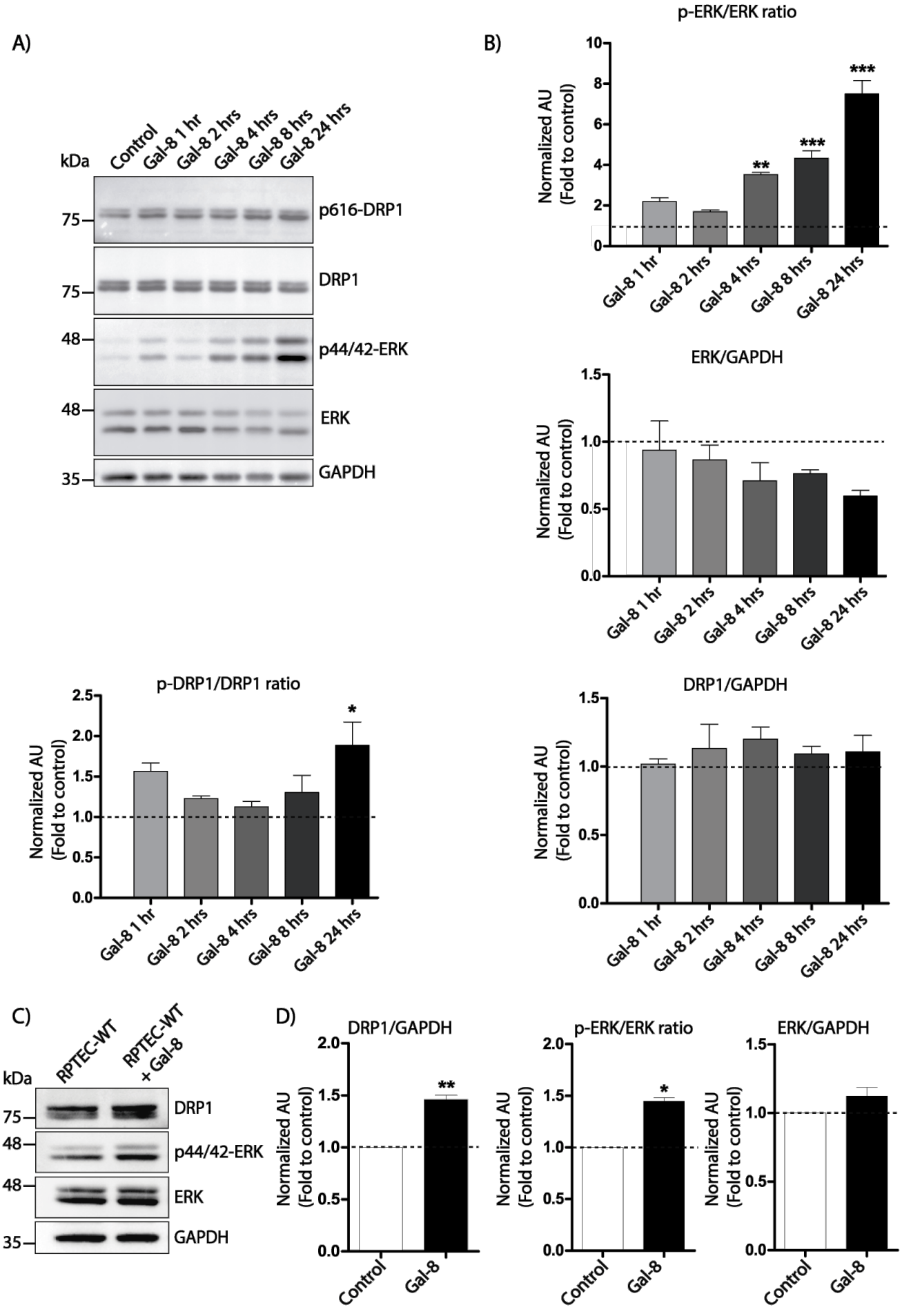
A)
kDa
Control
Gal-8 1 hr
Gal-8 2 hrs
Gal-8 4 hrs
Gal-8 8 hrs
Gal-8 24 hrs
75
p616-DRP1
75
DRP1
48
p44/42-ERK
48
ERK
35
GAPDH
B)
p-ERK/ERK ratio
Normalized AU
(Fold to control)
10
8
6
4
2
0
**
***
***
Gal-8 1 hr
Gal-8 2 hrs
Gal-8 4 hrs
Gal-8 8 hrs
Gal-8 24 hrs
ERK/GAPDH
Normalized AU
(Fold to control)
1.5
1.0
0.5
0.0
Gal-8 1 hr
Gal-8 2 hrs
Gal-8 4 hrs
Gal-8 8 hrs
Gal-8 24 hrs
p-DRP1/DRP1 ratio
Normalized AU
(Fold to control)
2.5
2.0
1.5
1.0
0.5
0.0
*
Gal-8 1 hr
Gal-8 2 hrs
Gal-8 4 hrs
Gal-8 8 hrs
Gal-8 24 hrs
DRP1/GAPDH
Normalized AU
(Fold to control)
1.5
1.0
0.5
0.0
Gal-8 1 hr
Gal-8 2 hrs
Gal-8 4 hrs
Gal-8 8 hrs
Gal-8 24 hrs
C)
kDa
RPTEC-WT
RPTEC-WT
+ Gal-8
75
DRP1
48
p44/42-ERK
48
ERK
35
GAPDH
D)
DRP1/GAPDH
Normalized AU
(Fold to control)
2.0
1.5
1.0
0.5
0.0
**
Control
Gal-8
p-ERK/ERK ratio
Normalized AU
(Fold to control)
2.0
1.5
1.0
0.5
0.0
*
Control
Gal-8
ERK/GAPDH
Normalized AU
(Fold to control)
1.5
1.0
0.5
0.0
Control
Gal-8

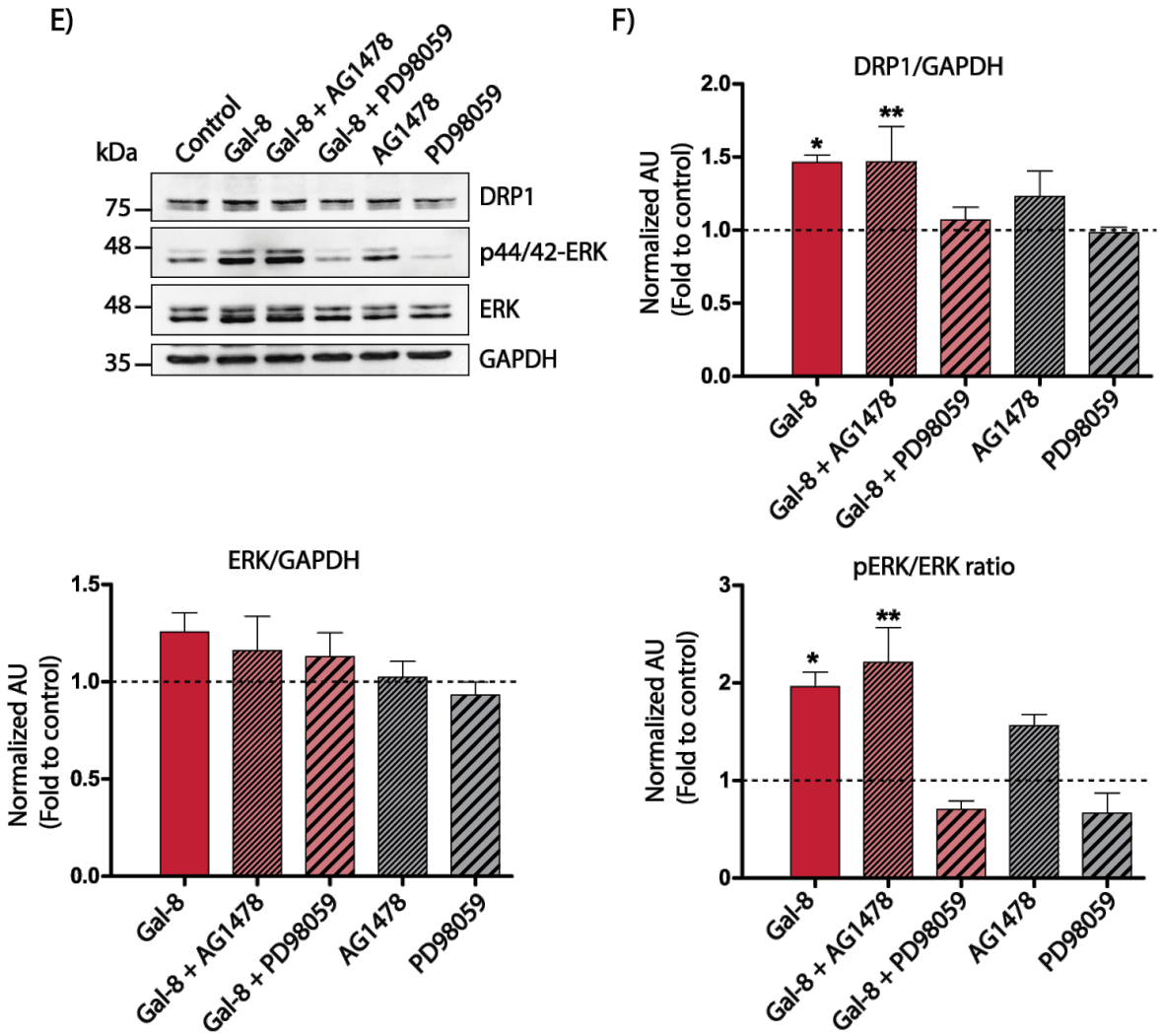

Figure 17. ERK activity is required for activation of DRP1 by Gal-8 in epithelial cells.

A) Immunoblots show phosphorylation of DRP1 (Serine 616), pERK and ERK in MDCK cells treated with 50 µg/ml of Gal-8 for indicated times. B) The graphs depict the quantified relative increase, measured in fold change, compared to the control for the immunoblots shown in A. C) Immunoblot show DRP1, pERK and ERK in RPTEC cells treated with 50 µg/ml of Gal-8 for 24 hours. D) The graphs depict the quantified relative increase, measured in fold change, compared to the control for the immunoblots shown in panel C. E) Immunoblots show the proteins levels of DRP1, pERK and ERK in RPTEC treated with Gal-8 (50 µg/ml) in the presence or absence of the MEK inhibitor PD98059 (25 µM) or EGFR inhibitor AG1478 (0,1 µM) for 24h. F) The graphs depict the quantified relative increase, measured in fold change, compared to the control for the immunoblots shown in panel E. (Means ± s.d. n=3 three independent experiments, T Student or One-Way ANOVA with a posterior Tukey, *p<0.05, **p < 0.01, ***p<0.001).

DRP1, a GTPase recognized as the key regulator of mitochondrial fission, plays a pivotal role in influencing the proper functioning of the organelle. To investigate the role of DRP1 in Gal-8-induced mitochondrial fragmentation and the redistribution of mitochondria to the perinuclear zone, were employed lentiviral infection to silence DRP1 in RPTEC cells (Figure 18A-B). Following this, the cells were treated with 50 µg/ml of Gal-8 for 24 hours. RPTEC-Sh-DRP1 shows more interconnected mitochondria, and upon treatment with Gal-8 (Figure 18C), they did not undergo mitochondrial fragmentation or redistribution of mitochondria to the perinuclear zone (Figure 18D-E). In contrast, RPTEC-sh-Control treated cells displayed both mitochondrial fragmentation and perinuclear redistribution after Gal-8 treatment (Figure 18C-E).

These findings indicate that DRP1 is necessary for mitochondrial fragmentation and perinuclear redistribution triggered by Gal-8.

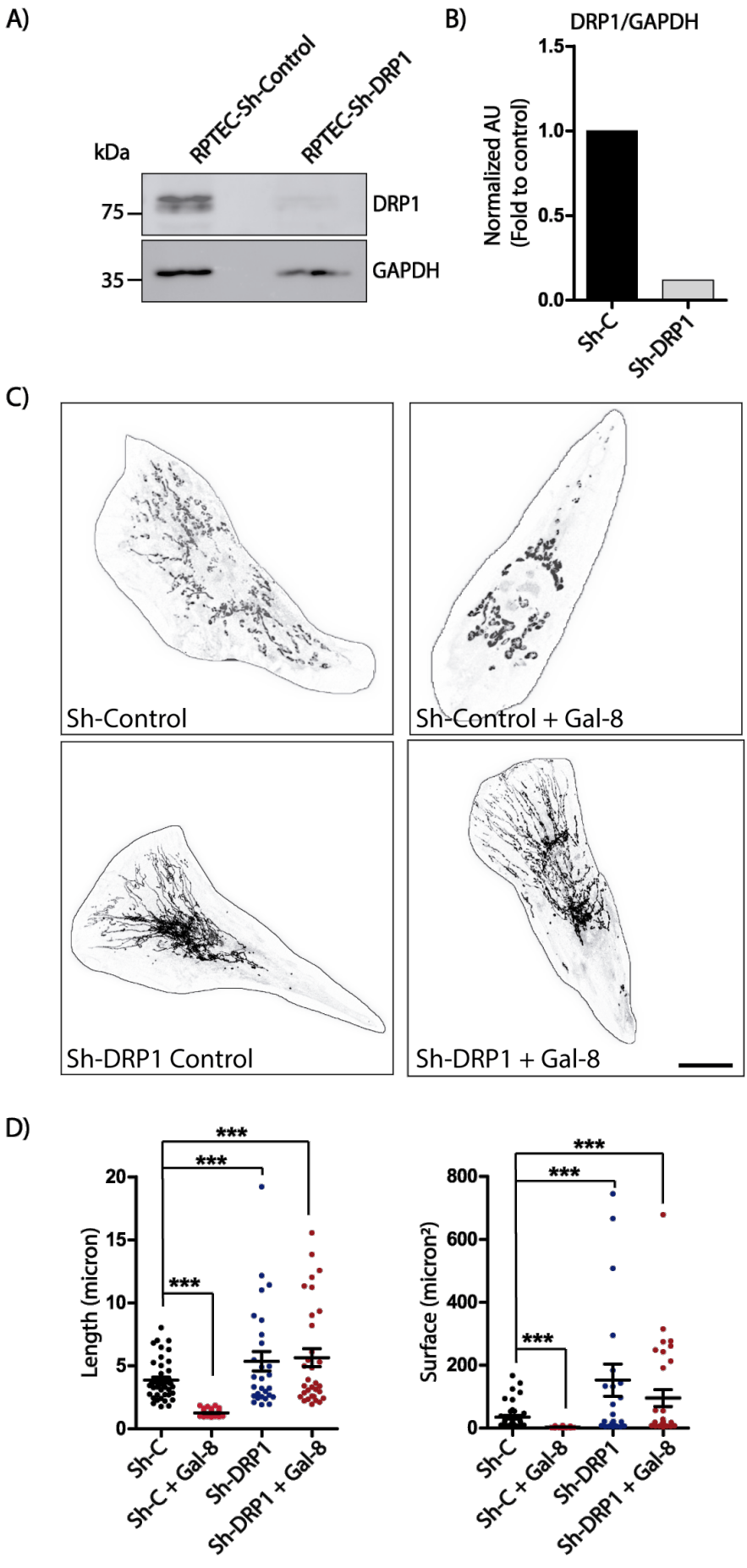
A)
RPTEC-Sh-Control
RPTEC-Sh-DRP1
kDa
75
DRP1
35
GAPDH
B)
DRP1/GAPDH
Normalized AU
(Fold to control)
1.5
1.0
0.5
0.0
Sh-C
Sh-DRP1
C)
Sh-Control
Sh-Control + Gal-8
Sh-DRP1 Control
Sh-DRP1 + Gal-8
D)
Length (micron)
20
15
10
5
0
***
***
***
Sh-C
Sh-C + Gal-8
Sh-DRP1
Sh-DRP1 + Gal-8
Surface (micron²)
800
600
400
200
0
***
***
***
Sh-C
Sh-C + Gal-8
Sh-DRP1
Sh-DRP1 + Gal-8

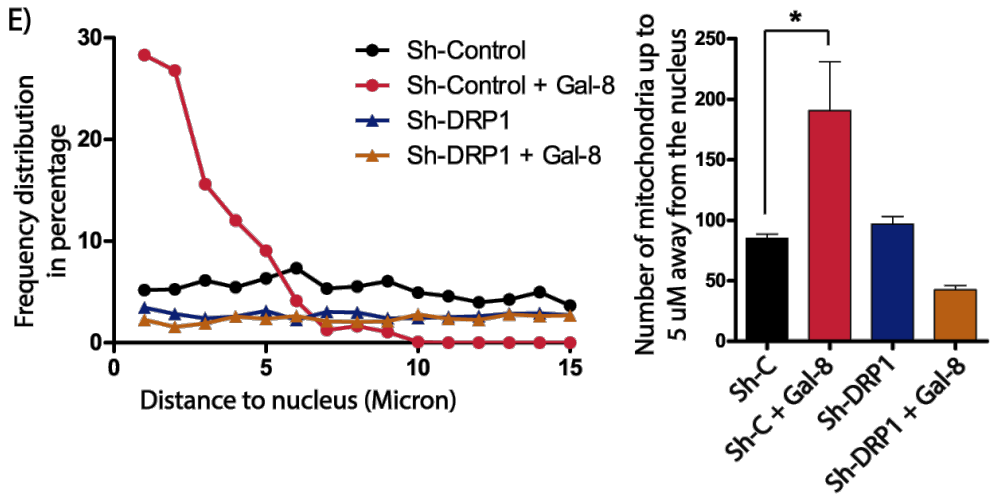

Figure 18. Fragmentation and redistribution of mitochondria to the perinuclear zone induced by Gal-8 depend on DRP1 in RPTEC cells.

A) Immunoblot show the level of DRP1 in RPTEC-Sh-Control and RPTEC-Sh-DRP1. B) Graph shows the quantification of the levels of DRP1 RPTEC-Sh-Control and RPTEC-Sh-DRP1. C) ImageJ reconstruction showing the distribution of the mitochondria. D) Graphs showing the length and surface of mitochondria quantified by Huygens Software. E) Frequency distribution of the distance of mitochondria to the nucleus quantified by Huygens Software (Means ± s.d., n=3, 15 cells per experiment, One-Way ANOVA with a posterior Tukey, *p<0.05, ***p<0.001). Scale bar = 10µm.

3.5. Gal-8 promotes mitophagy in a carbohydrate-dependent manner in MDCK cells.

Mitophagy is a cellular process that selectively removes damaged, old, or dysfunctional mitochondria. Several publications show that mitochondrial fragmentation is related to mitophagy because it facilitates the removal of damaged mitochondria under cellular stress conditions (Sun et al., 2017). To analyze if Gal-8-mediated fragmentation of mitochondria promotes autophagy, MDCK cells were treated with 50 µg/ml of Gal-8 for 1, 2, 4, 8, and 24 hours, and then the conversion of LC3-I to LC3-II and the levels of NDP52, an autophagy receptor, were evaluated by immunoblot. The results showed that Gal-8 promotes a significant increment in the LC3II/LC3I ratio after 24 hours of treatment and a significant decrease in NDP52 after 24 hours of treatment (Figure 19A). These results suggest that Gal-8 promotes autophagy at 24 hours of treatment.

To investigate mitophagy, MDCK cells were transfected with a Keima-FIS1 plasmid, coding for a pH-dependent fluorescent protein labeling the outer mitochondrial membrane (MDCK-Keima-FIS1). Keima is a pH-sensitive dual-excitation ratiometric fluorescent protein resistant to lysosomal proteases. Under the normal pH of mitochondria, shorter-wavelength excitation prevails (440 nm, indicating pH 7). Following mitophagy in the acidic lysosome (pH 4.5), Keima-FIS1 gradually shifts to longer-wavelength excitation (586 nm, indicating pH 4.5) (Sun et al., 2017). MDCK-Keima-FIS1 cells were exposed to 50 µg/ml of Gal-8 or CCCP, a mitophagy inducer, for 24 hours. Subsequently, live cell imaging confocal microscopy was used to analyze MDCK cells. Keima was excited at 440 nm (cyan) and 586 nm (red). Cells treated with Gal-8 and CCCP exhibited red fluorescence, indicating mitophagy (Figure 19B). Moreover, to determine if the interaction between Gal-8 and the carbohydrates is necessary to trigger mitophagy, MDCK-Keima-FIS1 cells were treated with 50 µg/ml of Gal-8, Gal-8-R69H, Gal-8-R275 or Gal-8-R69H-R275H for 24 hours. After this time, the MDCK cells were analyzed by live cell imaging confocal microscopy (Figure 19B). Gal-8 and Gal-8-R275H treated cells show red fluorescence, indicating mitophagy. This effect was not observed when cells were incubated with Gal-8-R69H or Gal-8-R69H-R275H (Figure 19B).

These results show that Gal-8 promotes mitophagy in a mitochondrial fraction in a carbohydrate-dependent manner, particularly through the N-terminal CRD.

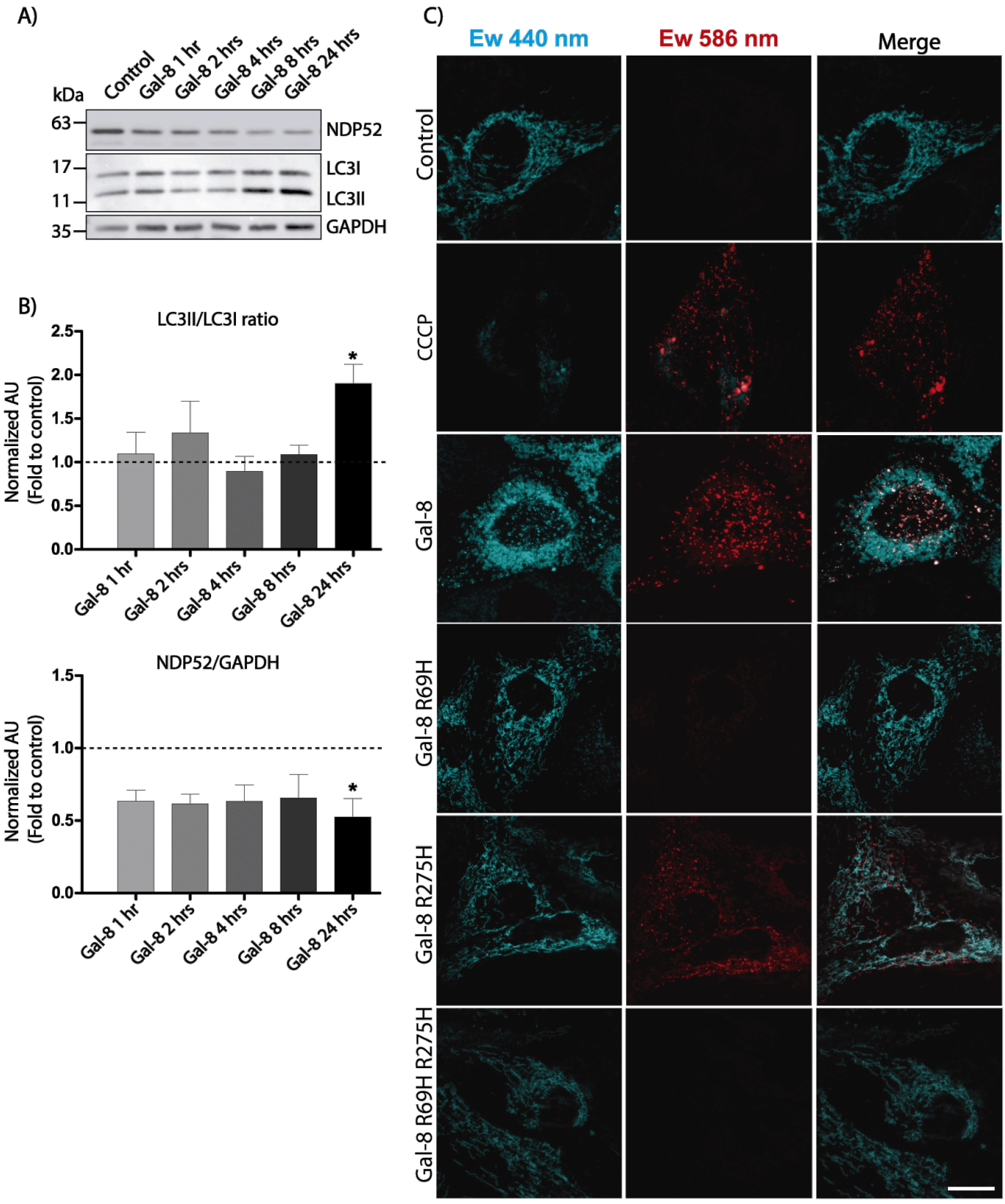
A)
kDa
Control
Gal-8 1 hr
Gal-8 2 hrs
Gal-8 4 hrs
Gal-8 8 hrs
Gal-8 24 hrs
63
NDP52
17
LC3I
11
LC3II
35
GAPDH
B)
LC3II/LC3I ratio
Normalized AU
(Fold to control)
2.5
2.0
1.5
1.0
0.5
0.0
*
Gal-8 1 hr
Gal-8 2 hrs
Gal-8 4 hrs
Gal-8 8 hrs
Gal-8 24 hrs
NDP52/GAPDH
Normalized AU
(Fold to control)
1.5
1.0
0.5
0.0
*
Gal-8 1 hr
Gal-8 2 hrs
Gal-8 4 hrs
Gal-8 8 hrs
Gal-8 24 hrs
C)
Ew 440 nm
Ew 586 nm
Merge
Control
CCCP
Gal-8
Gal-8 R69H
Gal-8 R275H
Gal-8 R69H R275H

Figure 19. Gal-8 promotes mitophagy in MDCK cells.

A) Immunoblot showing the conversion of LC3I to LC3II, and the levels of NDP52 in MDCK cells treated with 50 µg/ml of Gal-8 for indicated times. B) The graphs depict the quantified relative increase, measured in fold change, compared to the control for the immunoblots shown in A. C) Live-cell imaging confocal microscopy of MDCK-Keima-FIS1 cells treated with Gal-8, Gal-8-R69H, Gal-8-R275H, Gal-8-R69H-R275H (50 µg/ml) or CCCP (10 µM) for 24 hours. Keima- excited at 440 nm was pseudocolored as cyan and Keima- excited at 586 nm was pseudocolored as red. (Means ± s.d. n=3 three independent experiments, One-Way ANOVA with a posterior Tukey, *$p<0.05$). Scale bar = 10µm.

3.6. Gal-8 impact on mitochondrial function in epithelial cells.

Mitochondrial size affects mitochondrial function, as highly fused tubular mitochondrial networks demonstrate higher ATP synthase dimerization and ATP synthesis, and lower degradation compared to fragmented mitochondria (Gomes et al., 2011). In contrast, fragmented mitochondria have been largely associated with higher glycolytic flow rates and decreased oxidative phosphorylation activity (Chen & Chan, 2017).

To assess whether Gal-8 affects metabolic activity, MDCK cells were challenged to various mitochondrial stressors, and the resultant changes in oxygen consumption rate (OCR) and extracellular acidification rate (ECAR) were measured using a Seahorse XFp assay. The stress response was measurement by Seahorse Cell Mito Stress Test. This was evaluated by seeding MDCK cells into an 8-well microplate and monitoring metabolic changes in the presence of glucose, sodium pyruvate, and L-glutamine following the sequential addition of mitochondrial inhibitors: Oligomycin, FCCP and Rotenone/Antimycin-A (Figure 20A). Here, we show that Oligomycin did not reduce the OCR in Gal-8 treatment. The treatment of MDCK cells with Gal-8 resulted in decreased ATP production associated with OCR and an increased proton leak level in comparison to the control group (Figure 20B). Similarly, the metabolic rate was determined using a Seahorse Real-Time ATP Rate assay. For this purpose, the cells were seeded in the same type of microplate and data was recorded post-injection with Oligomycin, followed by Rotenone/Antimycin-A (Figure 20C). Furthermore, MDCK cells treated with Gal-8 exhibited an enhanced extracellular acidification rate (ECAR) rather than oxygen consumption rate (OCR) relative to control cells (Figure 20C).

This data suggest that Gal-8 induces a change in the metabolic rate of MDCK cells.

A)

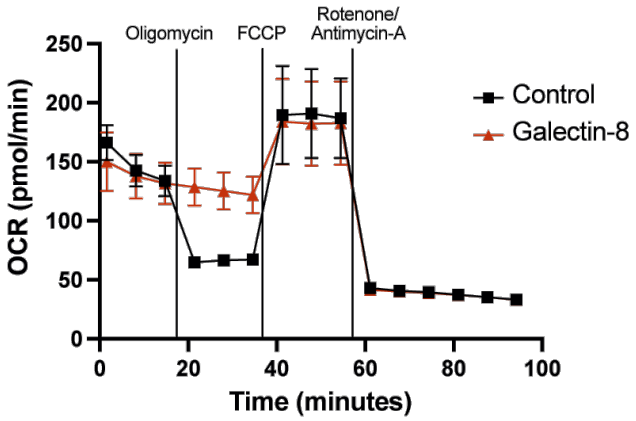
Oligomycin
FCCP
Rotenone/
Antimycin-A
Control
Galectin-8
OCR (pmol/min)
Time (minutes)
250
200
150
100
50
0
0
20
40
60
80
100

B)

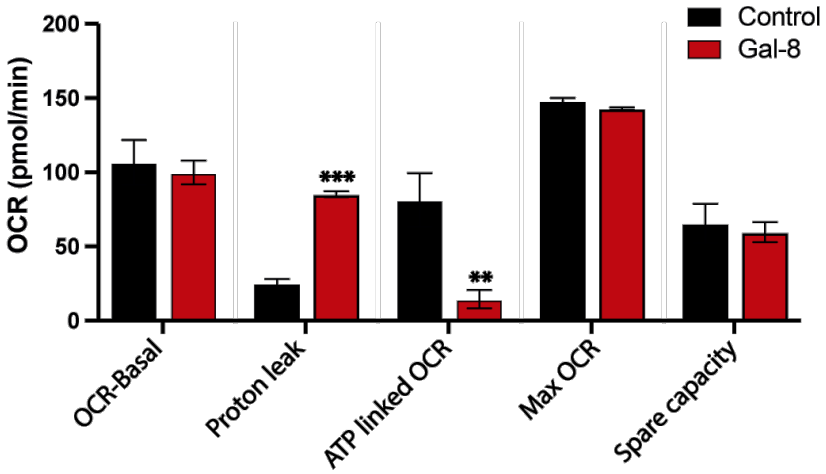
Control
Gal-8
OCR (pmol/min)
200
150
100
50
0
***
**
OCR-Basal
Proton leak
ATP linked OCR
Max OCR
Spare capacity

C)

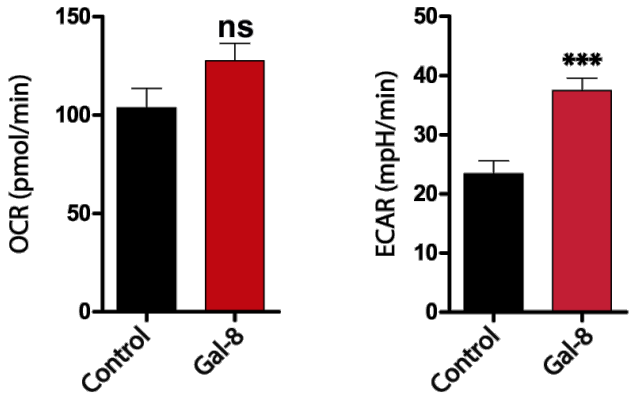
OCR (pmol/min)
150
100
50
0
ns
Control
Gal-8
ECAR (mpH/min)
50
40
30
20
10
0
***
Control
Gal-8

Figure 20. Gal-8 increases ECAR without ATP synthesis linked to OCR.

A) MDCK cells were seeded in an 8-well plate for a Seahorse Cell Mito Stress Test. The cells were exposed sequentially to oligomycin, FCCP and rotenone/antimycin in the presence or absence of Gal-8 (50 µg/ml). Oxygen consumption rate (OCR) with vertical lines indicates the time of addition of mitochondrial inhibitors. B) Graph showing the quantification of A. C) MDCK cells were seeded in an 8-well plate for a Seahorse Real-Time ATP Rate assay. Data were recorded post-injection with Oligomycin, followed by Rotenone/Antimycin-A. The results are shown as oxygen consumption rate (OCR) and extracellular acidification rate (ECAR) (Means ± s.d., n=3, T Student, **p < 0.01, ***p<0.001).

3.7. Gal-8 induces proliferation depended on carbohydrate recognition, and EMT depended on ERK activity in epithelial cells

As previously reported, exogenous Gal-8 induces cell proliferation in MDCK (Oyanadel et al., 2018). In this work, we analyzed whether Gal-8-induced cell proliferation depends on the interaction with sialylated glycans in α-2,3 position and the N-terminal CRD of Gal-8. For this purpose, MDCK cells were treated with 50 µg/ml of Gal-8, Gal-8-R69H, or Gal-8-R275H for 72 hours. Only Gal-8 and Gal-8-R275H show an increase in cell number measurement by Automated Cell Counter (Figure 21A). This result shows that mitochondrial fragmentation, the perinuclear distribution of mitochondria, and cell proliferation depend on the N-terminal domain of Gal-8.

NF-κB is a protein complex that functions as a transcription factor and can promote cell proliferation and survival by inducing the expression of genes involved in these processes. For example, it can upregulate the expression of cyclins and cyclin-dependent kinases (CDKs), which are crucial for cell cycle progression (Guttridge et al., 1999). Previous research has shown that Gal-8 promotes the activation of NF-κB in osteoblasts (Vinik et al., 2015). MDCK cells were transfected with a NF-κB-MetLuc2-reporter plasmid and treated with Gal-8 or Gal-8-R69H for 24 hours. NF-κB activation was increased by Gal-8, but not by the mutant Gal-8-R69H (Figure 21B).

Additionally, emerging evidence has linked NF-κB signaling to EMT (Oh et al., 2023). As previously reported (Oyanadel et al., 2018), MDCK cells that overexpress Gal-8 promotes EMT. In this work, MDCK cells were treated with recombinant Gal-8 and analyzed EMT markers. Gal-8 increased snail protein levels, a EMT transcription factor, and decreased levels of ZO-1, an epithelial marker. These changes were observed after 24 hours of treatment but not after 4 hours (Figure 21C).

To investigate the impact of Gal-8-driven proliferation on other epithelial cells, RPTEC cells were used and exposed to Gal-8 at a concentration of 50 µg/ml for a duration of 72 hours. The crystal violet assay was employed to evaluate proliferation, where the amount of dye retained by cells corresponds to cell mass, providing a quantitative measure of cell proliferation. Gal-8 increased the cell number in relation to the control (Figure 22A). Similar to MDCK cells, an increase in the protein levels of N-cadherin and Snail and a decrease in E-cadherin was observed in RPTEC cells (Figure 22B), indicating that Gal-8 promotes EMT in RPTEC cells.

To analyze if the activity of EGFR and ERK are necessary for the expression of snail, a common EMT marker in MDCK and RPTEC cells, RPTEC cells were treated with Gal-8 in the presence or absence of the ERK inhibitor PD98059 (25 μM) or the EGFR inhibitor AG1478 (0,1 μM) for 24 hours, then levels of Snail were measured by immunoblot (Figure 22C). The quantification of the immunoblots demonstrates that the expression of snail, induced by Gal-8, depends on ERK activity but not on the tyrosine kinase activity of EGFR.

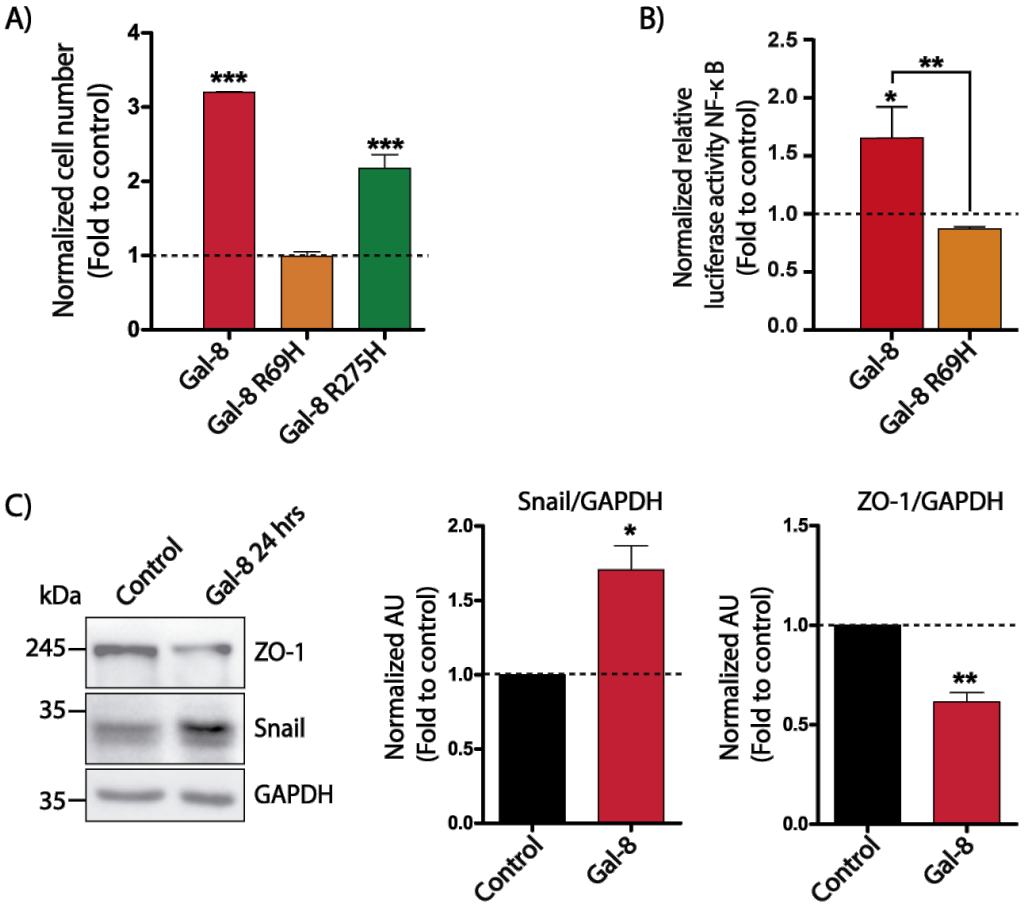

Figure 21. Gal-8 induces expression of NF-κB, EMT markers and proliferation in MDCK cells.

A) MDCK cells were treated with Gal-8, Gal-8-R69H, Gal-8-R275H (50 µg/ml) for 72 hours and counted using trypan blue in an Automated Cell Counter. B) Relative luciferase activity for NF-κB in MDCK cells after 24 hours of treatment with Gal-8 or Gal-8 R69H (50 µg/ml). The graphs depict the quantified relative increase, measured in fold change, compared to the control. C) Immunoblot and quantification of the epithelial (ZO-1) and mesenchymal (Snail) markers of MDCK treated with Gal-8 (50 µg/ml) for 24 hours. (Means ± s.d. n=3 three independent experiments, T Student or One-Way ANOVA with a posterior Tukey *p<0.05, **p < 0.01, ***p<0.001).

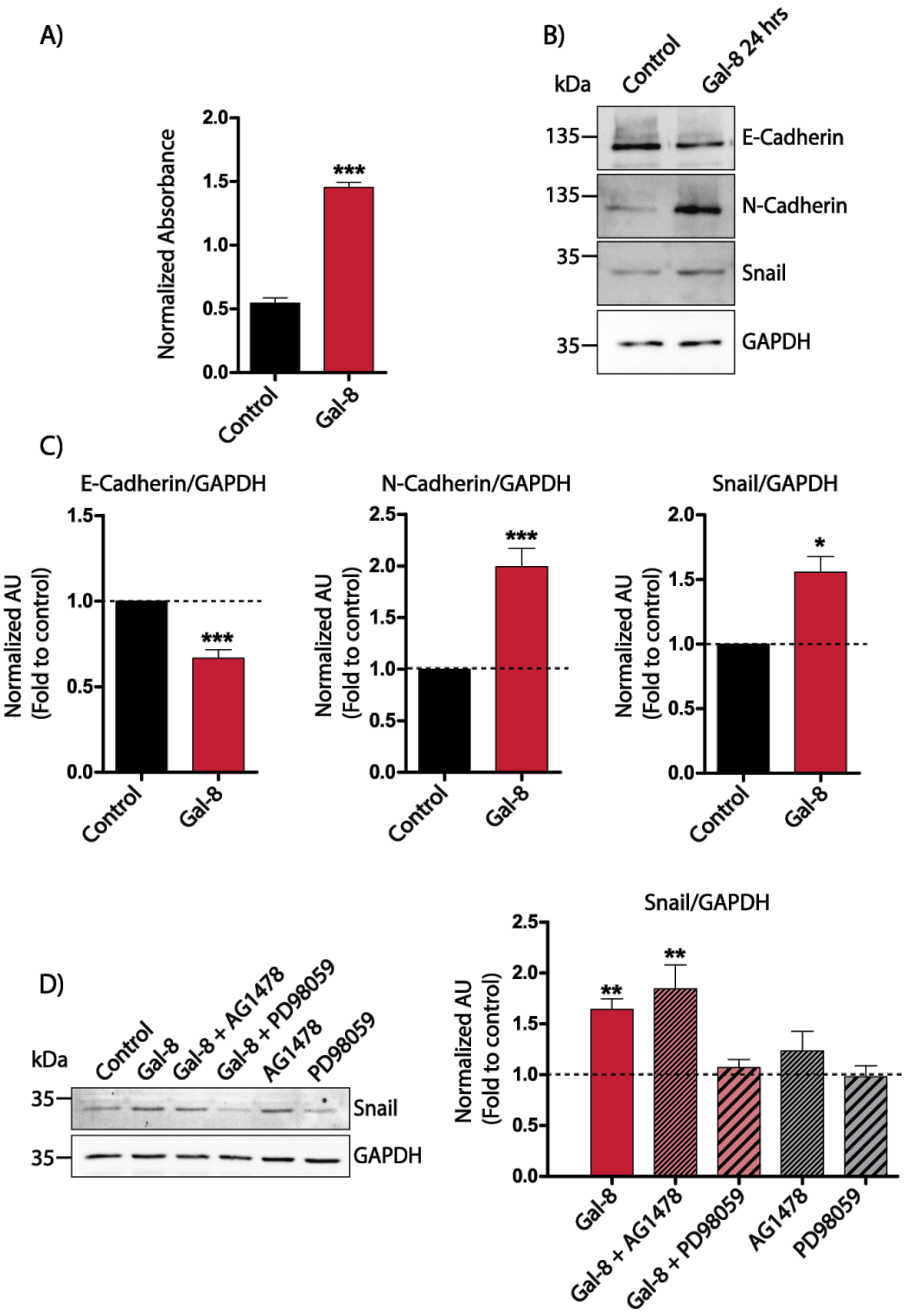
A)
Normalized Absorbance
2.0
1.5
1.0
0.5
0.0
***
Control
Gal-8
B)
kDa
Control
Gal-8 24 hrs
135
E-Cadherin
135
N-Cadherin
35
Snail
35
GAPDH
C)
E-Cadherin/GAPDH
Normalized AU
(Fold to control)
1.5
1.0
0.5
0.0
***
Control
Gal-8
N-Cadherin/GAPDH
Normalized AU
(Fold to control)
2.5
2.0
1.5
1.0
0.5
0.0
***
Control
Gal-8
Snail/GAPDH
Normalized AU
(Fold to control)
2.0
1.5
1.0
0.5
0.0
*
Control
Gal-8
D)
kDa
Control
Gal-8
Gal-8 + AG1478
Gal-8 + PD98059
AG1478
PD98059
35
Snail
35
GAPDH
Snail/GAPDH
Normalized AU
(Fold to control)
2.5
2.0
1.5
1.0
0.5
0.0
**
**
Gal-8
Gal-8 + AG1478
Gal-8 + PD98059
AG1478
PD98059

Figure 22. Gal-8 induces proliferation and changes in EMT markers depend on ERK activity in RPTEC cells.

A) Crystal violet staining shows an increment in the cell number in RPTEC cells treated with Gal-8 (50 µg/ml) for 72 hours compared to control cells. B) Immunoblots of E-Cadherin and N-Cadherin and Snail of RPTEC cells treated with Gal-8 (50 µg/ml) for 24 hours compared to the control. C) Graphs show the quantifications of B). D) RPTEC cells were treated with Gal-8 (50 µg/ml) in the presence or absence of the MEK inhibitor PD98059 (25 µM) or EGFR inhibitor AG1478 (0,1 µM) for 24 hours. The graphs depict the quantified relative increase of Snail, measured in fold change, compared to the control (Means ± SEM n=3 three independent experiments, T Student or One-Way ANOVA with a posterior Tukey *$p<0.05$, **$p < 0.01$, ***$p<0.001$).

3.8. DRP1 is essential for proliferation and epithelial phenotype

DRP1 silenced RPTEC cells (Sh-DRP1) were used to investigate the role of DRP1 in modulating cell proliferation and EMT induced by Gal-8 (Figure 23). The results show that DRP1 silencing reduced the number of cells compared to the control, and no proliferation was observed in RPTEC Sh-DRP1 treated with Gal-8 (Figure 23A). Additionally, RPTEC Sh-DRP1 reduced the protein levels of E-cadherin and N-cadherin, accompanied by an increase in snail protein levels, suggesting that DRP1 silencing leads to a more mesenchymal phenotype (Figure 23B-C). Treatment with Gal-8 did not change the levels of E-Cadherin, N-Cadherin, Snail and Vimentin protein levels in RPTEC Sh-DRP1 (Figure 23B-C). Also, Gal-8 increased DRP1 and pERK levels in RPTEC-Sh-Control cells (Figure 23D), as well as in RPTEC-WT cells (Figure 17C). However, RPTEC-Sh-DRP1 cells show increased levels of pERK, that were decreased in the presence of Gal-8 (Figure 23D). Because DRP1 silencing affects proliferation, EMT markers and ERK signaling, it is difficult to determine the role of DRP1 in Gal-8 mediated effects. Therefore, further experiments are necessary to fully understand the role of DRP1 in proliferation and EMT induced by Gal-8.

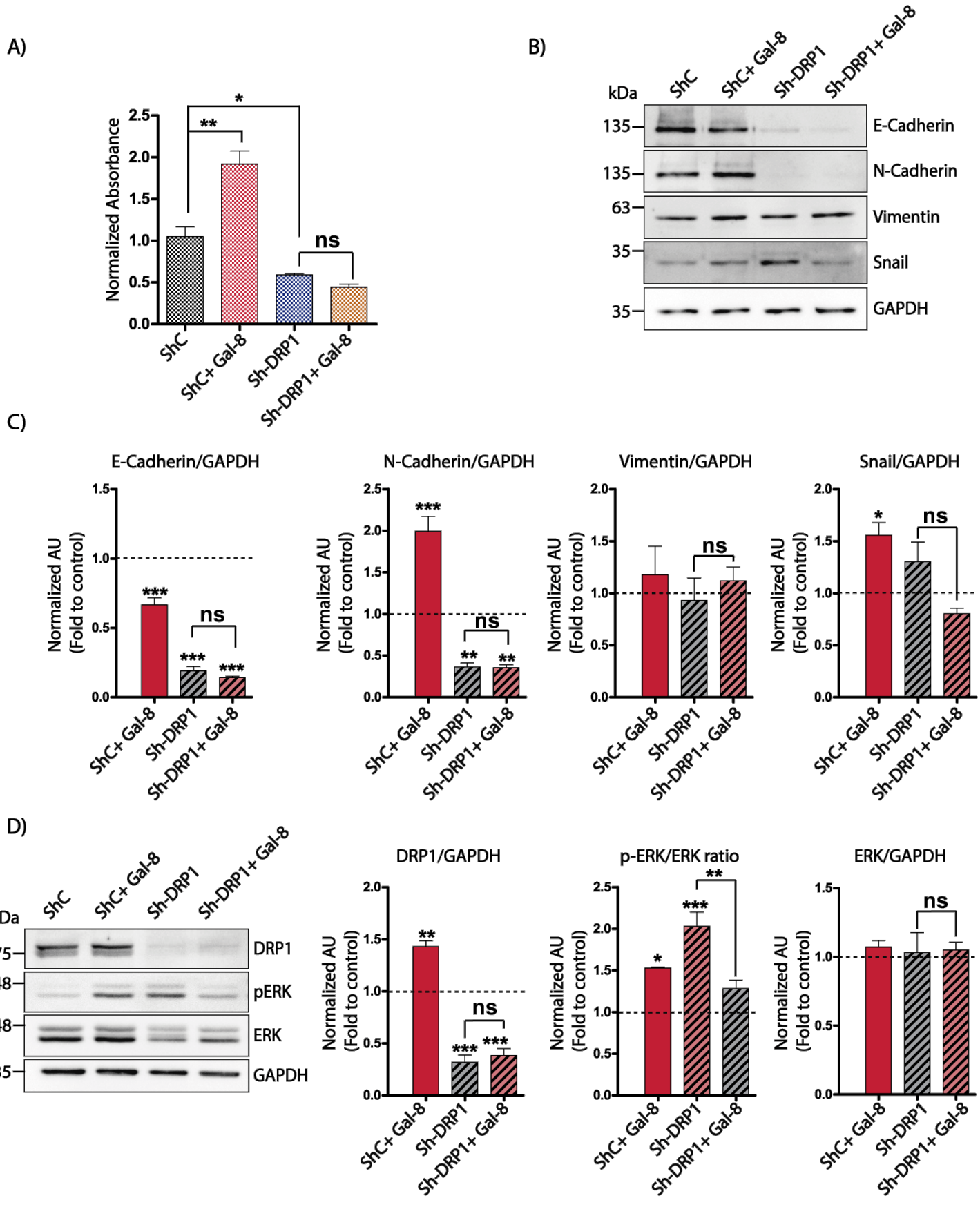
A)
Normalized Absorbance
2.5
2.0
1.5
1.0
0.5
0.0
*
**
ns
ShC
ShC+ Gal-8
Sh-DRP1
Sh-DRP1+ Gal-8
B)
kDa
ShC
ShC+ Gal-8
Sh-DRP1
Sh-DRP1+ Gal-8
135
E-Cadherin
135
N-Cadherin
63
Vimentin
35
Snail
35
GAPDH
C)
E-Cadherin/GAPDH
N-Cadherin/GAPDH
Vimentin/GAPDH
Snail/GAPDH
Normalized AU
(Fold to control)
***
**
*
ns
ShC+ Gal-8
Sh-DRP1
Sh-DRP1+ Gal-8
D)
kDa
75
DRP1
48
pERK
48
ERK
35
GAPDH
DRP1/GAPDH
p-ERK/ERK ratio
ERK/GAPDH

Figure 23. DRP1 is essential for proliferation and epithelial phenotype

A) Absorbance of crystal violet assay performed in RPTEC-Sh-Control and RPTEC-Sh-DRP1 cells treated with Gal-8 (50 µg/ml) for 72 hours. B) Immunoblots of the epithelial marker E-Cadherin, and mesenchymal markers Snail, N-Cadherin and vimentin after 24h of Gal-8 (50 µg/ml) treatment of RPTEC-Sh-Control and RPTEC-Sh-DRP1. C) The graphs depict the quantified relative changes of EMT markers, measured in fold change, compared to the control of immunoblot shown in B. D) Immunoblot detection of DRP1, p-ERK, and ERK after 24h of Gal-8 (50 µg/ml) treatment of RPTEC-Sh-Control and RPTEC-Sh-DRP1 compared to the control. The graphs depict the quantified relative changes, measured in fold change, compared to the control. (Means ± SEM, n=3, three independent experiments, One-Way ANOVA with a posterior Tukey, *$p<0.05$, **$p<0.01$, ***$p<0.001$).

IV. DISCUSSION

In this work, we have described that Gal-8 promotes mitochondrial fragmentation and redistribution to the perinuclear zone in epithelial cells (MDCK, CHO and RPTEC cells). This repositioning process is uniquely mediated by Gal-8, setting it apart from other galectins we examined. We show that mitochondrial fragmentation and redistribution to the perinuclear zone involve cell signaling pathway SRC and ERK activated by Gal-8, leading to the activation of GTPase DRP1. Mitochondrial fragmentation, redistribution and proximity to the nucleus are initiated by Gal-8 through binding to α-2-3 sialylated carbohydrate structure present in proteins on the cell surface, most likely β-1 integrin. Mitochondrial changes induced by Gal-8 affect cell metabolism, increasing cell proliferation and EMT induction. Additionally, Gal-8 promotes mitophagy and an increment in ECAR without ATP associated with OCR, suggesting metabolic reprogramming.

4.1. Role of carbohydrate and galectin in mitochondrial dynamic

In this work, we have described that Gal-8 added to the cells triggers an intracellular response, leading to mitochondrial fragmentation and redistribution of mitochondria to the perinuclear zone in a carbohydrate-dependent manner. This dependency was detected using Gal-8 mutants in its N- or C- CRD and the CHO-LEC3.2.8.1 that have N-glycosylation deficiency but conserve the ability to synthesize O-glycoproteins (Stanley, 1989). Specifically, Gal-8, through its N-terminal domain, interacts with sialylated N-glycans in the α-2,3 position, promoting mitochondrial fragmentation and perinuclear distribution. Interestingly, there are differences in mitochondrial fragmentation between CHO-WT cells and CHO-LEC3.2.8.1 cells. CHO-LEC3.2.8.1 cells have more fragmented mitochondria than the control CHO-WT cells, suggesting that modifying the glycome can impact on the mitochondrial dynamics.

Studies on the extracellular function of mitochondria-related galectins are just a few. It has been reported that Gal-1 and Gal-9 are associated to mediated apoptosis (Chiyo et al., 2019; Ion et al., 2006; Lange et al., 2009) and linked to mitochondria as a consequence of apoptosis. Nevertheless, only Gal-3 has been associated with

changes in mitochondrial dynamics (Coppin et al., 2020; Marin-Royo et al., 2018). Wang et al. reported that extracellular Gal-3 downregulates genes of the respiratory chain complex and inhibits mitochondrial biogenesis (Wang et al., 2023). Moreover, Gal-3 inhibition by citrus pectin partially prevents mitochondrial damage induced by lipotoxicity in a model of a high-fat diet in rats (Wang et al., 2023). Otherwise, the intracellular function of galectins concerning mitochondria has been studied. Gal-3 has been described as an antiapoptotic protein, where Gal-3 interacts with Bcl-2 at the mitochondria and prevents mitochondrial damage and cytochrome c release (Yu et al., 2002). Moreover, Gal-3 is present in mitochondria-associated membranes (MAM) and interacts with proteins located at the ER or mitochondrial membrane, preventing the activation and recruitment of the mitochondrial fission protein DRP1. This coordination maintains the integrity of the mitochondrial network and modulates the ER stress response (Coppin et al., 2020). Besides, it has been reported that the presence of Gal-7 at the mitochondrial membrane sensitizes the mitochondria to apoptotic stimuli (Villeneuve et al., 2011).

In this thesis, we found that Gal-8 induced mitochondrial fragmentation and redistribution to the perinuclear zone, while Gal-4 induced mitochondrial fragmentation without affecting their distribution. Notably, both galectins are classified as tandem repeats and have an affinity for glycans containing Galβ1-3GlcNAcβ. However, Gal-8 has an affinity for Galβ1-3GalNAcα and Galβ1-3GalNAcβ. In particular, the N-terminal of Gal-8 has a high affinity for sialylated glycans in the α-2,3 position, giving it a unique characteristic (Rapoport & Bovin, 2015). These data suggest that the presence of sialylated glycosylation in the α-2,3 position of glycoproteins and glycolipids on the surface of cells is necessary. The recognition of this sialylated glycosylation triggers mitochondrial fragmentation and redistribution to the perinuclear zone. Our results also show that mitochondrial fragmentation alone is insufficient to trigger the movement of mitochondria to the perinuclear zone.

We show that the N-terminal domain of Gal-8, the arginine 69, is essential to recognize glycoconjugates that contain α-2,3-sialic acid (Hirabayashi et al., 2002) and is necessary to trigger the fragmentation and redistribution to the perinuclear zone of mitochondria. However, we did not evaluate the influence of the lattice formed by Gal-8 in mitochondrial dynamics. The lattice is produced when galectins form complexes that crosslink glycosylated ligands to form a dynamic lattice (Nabi et al., 2015). The

galectin lattice regulates the diffusion, compartmentalization and endocytosis of plasma membrane glycoproteins and glycolipids. Also, it regulates the selection, activation, and arrest of T cells, receptor kinase signaling, and the functionality of membrane receptors, including the glucagon receptor, glucose, and amino acid transporters, cadherins, and integrins (Nabi et al., 2015). It would be interesting to evaluate the possible influence of the Gal-8 lattice over mitochondrial dynamics using the N- or C- terminal domain of Gal-8.

In summary, glycosylation is becoming increasingly important as it provides rapid, reversible adaptations to stressors. Altered protein glycosylation can mediate many cellular changes, including cell-cell adhesion, responsiveness to growth factors, and signal transduction programs (Taparra et al., 2016).

4.2. Gal-8 and nucleus-mitochondria communication

Our results suggest that Gal-8 could induce possible contact site mitochondria-nucleus through MFN2 that may have significant functional implications; nevertheless, to establish this contact site will be needed more experiments. Moreover, stable mitochondria-nucleus contact sites have not been described. It has been shown in electron microscopy a close association of the mitochondria with the nucleus in various cell types (Walker & Moraes, 2022). Frederic et al., described that the interaction between mitochondria-nucleus increased with the addition of 2,4-dinitrophenol, an OXPHOS uncoupler (Frederic, 1951). Prachar et al. observed mitochondria in close proximity to the nucleus and described that mitochondria can be seen perinuclearly in almost all metabolically active cells. Prachar et al. suggested the contacts between the nucleus and the mitochondria could act as an energy reservoir for mRNA and protein transport (Prachar, 2003). Dzeja et al. observed that mitochondria clustered around the nucleus, although structures in the perinuclear space hindered direct contact, and hypothesized this proximity is required due to the high-energy demands of the nucleus (Dzeja et al., 2002). ATP is required for nuclear transport, and more specifically, inhibition of OXPHOS abolishes transport, while inhibitors of glycolysis decreased ATP production but did not abolish transport (Dzeja et al., 2002). In a study by Al-Mehdi et al., hypoxia triggers the perinuclear localization of mitochondria in pulmonary artery endothelial cells (PAEC) (Al-Mehdi et al., 2012). Consequently,

reactive oxygen species (ROS) accumulate in the perinuclear and nuclear regions, introducing an oxidative base modification in hypoxia response elements of hypoxia-inducible promotors, which is important for transcriptional activation (Al-Mehdi et al., 2012). Additionally, mitochondria generate ROS influenced by factors like substrate availability, membrane potential, and oxygen levels. Disruption of respiration-related genes can elevate intracellular oxygen, leading to oxidative damage. Lower oxygen levels alleviate damage and enhance cell growth. Recent techniques confirm mitochondrial oxygen levels are lower than cytosol, suggesting nuclear oxygen levels are also regulated by mitochondria (Mori et al., 2023). This mitochondrial-nuclear oxygen dependency may impact cellular processes and cancer metabolism. Otherwise, in 2020, Desai and their collaborators reported that mitochondria cluster around the nucleus in response to proliferative stimuli and tether onto the nuclear envelope (NE) via MFN2-enriched contact points (Desai et al., 2013). This facilitates the translocation of mitochondrial pyruvate dehydrogenase complex (PDC) into the nucleus, producing acetyl-CoA and promoting histone acetylation (Zervopoulos et al., 2022).

It is necessary to conduct further studies to define the proteins involved in the contact site between mitochondria and the nucleus, as the reticulum cannot be discarded in this interaction. The proteins between mitochondria and reticulum, such as IP3Rs-Grp75-VDACs Complex, VAPB-PTPIP51 Complex, MOSPD2-PTPIP51 Complex, and/or REEP1 must be considered. More studies are necessary to put Gal-8 as a novel inductor of contact sites of mitochondria-nucleus. Also, published data show that Gal-8 promotes actin cytoskeletal rearrangements (Carcamo et al., 2006), which could stabilize the redistribution of mitochondria to the perinuclear zone and/or allow the movement of mitochondria to the nucleus.

What are the functional consequences of this proximity between the nucleus and mitochondria? The two main signaling systems that link the mitochondria and the nucleus are nucleus-to-mitochondria anterograde signaling and mitochondria-to-nucleus retrograde signaling, which comprises bi-directional communication between the mitochondria and the nucleus. The nucleus controls the proteins and information transmitted to the mitochondria by anterograde regulation. Anterograde regulation reflects different stressors through the nuclear genome reprograming which modulate mitochondria biogenesis. When cells are under stress such as calcium overloading,

oxidative pressure, and DNA damage, different stressors activate different downstream cascades, resulting in the activation of different cascades (Xia et al., 2019). Otherwise, alterations and adaptations in mitochondrial function depend heavily on the nucleus responding to signals originating at the mitochondria, a process known as “retrograde signaling” (Tang et al., 2018). The retrograde response may be stimulated by the ATP/ADP ratio, disruption of the mitochondrial membrane potential, reactive oxygen species (ROS), calcium, or general cellular stress (Xia et al., 2019).

There are a few examples of retrograde signals that show a proximity between mitochondria-nucleus and can trigger proliferation and/or EMT. It has been reported that the activation of Ca^{2+}-Calcineurin signaling induced pathways involved with EMT accompany with a proximity between mitochondria-nucleus (Guha et al., 2014). Also, it’s have been reported that the proximity between mitochondria nucleus could exchange Acetyl-CoA, a metabolite intermediate produced in the TCA cycle, lead to increased histone acetylation, promoting cell growth and proliferation (Shi & Tu, 2015). Likewise, ROS stimulates signaling cascades that promote cell proliferation, growth, and resistance to apoptosis (Porporato et al., 2018). For example, defects in Complex I lead to an accumulation of ROS, which activates Akt. Akt is recruited to the mitochondria and phosphorylates the pyruvate dehydrogenase kinase 1 (PDK1). The Akt-PDK1 axis is important for metabolic programming and cell proliferation (Sharma et al., 2011).

In summary, the data shown here suggest that Gal-8 leads to mitochondria-nucleus contact sites and that this proximity of mitochondria to the nucleus driven by Gal-8 could facilitate retrograde signals. The identity of the specific signaling molecules that can trigger the communication between mitochondria to the nucleus after Gal-8 treatment is unknown. Since mitochondria fragmentation, there could be a release of calcium, ROS and/or metabolites from mitochondria that could lead to a retrograde signal promoting proliferation and EMT.

4.3. Gal-8 and mitochondrial distribution

The cytoskeleton is a structure that helps cells maintain their shape and internal organization, and it also provides mechanical support that enables cells to carry out essential functions as spatially organizes the contents of the cell (Fletcher & Mullins,

2010). Mammalian cells must constantly reorganize the distribution of mitochondria to meet the local demands for energy, calcium, redox balance, and other mitochondrial functions. Mitochondrial localization inside the cell results from a combination of movement along the microtubule tracks and anchoring to actin filaments (Furnish & Caino, 2020). Changes in cytoskeletal organization and/or motor activities can impact mitochondrial distribution and function because mitochondria are trafficked intracellularly through the action of molecular motors operating on microtubules and actin filaments (Hu et al., 2019).

In this thesis, we show that Gal-8 triggers a perinuclear distribution of mitochondria. However, this distribution to the perinuclear zone is symmetric in MDCK and RPTEC cells but not in CHO cells, where the perinuclear distribution of mitochondria is asymmetric. Furthermore, it seems that the asymmetric cluster of perinuclear mitochondria in CHO cells is surrounded by the microtubule organizing center (MTOC). To clarify if the movement of mitochondria to the perinuclear zone is dependent on microtubules and/or actin and if there is any difference between MDCK/RPTEC and CHO cells, it is necessary to do more experiments using agents that depolymerize/destabilize the actin or microtubule networks. Further, small interference RNAs targeting the molecular motors of actin or microtubules will be necessary to elucidate the precise mechanism of mitochondrial movement.

4.4. Gal-8 activates ERK, promoting DRP1 activation leading to mitochondrial fragmentation and perinuclear redistribution

Here, we show that mitochondrial fragmentation and redistribution to the perinuclear zone induced by Gal-8 required ERK and SRC activity but were independent of the tyrosine kinase activity of EGFR. Additionally, Gal-8 promotes DRP1 activation in an ERK-dependent manner in epithelial cells. These results differ from those shown by the overexpression of Gal-8 (Oyanadel et al., 2018). In that work, it was described that Gal-8 binds to integrin and transactivates the epidermal growth receptor EGFR via FAK only in sub-confluent cells, promoting activation of ERK. However, in this study, when epithelial cells were treated with Gal-8, the activity of the tyrosine kinase activity of EGFR was not required to activate ERK and DRP1. These differences could be attributed to the modulation of the expression of a protein, which

could promote a radical change in the phenotype of the cell rather than a single treatment with an exogenous protein.

Besides integrins, other glycoproteins could be involved in the effects described for Gal-8. Unpublished data from our laboratory indicate that Gal-8 may interact with α1 Na+/K+-ATPase. Previous reports have suggested that Na+/K+-ATPase regulates SRC and ERK activity by phosphorylating the Y260 of α1 Na+/K+-ATPase (Banerjee et al., 2018). Moreover, the activation of this axis enhances proliferation, migration, wound healing (Chen et al., 2019), and enables dynamic control of aerobic glycolysis (Banerjee et al., 2018). Thus, studying the interaction between Gal-8 and α1 Na+/K+-ATPase, along with its consequent effects on SRC and ERK signaling pathways, could provide valuable insights into a potential mechanism that leads to mitochondrial fragmentation and redistribution.

4.5. Gal-8 promotes a metabolic change.

We found that Gal-8-induced changes in mitochondrial dynamics affect cellular metabolism. This is reflected in increased mitophagy and ECAR, without ATP synthesis linked to OCR. These data suggest metabolic reprogramming since there is an increase in cell proliferation and EMT induction.

Mitophagy is a specific autophagy phenomenon in which damaged, redundant and/or fragmented mitochondria are selectively cleared by autophagic lysosomes. In mitophagy, damaged or redundant mitochondria are “tagged” and surrounded by phagocytic vesicles that elongate to form a double-membranous vesicle of the autophagosome. The autophagosome fuses with the lysosome to form the autolysosome, releasing a set of potent lysosomal hydrolases to degrade enveloped mitochondria (Lin et al., 2021). Defected mitochondria produce toxic byproducts, particularly reactive oxygen species (ROS), that threaten themselves, neighboring mitochondria, and host cells. Injured mitochondria could release proapoptotic factors to induce apoptosis or self-elimination through autophagy, which helps to maintain cell viability. Mitophagy can selectively clear dysfunctional mitochondria, but if defective mitochondria are not cleared in time, they become a source of oxidative stress and damage the health of the entire mitochondrial network. Dysregulation of mitophagy

has been linked to the development of diseases and metabolic disorders (Li et al., 2017).

Keima probe is a powerful tool to monitor mitophagy. By targeting Keima to the mitochondria, changes in the pH of the mitochondrial environment can be monitored and correlated with the degree of mitophagy. In this case, an acidic environment, such as that found in lysosomes, will cause Keima to emit light at a longer wavelength than in a neutral pH environment (Katayama et al., 2011). The results obtained with the Keima probe in MDCK cells treated with Gal-8 show an increased level of red punctate Keima, indicating an increase in mitophagy that was dependent on the N-terminal domain of Gal-8. It would be attractive to link this mitophagy to a selective form, such as bit-by-bit mitophagy, where mitochondria actively shed dysfunctional protein components before overt dysfunction ensues (Yang & Yang, 2013). Ultimately, this could lead to new therapeutic approaches for diseases involving mitochondrial dysfunction.

Furthermore, we aim to investigate whether treatment with Gal-8, which results in increased mitochondrial fragmentation, the relocation of mitochondria to the perinuclear zone, and the induction of mitophagy, subsequently affects mitochondrial function. For this purpose, we performed a Seahorse Cell Mito Stress Test to measure mitochondrial function as oxygen consumption rate - OCR, where Gal-8 treatment led to less production of ATP linked to the mitochondria respiration and increased levels of proton leak, compared to the control. Also, we performed a Seahorse Real-Time ATP Rate assay, where treatment with Gal-8 shows an increase in ECAR, but not on OCR, compared to the control.

In summary, the data from the Seahorse Cell Mito Stress Test shows that cells treated with Gal-8 maintain the OCR. However, it does not lead to the production of ATP. Since, even in the presence of an ATP synthase inhibitor, Oligomycin, the OCR is stable in time. This data suggests that the ETC is working but not producing ATP. Further experiments are necessary to corroborate the total and ATP production in an enriched mitochondrial fraction. A function of ETC not associated with ATP synthesis is modulate ROS (Mills et al., 2016). ROS are generated by incomplete reduction of molecular oxygen during oxidative phosphorylation. It has been suggested that during the transfer of electrons, 1–5% will ‘escape’ the OXPHOS system and participate in forming super-oxides that are more readily released by mitochondria. CI and CIII,

especially CI, are considered to be the main sites of ROS production in mitochondria (Kowaltowski et al., 2009). The amount of ROS generated from a stimulus determines whether ROS plays beneficial or harmful roles, which means different physiological or pathological pathways are activated. ROS could act through the oxidative modification of numerous types of proteins, particularly receptors, kinases, phosphatases, caspases, ion channels and transcription factors (Zhao et al., 2019). Moreover, our results show a more proton leak in Gal-8 treated cells. Proton leak occurs when protons return to the matrix independently of ATP synthase (Jastroch et al., 2010). The existence of a feedback loop between ROS and proton leak has been reported. Where proton leak decreases ROS generation, whereas ROS have been shown to induce proton leak (Brookes, 2005). Interestingly, although proton leak is detrimental to ATP synthesis, several recent reports have identified mitochondrial uncoupling as a cytoprotective strategy, especially in the heart and brain, under conditions of oxidative stress such as diabetes, I-R injury, or aging (Brookes, 2005). Therefore, it will be attractive to determine ROS production as a signaling molecule modulated by Gal-8. We still need to determine whether Gal-8 induces an increase in ROS and if this is the mitochondria-nucleus retrograde signal responsible for the effects on proliferation and EMT.

Finally, a Seahorse Real-Time ATP Rate assay determined that Gal-8 increases ECAR, but not in basal OCR, compared to the control. This data suggests that Gal-8 can induce a change in the metabolic rate of the epithelial cells. However, further experiments are required to ascertain the metabolic effects on cells treated with Gal-8. Since ECAR is proportional to glycolysis, ECAR is not a direct measurement of glycolysis (Schmidt et al., 2021). In order to establish a glycolytic phenotype induced by Gal-8, we require an additional Seahorse test called Seahorse XF Glycolytic Rate Assay Kit. This kit accurately measures glycolysis in living cells, allowing us to observe quick metabolic changes and temporary responses (Qing et al., 2021). Additionally, this test reveals how cells can compensate for inhibited mitochondrial respiration through glycolysis. Furthermore, it is necessary to determine if there is more use of glucose, measurement by GLUTs transporters, and glycolytic enzymes.

4.6. Gal-8, mitochondrial dynamics and EMT induction

Currently, the role of galectins in mitochondrial dynamics in the context of cell proliferation and EMT remains unexplored. Consequently, delineating the relationship between Gal-8 mediated mitochondrial dynamics and the processes of proliferation and EMT would be a significant advance in the field. Here we show that Gal-8 promotes proliferation and expression of NF-κB, concomitant with EMT markers in epithelial cells.

It has been shown that activation of the NF-κB pathway is the major signal for the stabilization of Snail and the induction of EMT (Lee et al., 2020). Activation of NF-κB correlated with the level of Snail in breast cancer cell lines and tumor samples (Wu et al., 2009). Also, the signaling pathway between Snail and NF-κB is highly conserved from fly to mammal (Julien et al., 2007). Snail has been shown to be increased at the transcriptional level by the NF-κB pathway (Julien et al., 2007). Also, the stabilization of Snail occurred at the post-translational level. Therefore, it is likely that NF-κB regulates the activity of Snail through both transcriptional and post-translational mechanisms during EMT (Huber et al., 2004). Furthermore, NF-κB pathway controls mitochondrial dynamics. A study by Laforge et al., demonstrate that the absence of IκB kinase-α, which is a key element of the nonclassical NF-κB pathway, has an impact on the mitochondrial network morphology and OPA1 expression, driven by a more fragmented mitochondria phenotype (Laforge et al., 2016). On the other hand, NF-κB has the ability to regulate cell metabolism, acting both on glycolysis and OXPHOS (Mauro et al., 2011). It has been reported that the inhibition of NF-κB causes cellular reprogramming to aerobic glycolysis under basal conditions. Otherwise, NF-κB stimulates oxidative phosphorylation by upregulating mitochondrial synthesis of cytochrome c oxidase 2 (Mauro et al., 2011). Since it depends on the interaction through carbohydrates, we can hypothesize that mitochondrial fragmentation and redistribution to the perinuclear zone driven by Gal-8 could control the expression of NF-κB and, with that, proliferation, EMT progression, and the cell metabolic state.

Otherwise, Gal-8 promotes an increment of Snail depending on ERK activity but not on tyrosine kinase activity of EGFR. Numerous studies have focused on the activation of Snail in cancer cells through the EGFR/SRC/ERK pathway. They describe that SRC activation is primarily regulated by receptor tyrosine kinases and

by the direct binding of FAK to the SH2 domain (Aleshin & Finn, 2010). In contrast, integrin could activate the axis SRC/ERK and lead to Snail expression, independent of EGFR (Badarinath et al., 2022). A study by Banerjee et al. shows that α1 Na/K-ATPase phosphorylate SRC in Y260 and active ERK (Banerjee et al., 2018), downregulated snail expression (Rajasekaran et al., 2010).

On the other hand, it has recently been reported that mitochondrial fragmentation mediated bioenergetic alteration and EMT invasion in cancer cells (Ghosh et al., 2023). According to a study conducted by Ghosh, Ets-1, an oncoprotein belonging to the Ets family, is a well-known promoter of EMT. It promotes mitochondrial fragmentation by enhancing DRP1 through direct binding at the DNM1L (DRP1) promoter in ovarian cancer cells (Ghosh et al., 2023). Interestingly, our results show a correlation between increased levels of DRP1, mitochondrial fragmentation, and EMT induction in Gal-8 treated cells. However, MDCK cells induce mitochondrial fragmentation via phosphorylation at Serine 616 of DRP1, whereas RPTEC cells achieve this through upregulation of DRP1 levels. But both types of cells have the same outcome with Gal-8 treatment, mitochondria fragmentation, redistribution of mitochondria to the perinuclear zone, and increased proliferation and EMT markers. DRP1 activation and subsequent mitochondrial fragmentation are triggered not only by phosphorylation at Serine 616 but also by an accumulation of DRP1, S-Nitrosylation at Cysteine 644, phosphorylation at Serine 656, and less frequently studied phosphorylation at Serine residues 579, 585, 592, and 693 (Zerihun et al., 2023).

Additionally, we want to study the relationship between DRP1, proliferation, and EMT induction by Gal-8 to determine if DRP1 is essential to promote mitochondrial fragmentation and control proliferation and EMT driven by Gal-8 in epithelial cells. For this purpose, DRP1 was silenced in RPTEC cells. Our results show that Gal-8 promotes EMT and proliferation in RPTEC and MDCK cells as previously described (Oyanadel et al., 2018). However, silencing DRP1 in RPTEC promotes a more mesenchymal phenotype and a dramatic reduction in N- and E- Cadherin protein levels, accompanied by an increment of Snail and a reduction in cell proliferation. Certainly, it has been shown that DRP1 knockdown reduces proliferation and promotes apoptosis. Inoue-Yamauchi and Oda have demonstrated that DRP1 knockdown in human colon cancer cells resulted in significantly reduced proliferation, increased percentage of cells in the sub-G0/G1 cell cycle phase, caspase-3 activation,

and apoptosis. Interestingly, a reduction in mitochondrial membrane potential was also observed, which may explain the cytochrome c release in apoptosis following caspase activation (Inoue-Yamauchi & Oda, 2012). Parone et al. showed that downregulation of DRP1 in HeLa cell lines causes mitochondrial dysfunction, with an increase in ROS levels, a loss of mtDNA, a reduction in cellular ATP, proliferation arrest, and autophagy (Parone et al., 2008). Zhan et al. have shown that DRP1 knockdown induced a significant G1 phase arrest in vitro, and reduced tumor growth in vivo (Zhan et al., 2016). Therefore, it seems that cellular homeostasis depends on DRP1-dependent mitochondrial fission. To determine whether Gal-8 promotes EMT driven by the mitochondrial fission machinery, a less aggressive approach is needed. For this, the inactive DRP1 form of its GTPase activity, DRP1 K38A, will be necessary.

In summary, mitochondria serve as primary energy production centers within cells. In addition to driving respiration and ATP synthesis, they play pivotal roles in regulating cellular functions, including cell death, differentiation, signaling, inflammation, and anabolism (Trinchese et al., 2024). Mitochondrial integrity, efficiency, and dynamics are referred to as “Mitochondrial fitness”. Mitochondrial fitness led to an appropriate response and maintained cellular homeostasis. This concept emphasizes the crucial role of mitochondria in cells and how the proper function of mitochondria can prevent malfunctions in cells and regulate apoptosis (Clemente-Suarez et al., 2023). Given their critical importance, mitochondria necessitate constant surveillance to uphold functional integrity. Several mechanisms are involved in mitochondrial quality control, encompassing mitochondrial dynamics, the mitochondrial unfolded protein response (UPR), and the selective degradation of damaged mitochondria via mitophagy (Guo et al., 2024). Importantly, dysregulation of these processes has been implicated in the onset and progression of various diseases, such as metabolic disorders, inflammatory conditions, cancer, sarcopenia, and aging (Guo et al., 2024; Qin et al., 2024).

The comprehensive dataset in this thesis suggests that Gal-8-induced fragmentation of mitochondria enhances mitochondrial function, synonyms of mitochondrial fitness. The improvement of mitochondrial fitness by Gal-8 is evidenced by the lack of change in mitochondrial integrity and the basal respiration observed in Seahorse assay measurements following Gal-8 treatment. Furthermore, Gal-8

promotes mitochondrial degradation, correlating with increased cell proliferation. The interpretation of these findings varies depending on the cellular context, owing to the multifaceted roles of mitochondria and their potential dysfunctions. In a cancer context, enhanced mitochondrial fitness is pivotal for cancer development (Kossenkov et al., 2022). Similarly, maintaining healthy mitochondria is crucial for sustaining metabolic processes and regulating cellular apoptosis during tissue repair. However, in the presence of chronic inflammation, mitochondria may struggle to support and regulate cells, potentially impairing tissue regeneration and causing damage to the affected organ (Clemente-Suarez et al., 2023; Guo et al., 2024).

V. CONCLUSIONS

- Gal-8 promotes mitochondrial fragmentation and redistribution of mitochondria to the perinuclear zone involving carbohydrate recognition, ERK and DRP1 activity in epithelial cells.
- Gal-8 promotes mitophagy in a carbohydrate-dependent manner in MDCK cells.
- Gal-8 impacts mitochondrial function, increasing ECAR, without ATP synthesis linked to OCR in MDCK cells.
- Gal-8 induces proliferation, NF-κB expression depending on carbohydrate recognition, and EMT depending on ERK activity in epithelial cells.
- DRP1 is essential for epithelial phenotype.

VI. PROPOSED MODEL

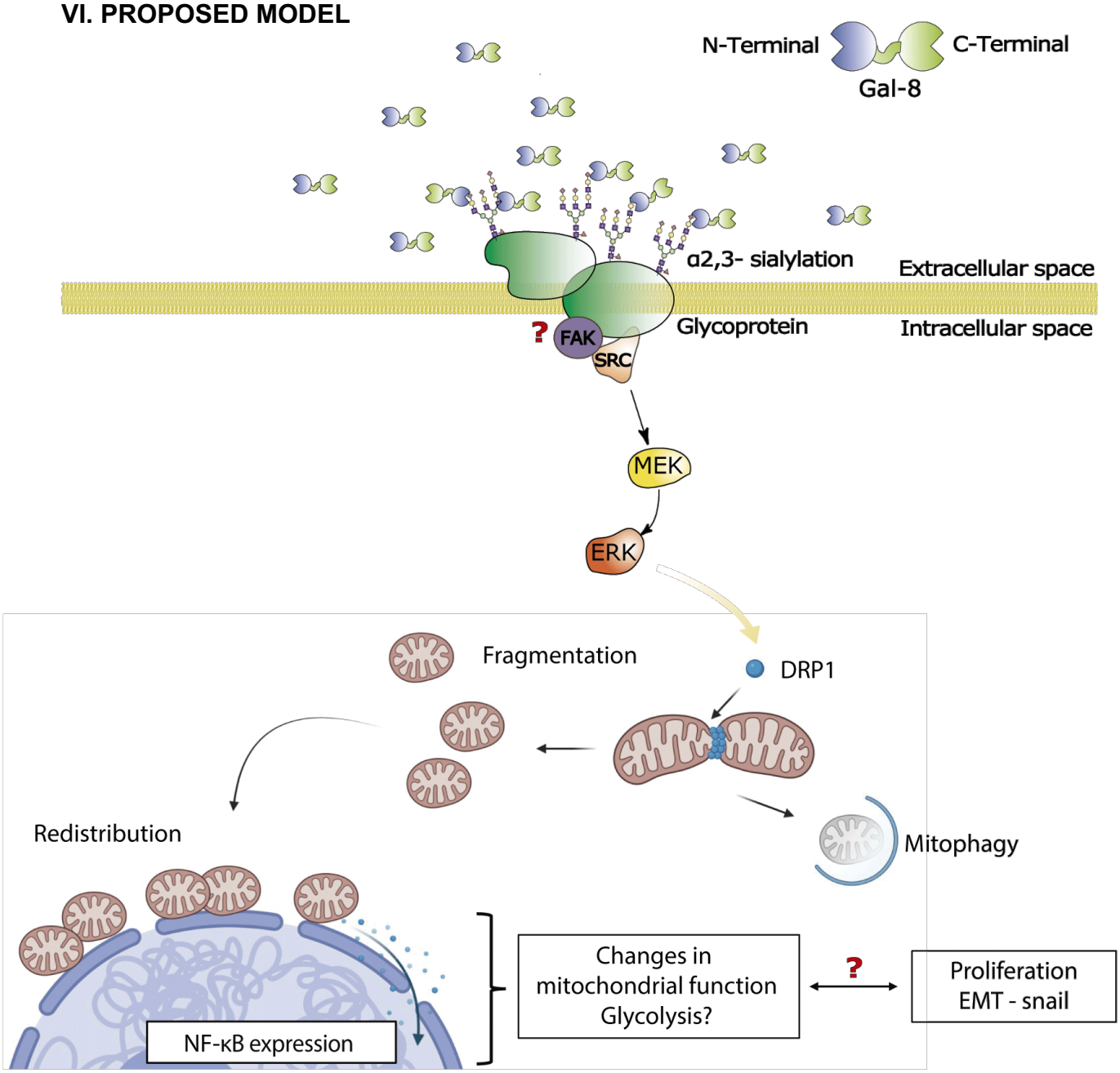

Figure 24. Proposed model.

Gal-8 binds through its N-terminal domain to α-2,3 sialylation proteins on the cell surface, triggering SRC and ERK kinase activation, leading to DRP1 activation. This pathway promotes mitochondrial fragmentation, redistribution of mitochondria to the perinuclear zone. Also, Gal-8 promotes NF-kB expression, cell proliferation and mitophagy coupled with an increase in ECAR without ATP synthesis linked to OCR. This suggests that Gal-8 may shift cellular metabolism toward a more glycolytic phenotype.

VII. PROYECTIONS

- Characterize the contact sites between mitochondria and nucleus induced by Gal-8
- Identify the molecules responsible for communication between mitochondria and nucleus after Gal-8 treatment and their implications on proliferation and EMT.
- Identify the plasma membrane glycoproteins that bind Gal-8 to activate the SRC/ERK pathway and the consequent changes in mitochondrial dynamics.
- Analyze changes in the metabolic profile after Gal-8 treatment
- Investigate mitochondrial dynamics to assess its influence on proliferation and EMT.
- Analyze the Mass Spectrometry and defined new possible proteins interaction with Gal-8

VIII. REFERENCES

Al-Mehdi, A. B., Pastukh, V. M., Swiger, B. M., Reed, D. J., Patel, M. R., Bardwell, G. C., Pastukh, V. V., Alexeyev, M. F., & Gillespie, M. N. (2012). Perinuclear mitochondrial clustering creates an oxidant-rich nuclear domain required for hypoxia-induced transcription. *Sci Signal*, *5*(231), ra47. https://doi.org/10.1126/scisignal.2002712

Aleshin, A., & Finn, R. S. (2010). SRC: a century of science brought to the clinic. *Neoplasia*, *12*(8), 599-607. https://doi.org/10.1593/neo.10328

Anderson, C. C., Aivazidis, S., Kuzyk, C. L., Jain, A., & Roede, J. R. (2018). Acute Maneb Exposure Significantly Alters Both Glycolysis and Mitochondrial Function in Neuroblastoma Cells. *Toxicol Sci*, *165*(1), 61-73. https://doi.org/10.1093/toxsci/kfy116

Anesti, V., & Scorrano, L. (2006). The relationship between mitochondrial shape and function and the cytoskeleton. *Biochim Biophys Acta*, *1757*(5-6), 692-699. https://doi.org/10.1016/j.bbabio.2006.04.013

Badarinath, K., Dam, B., Kataria, S., Zirmire, R. K., Dey, R., Kansagara, G., Ajnabi, J., Hegde, A., Singh, R., Masudi, T., Sambath, J., Sachithanandan, S. P., Kumar, P., Gulyani, A., He, Y. W., Krishna, S., & Jamora, C. (2022). Snail maintains the stem/progenitor state of skin epithelial cells and carcinomas through the autocrine effect of matricellular protein Mindin. *Cell Rep*, *40*(12), 111390. https://doi.org/10.1016/j.celrep.2022.111390

Banerjee, M., Cui, X., Li, Z., Yu, H., Cai, L., Jia, X., He, D., Wang, C., Gao, T., & Xie, Z. (2018). Na/K-ATPase Y260 Phosphorylation-mediated Src Regulation in Control of Aerobic Glycolysis and Tumor Growth. *Sci Rep*, *8*(1), 12322. https://doi.org/10.1038/s41598-018-29995-2

Barake, F., Soza, A., & Gonzalez, A. (2020). Galectins in the brain: advances in neuroinflammation, neuroprotection and therapeutic opportunities. *Curr Opin Neurol*, *33*(3), 381-390. https://doi.org/10.1097/WCO.0000000000000812

Bergman, O., & Ben-Shachar, D. (2016). Mitochondrial Oxidative Phosphorylation System (OXPHOS) Deficits in Schizophrenia: Possible Interactions with Cellular Processes. *Can J Psychiatry*, *61*(8), 457-469. https://doi.org/10.1177/0706743716648290

Brookes, P. S. (2005). Mitochondrial H(+) leak and ROS generation: an odd couple. *Free Radic Biol Med*, *38*(1), 12-23. https://doi.org/10.1016/j.freeradbiomed.2004.10.016

Cagnoni, A. J., Troncoso, M. F., Rabinovich, G. A., Marino, K. V., & Elola, M. T. (2020). Full-length galectin-8 and separate carbohydrate recognition domains: the whole is greater than the sum of its parts? *Biochem Soc Trans*, *48*(3), 1255-1268. https://doi.org/10.1042/BST20200311

Carcamo, C., Pardo, E., Oyanadel, C., Bravo-Zehnder, M., Bull, P., Caceres, M., Martinez, J., Massardo, L., Jacobelli, S., Gonzalez, A., & Soza, A. (2006). Galectin-8 binds specific beta1 integrins and induces polarized spreading highlighted by asymmetric lamellipodia in Jurkat T cells. *Exp Cell Res*, *312*(4), 374-386. https://doi.org/10.1016/j.yexcr.2005.10.025

Chang, C. R., & Blackstone, C. (2010). Dynamic regulation of mitochondrial fission through modification of the dynamin-related protein Drp1. *Ann N Y Acad Sci*, *1201*, 34-39. https://doi.org/10.1111/j.1749-6632.2010.05629.x

Che, T. F., Lin, C. W., Wu, Y. Y., Chen, Y. J., Han, C. L., Chang, Y. L., Wu, C. T., Hsiao, T. H., Hong, T. M., & Yang, P. C. (2015). Mitochondrial translocation of EGFR regulates mitochondria dynamics and promotes metastasis in NSCLC. *Oncotarget*, *6*(35), 37349-37366. https://doi.org/10.18632/oncotarget.5736

Chen, H., & Chan, D. C. (2017). Mitochondrial Dynamics in Regulating the Unique Phenotypes of Cancer and Stem Cells. *Cell Metab*, *26*(1), 39-48. https://doi.org/10.1016/j.cmet.2017.05.016

Chen, H., Detmer, S. A., Ewald, A. J., Griffin, E. E., Fraser, S. E., & Chan, D. C. (2003). Mitofusins Mfn1 and Mfn2 coordinately regulate mitochondrial fusion and are essential for embryonic development. *J Cell Biol*, *160*(2), 189-200. https://doi.org/10.1083/jcb.200211046

Chen, L., Jiang, P., Li, J., Xie, Z., Xu, Y., Qu, W., Feng, F., & Liu, W. (2019). Periplocin promotes wound healing through the activation of Src/ERK and PI3K/Akt pathways mediated by Na/K-ATPase. *Phytomedicine*, *57*, 72-83. https://doi.org/10.1016/j.phymed.2018.12.015

Chen, W., Zhao, H., & Li, Y. (2023). Mitochondrial dynamics in health and disease: mechanisms and potential targets. *Signal Transduct Target Ther*, *8*(1), 333. https://doi.org/10.1038/s41392-023-01547-9

Chiaradonna, F., Ricciardiello, F., & Palorini, R. (2018). The Nutrient-Sensing Hexosamine Biosynthetic Pathway as the Hub of Cancer Metabolic Rewiring. *Cells*, *7*(6). https://doi.org/10.3390/cells7060053

Chiyo, T., Fujita, K., Iwama, H., Fujihara, S., Tadokoro, T., Ohura, K., Matsui, T., Goda, Y., Kobayashi, N., Nishiyama, N., Yachida, T., Morishita, A., Kobara, H., Mori, H., Niki, T., Hirashima, M., Himoto, T., & Masaki, T. (2019). Galectin-9 Induces Mitochondria-Mediated Apoptosis of Esophageal Cancer In Vitro and In Vivo in a Xenograft Mouse Model. *Int J Mol Sci*, *20*(11). https://doi.org/10.3390/ijms20112634

Clemente-Suarez, V. J., Martin-Rodriguez, A., Redondo-Florez, L., Ruisoto, P., Navarro-Jimenez, E., Ramos-Campo, D. J., & Tornero-Aguilera, J. F. (2023). Metabolic Health, Mitochondrial Fitness, Physical Activity, and Cancer. *Cancers (Basel)*, *15*(3). https://doi.org/10.3390/cancers15030814

Collins, T. J., Berridge, M. J., Lipp, P., & Bootman, M. D. (2002). Mitochondria are morphologically and functionally heterogeneous within cells. *EMBO J*, *21*(7), 1616-1627. https://doi.org/10.1093/emboj/21.7.1616

Coppin, L., Jannin, A., Ait Yahya, E., Thuillier, C., Villenet, C., Tardivel, M., Bongiovanni, A., Gaston, C., de Beco, S., Barois, N., van Seuningen, I., Durand, E., Bonnefond, A., Vienne, J. C., Vamecq, J., Figeac, M., Vincent, A., Delacour, D., Porchet, N., & Pigny, P. (2020). Galectin-3 modulates epithelial cell adaptation to stress at the ER-mitochondria interface. *Cell Death Dis*, *11*(5), 360. https://doi.org/10.1038/s41419-020-2556-3

Cribbs, J. T., & Strack, S. (2007). Reversible phosphorylation of Drp1 by cyclic AMP-dependent protein kinase and calcineurin regulates mitochondrial fission and cell death. *EMBO Rep*, *8*(10), 939-944. https://doi.org/10.1038/sj.embor.7401062

Cummings, R. D. (2009). The repertoire of glycan determinants in the human glycome. *Mol Biosyst*, *5*(10), 1087-1104. https://doi.org/10.1039/b907931a

Davies, V. J., Hollins, A. J., Piechota, M. J., Yip, W., Davies, J. R., White, K. E., Nicols, P. P., Boulton, M. E., & Votruba, M. (2007). Opa1 deficiency in a mouse model of autosomal dominant optic atrophy impairs mitochondrial morphology, optic nerve structure and visual function. *Hum Mol Genet*, *16*(11), 1307-1318. https://doi.org/10.1093/hmg/ddm079

DeBerardinis, R. J., & Chandel, N. S. (2020). We need to talk about the Warburg effect. *Nat Metab*, *2*(2), 127-129. https://doi.org/10.1038/s42255-020-0172-2

Desai, S. P., Bhatia, S. N., Toner, M., & Irimia, D. (2013). Mitochondrial localization and the persistent migration of epithelial cancer cells. *Biophys J*, *104*(9), 2077-2088. https://doi.org/10.1016/j.bpj.2013.03.025

Diskin, S., Chen, W. S., Cao, Z., Gyawali, S., Gong, H., Soza, A., Gonzalez, A., & Panjwani, N. (2012). Galectin-8 promotes cytoskeletal rearrangement in trabecular meshwork cells through activation of Rho signaling. *PLoS One*, *7*(9), e44400. https://doi.org/10.1371/journal.pone.0044400

Dube, D. H., & Bertozzi, C. R. (2005). Glycans in cancer and inflammation--potential for therapeutics and diagnostics. *Nat Rev Drug Discov*, *4*(6), 477-488. https://doi.org/10.1038/nrd1751

Dzeja, P. P., Bortolon, R., Perez-Terzic, C., Holmuhamedov, E. L., & Terzic, A. (2002). Energetic communication between mitochondria and nucleus directed by catalyzed phosphotransfer. *Proc Natl Acad Sci U S A*, *99*(15), 10156-10161. https://doi.org/10.1073/pnas.152259999

Eberhardt, E. L., Ludlam, A. V., Tan, Z., & Cianfrocco, M. A. (2020). Miro: A molecular switch at the center of mitochondrial regulation. *Protein Sci*, *29*(6), 1269-1284. https://doi.org/10.1002/pro.3839

Elola, M. T., Ferragut, F., Cardenas Delgado, V. M., Nugnes, L. G., Gentilini, L., Laderach, D., Troncoso, M. F., Compagno, D., Wolfenstein-Todel, C., & Rabinovich, G. A. (2014). Expression, localization and function of galectin-8, a tandem-repeat lectin, in human tumors. *Histol Histopathol*, *29*(9), 1093-1105. https://doi.org/10.14670/HH-29.1093

Ferro, F., Servais, S., Besson, P., Roger, S., Dumas, J. F., & Brisson, L. (2020). Autophagy and mitophagy in cancer metabolic remodelling. *Semin Cell Dev Biol*, *98*, 129-138. https://doi.org/10.1016/j.semcdb.2019.05.029

Flannery, P. J., & Trushina, E. (2019). Mitochondrial dynamics and transport in Alzheimer's disease. *Mol Cell Neurosci*, *98*, 109-120. https://doi.org/10.1016/j.mcn.2019.06.009

Fletcher, D. A., & Mullins, R. D. (2010). Cell mechanics and the cytoskeleton. *Nature*, *463*(7280), 485-492. https://doi.org/10.1038/nature08908

Frederic, J. (1951). [Relation between the nuclear membrane and nucleoli and mitochondria; study of living and contrast phase]. *C R Seances Soc Biol Fil*, *145*(23-24), 1913-1916. https://www.ncbi.nlm.nih.gov/pubmed/14936368 (Rapports de la membrane nucleaire avec les nucleoles et les chondriomes; etude sur le vivant et en contraste de phase.)

Furnish, M., & Caino, M. C. (2020). Altered mitochondrial trafficking as a novel mechanism of cancer metastasis. *Cancer Rep (Hoboken)*, *3*(1), e1157. https://doi.org/10.1002/cnr2.1157

Gentilini, L. D., Jaworski, F. M., Tiraboschi, C., Perez, I. G., Kotler, M. L., Chauchereau, A., Laderach, D. J., & Compagno, D. (2017). Stable and high expression of Galectin-8 tightly controls metastatic progression of prostate cancer. *Oncotarget*, *8*(27), 44654-44668. https://doi.org/10.18632/oncotarget.17963

Georgakopoulos, N. D., Wells, G., & Campanella, M. (2017). The pharmacological regulation of cellular mitophagy. *Nat Chem Biol*, *13*(2), 136-146. https://doi.org/10.1038/nchembio.2287

Ghosh, D., Pakhira, S., Ghosh, D. D., Roychoudhury, S., & Roy, S. S. (2023). Ets1 facilitates EMT/invasion through Drp1-mediated mitochondrial fragmentation in ovarian cancer. *iScience*, *26*(9), 107537. https://doi.org/10.1016/j.isci.2023.107537

Gomes, L. C., Di Benedetto, G., & Scorrano, L. (2011). During autophagy mitochondria elongate, are spared from degradation and sustain cell viability. *Nat Cell Biol*, *13*(5), 589-598. https://doi.org/10.1038/ncb2220

Guha, M., Srinivasan, S., Ruthel, G., Kashina, A. K., Carstens, R. P., Mendoza, A., Khanna, C., Van Winkle, T., & Avadhani, N. G. (2014). Mitochondrial retrograde signaling induces epithelial-mesenchymal transition and generates breast cancer stem cells. *Oncogene*, *33*(45), 5238-5250. https://doi.org/10.1038/onc.2013.467

Guo, Y., Che, R., Wang, P., & Zhang, A. (2024). Mitochondrial dysfunction in the pathophysiology of renal diseases. *Am J Physiol Renal Physiol*. https://doi.org/10.1152/ajprenal.00189.2023

Guttridge, D. C., Albanese, C., Reuther, J. Y., Pestell, R. G., & Baldwin, A. S., Jr. (1999). NF-kappaB controls cell growth and differentiation through

transcriptional regulation of cyclin D1. *Mol Cell Biol*, *19*(8), 5785-5799. https://doi.org/10.1128/MCB.19.8.5785

Hirabayashi, J., Hashidate, T., Arata, Y., Nishi, N., Nakamura, T., Hirashima, M., Urashima, T., Oka, T., Futai, M., Muller, W. E., Yagi, F., & Kasai, K. (2002). Oligosaccharide specificity of galectins: a search by frontal affinity chromatography. *Biochim Biophys Acta*, *1572*(2-3), 232-254. https://doi.org/10.1016/s0304-4165(02)00311-2

Hong, M. H., Weng, I. C., Li, F. Y., Lin, W. H., & Liu, F. T. (2021). Intracellular galectins sense cytosolically exposed glycans as danger and mediate cellular responses. *J Biomed Sci*, *28*(1), 16. https://doi.org/10.1186/s12929-021-00713-x

Hoyer, M. J., Swarup, S., & Harper, J. W. (2022). Mechanisms Controlling Selective Elimination of Damaged Lysosomes. *Curr Opin Physiol*, *29*. https://doi.org/10.1016/j.cophys.2022.100590

Hu, H. H., Kannengiesser, C., Lesage, S., Andre, J., Mourah, S., Michel, L., Descamps, V., Basset-Seguin, N., Bagot, M., Bensussan, A., Lebbe, C., Deschamps, L., Saiag, P., Leccia, M. T., Bressac-de-Paillerets, B., Tsalamlal, A., Kumar, R., Klebe, S., Grandchamp, B., . . . Soufir, N. (2016). PARKIN Inactivation Links Parkinson's Disease to Melanoma. *J Natl Cancer Inst*, *108*(3). https://doi.org/10.1093/jnci/djv340

Hu, M., Schulze, K. E., Ghildyal, R., Henstridge, D. C., Kolanowski, J. L., New, E. J., Hong, Y., Hsu, A. C., Hansbro, P. M., Wark, P. A., Bogoyevitch, M. A., & Jans, D. A. (2019). Respiratory syncytial virus co-opts host mitochondrial function to favour infectious virus production. *Elife*, *8*. https://doi.org/10.7554/eLife.42448

Huang, C. Y., Lai, C. H., Kuo, C. H., Chiang, S. F., Pai, P. Y., Lin, J. Y., Chang, C. F., Viswanadha, V. P., Kuo, W. W., & Huang, C. Y. (2018). Inhibition of ERK-Drp1 signaling and mitochondria fragmentation alleviates IGF-IIR-induced mitochondria dysfunction during heart failure. *J Mol Cell Cardiol*, *122*, 58-68. https://doi.org/10.1016/j.yjmcc.2018.08.006

Huber, M. A., Beug, H., & Wirth, T. (2004). Epithelial-mesenchymal transition: NF-kappaB takes center stage. *Cell Cycle*, *3*(12), 1477-1480. https://doi.org/10.4161/cc.3.12.1280

Inoue-Yamauchi, A., & Oda, H. (2012). Depletion of mitochondrial fission factor DRP1 causes increased apoptosis in human colon cancer cells. *Biochem Biophys Res Commun*, *421*(1), 81-85. https://doi.org/10.1016/j.bbrc.2012.03.118

Ion, G., Fajka-Boja, R., Kovacs, F., Szebeni, G., Gombos, I., Czibula, A., Matko, J., & Monostori, E. (2006). Acid sphingomyelinase mediated release of ceramide is essential to trigger the mitochondrial pathway of apoptosis by galectin-1. *Cell Signal*, *18*(11), 1887-1896. https://doi.org/10.1016/j.cellsig.2006.02.007

Jastroch, M., Divakaruni, A. S., Mookerjee, S., Treberg, J. R., & Brand, M. D. (2010). Mitochondrial proton and electron leaks. *Essays Biochem*, *47*, 53-67. https://doi.org/10.1042/bse0470053

Jia, J., Abudu, Y. P., Claude-Taupin, A., Gu, Y., Kumar, S., Choi, S. W., Peters, R., Mudd, M. H., Allers, L., Salemi, M., Phinney, B., Johansen, T., & Deretic, V. (2018). Galectins Control mTOR in Response to Endomembrane Damage. *Mol Cell*, *70*(1), 120-135 e128. https://doi.org/10.1016/j.molcel.2018.03.009

Jia, J., Abudu, Y. P., Claude-Taupin, A., Gu, Y., Kumar, S., Choi, S. W., Peters, R., Mudd, M. H., Allers, L., Salemi, M., Phinney, B., Johansen, T., & Deretic, V. (2019). Galectins control MTOR and AMPK in response to lysosomal damage to induce autophagy. *Autophagy*, *15*(1), 169-171. https://doi.org/10.1080/15548627.2018.1505155

Jia, J., Claude-Taupin, A., Gu, Y., Choi, S. W., Peters, R., Bissa, B., Mudd, M. H., Allers, L., Pallikkuth, S., Lidke, K. A., Salemi, M., Phinney, B., Mari, M., Reggiori, F., & Deretic, V. (2020). Galectin-3 Coordinates a Cellular System for Lysosomal Repair and Removal. *Dev Cell*, *52*(1), 69-87 e68. https://doi.org/10.1016/j.devcel.2019.10.025

Johannes, L., Jacob, R., & Leffler, H. (2018). Galectins at a glance. *J Cell Sci*, *131*(9). https://doi.org/10.1242/jcs.208884

Julien, S., Puig, I., Caretti, E., Bonaventure, J., Nelles, L., van Roy, F., Dargemont, C., de Herreros, A. G., Bellacosa, A., & Larue, L. (2007). Activation of NF-kappaB by Akt upregulates Snail expression and induces epithelium mesenchyme transition. *Oncogene*, *26*(53), 7445-7456. https://doi.org/10.1038/sj.onc.1210546

Kaelin, W. G., Jr., & McKnight, S. L. (2013). Influence of metabolism on epigenetics and disease. *Cell*, *153*(1), 56-69. https://doi.org/10.1016/j.cell.2013.03.004

Kalia, R., Wang, R. Y., Yusuf, A., Thomas, P. V., Agard, D. A., Shaw, J. M., & Frost, A. (2018). Structural basis of mitochondrial receptor binding and constriction by DRP1. *Nature*, *558*(7710), 401-405. https://doi.org/10.1038/s41586-018-0211-2

Kamerkar, S. C., Kraus, F., Sharpe, A. J., Pucadyil, T. J., & Ryan, M. T. (2018). Dynamin-related protein 1 has membrane constricting and severing abilities sufficient for mitochondrial and peroxisomal fission. *Nat Commun*, *9*(1), 5239. https://doi.org/10.1038/s41467-018-07543-w

Kashatus, J. A., Nascimento, A., Myers, L. J., Sher, A., Byrne, F. L., Hoehn, K. L., Counter, C. M., & Kashatus, D. F. (2015). Erk2 phosphorylation of Drp1 promotes mitochondrial fission and MAPK-driven tumor growth. *Mol Cell*, *57*(3), 537-551. https://doi.org/10.1016/j.molcel.2015.01.002

Katayama, H., Kogure, T., Mizushima, N., Yoshimori, T., & Miyawaki, A. (2011). A sensitive and quantitative technique for detecting autophagic events based on lysosomal delivery. *Chem Biol*, *18*(8), 1042-1052. https://doi.org/10.1016/j.chembiol.2011.05.013

Korobova, F., Ramabhadran, V., & Higgs, H. N. (2013). An actin-dependent step in mitochondrial fission mediated by the ER-associated formin INF2. *Science*, *339*(6118), 464-467. https://doi.org/10.1126/science.1228360

Kossenkov, A. V., Milcarek, A., Notta, F., Jang, G. H., Wilson, J. M., Gallinger, S., Zhou, D. C., Ding, L., Ghosh, J. C., Perego, M., Morotti, A., Locatelli, M., Robert, M. E., Vaira, V., & Altieri, D. C. (2022). Mitochondrial fitness and cancer risk. *PLoS One*, *17*(10), e0273520. https://doi.org/10.1371/journal.pone.0273520

Kotova, E. A., & Antonenko, Y. N. (2022). Fifty Years of Research on Protonophores: Mitochondrial Uncoupling As a Basis for Therapeutic Action. *Acta Naturae*, *14*(1), 4-13. https://doi.org/10.32607/actanaturae.11610

Kowaltowski, A. J., de Souza-Pinto, N. C., Castilho, R. F., & Vercesi, A. E. (2009). Mitochondria and reactive oxygen species. *Free Radic Biol Med*, *47*(4), 333-343. https://doi.org/10.1016/j.freeradbiomed.2009.05.004

Laforge, M., Rodrigues, V., Silvestre, R., Gautier, C., Weil, R., Corti, O., & Estaquier, J. (2016). NF-kappaB pathway controls mitochondrial dynamics. *Cell Death Differ*, *23*(1), 89-98. https://doi.org/10.1038/cdd.2015.42

Lange, F., Brandt, B., Tiedge, M., Jonas, L., Jeschke, U., Pohland, R., & Walzel, H. (2009). Galectin-1 induced activation of the mitochondrial apoptotic pathway: evidence for a connection between death-receptor and mitochondrial pathways in human Jurkat T lymphocytes. *Histochem Cell Biol*, *132*(2), 211-223. https://doi.org/10.1007/s00418-009-0597-x

Lazarou, M., Sliter, D. A., Kane, L. A., Sarraf, S. A., Wang, C., Burman, J. L., Sideris, D. P., Fogel, A. I., & Youle, R. J. (2015). The ubiquitin kinase PINK1 recruits autophagy receptors to induce mitophagy. *Nature*, *524*(7565), 309-314. https://doi.org/10.1038/nature14893

Leboucher, G. P., Tsai, Y. C., Yang, M., Shaw, K. C., Zhou, M., Veenstra, T. D., Glickman, M. H., & Weissman, A. M. (2012). Stress-induced phosphorylation and proteasomal degradation of mitofusin 2 facilitates mitochondrial fragmentation and apoptosis. *Mol Cell*, *47*(4), 547-557. https://doi.org/10.1016/j.molcel.2012.05.041

Lee, J. V., Carrer, A., Shah, S., Snyder, N. W., Wei, S., Venneti, S., Worth, A. J., Yuan, Z. F., Lim, H. W., Liu, S., Jackson, E., Aiello, N. M., Haas, N. B., Rebbeck, T. R., Judkins, A., Won, K. J., Chodosh, L. A., Garcia, B. A., Stanger, B. Z., . . . Wellen, K. E. (2014). Akt-dependent metabolic reprogramming regulates tumor cell histone acetylation. *Cell Metab*, *20*(2), 306-319. https://doi.org/10.1016/j.cmet.2014.06.004

Lee, J. Y., Kapur, M., Li, M., Choi, M. C., Choi, S., Kim, H. J., Kim, I., Lee, E., Taylor, J. P., & Yao, T. P. (2014). MFN1 deacetylation activates adaptive mitochondrial fusion and protects metabolically challenged mitochondria. *J Cell Sci*, *127*(Pt 22), 4954-4963. https://doi.org/10.1242/jcs.157321

Lee, Y. J., Park, J. H., & Oh, S. M. (2020). Activation of NF-kappaB by TOPK upregulates Snail/Slug expression in TGF-beta1 signaling to induce epithelial-mesenchymal transition and invasion of breast cancer cells. *Biochem Biophys Res Commun*, *530*(1), 122-129. https://doi.org/10.1016/j.bbrc.2020.07.015

Li, C., Zhang, Y., Cheng, X., Yuan, H., Zhu, S., Liu, J., Wen, Q., Xie, Y., Liu, J., Kroemer, G., Klionsky, D. J., Lotze, M. T., Zeh, H. J., Kang, R., & Tang, D. (2018). PINK1 and PARK2 Suppress Pancreatic Tumorigenesis through Control of Mitochondrial Iron-Mediated Immunometabolism. *Dev Cell*, *46*(4), 441-455 e448. https://doi.org/10.1016/j.devcel.2018.07.012

Li, Q., Gao, Z., Chen, Y., & Guan, M. X. (2017). The role of mitochondria in osteogenic, adipogenic and chondrogenic differentiation of mesenchymal stem cells. *Protein Cell*, *8*(6), 439-445. https://doi.org/10.1007/s13238-017-0385-7

Li, Y., Yang, Z., Zhang, S., & Li, J. (2024). Miro-mediated mitochondrial transport: A new dimension for disease-related abnormal cell metabolism? *Biochem Biophys Res Commun*, *705*, 149737. https://doi.org/10.1016/j.bbrc.2024.149737

Lin, Q., Chen, J., Gu, L., Dan, X., Zhang, C., & Yang, Y. (2021). New insights into mitophagy and stem cells. *Stem Cell Res Ther*, *12*(1), 452. https://doi.org/10.1186/s13287-021-02520-5

Liu, J., Zhang, C., Zhao, Y., Yue, X., Wu, H., Huang, S., Chen, J., Tomsky, K., Xie, H., Khella, C. A., Gatza, M. L., Xia, D., Gao, J., White, E., Haffty, B. G., Hu, W., & Feng, Z. (2017). Parkin targets HIF-1alpha for ubiquitination and degradation to inhibit breast tumor progression. *Nat Commun*, *8*(1), 1823. https://doi.org/10.1038/s41467-017-01947-w

Ma, K., Chen, G., Li, W., Kepp, O., Zhu, Y., & Chen, Q. (2020). Mitophagy, Mitochondrial Homeostasis, and Cell Fate. *Front Cell Dev Biol*, *8*, 467. https://doi.org/10.3389/fcell.2020.00467

MacKenzie, E. D., Selak, M. A., Tennant, D. A., Payne, L. J., Crosby, S., Frederiksen, C. M., Watson, D. G., & Gottlieb, E. (2007). Cell-permeating alpha-ketoglutarate derivatives alleviate pseudohypoxia in succinate dehydrogenase-deficient cells. *Mol Cell Biol*, *27*(9), 3282-3289. https://doi.org/10.1128/MCB.01927-06

Maes, H., Van Eygen, S., Krysko, D. V., Vandenabeele, P., Nys, K., Rillaerts, K., Garg, A. D., Verfaillie, T., & Agostinis, P. (2014). BNIP3 supports melanoma cell migration and vasculogenic mimicry by orchestrating the actin cytoskeleton. *Cell Death Dis*, *5*(3), e1127. https://doi.org/10.1038/cddis.2014.94

Marin-Royo, G., Gallardo, I., Martinez-Martinez, E., Gutierrez, B., Jurado-Lopez, R., Lopez-Andres, N., Gutierrez-Tenorio, J., Rial, E., Bartolome, M. A. V., Nieto, M. L., & Cachofeiro, V. (2018). Inhibition of galectin-3 ameliorates the consequences of cardiac lipotoxicity in a rat model of diet-induced obesity. *Dis Model Mech*, *11*(2). https://doi.org/10.1242/dmm.032086

Mauro, C., Leow, S. C., Anso, E., Rocha, S., Thotakura, A. K., Tornatore, L., Moretti, M., De Smaele, E., Beg, A. A., Tergaonkar, V., Chandel, N. S., & Franzoso, G.

(2011). NF-kappaB controls energy homeostasis and metabolic adaptation by upregulating mitochondrial respiration. *Nat Cell Biol*, *13*(10), 1272-1279. https://doi.org/10.1038/ncb2324

McLelland, G. L., & Fon, E. A. (2018). MFN2 retrotranslocation boosts mitophagy by uncoupling mitochondria from the ER. *Autophagy*, *14*(9), 1658-1660. https://doi.org/10.1080/15548627.2018.1505154

Mills, E. L., Kelly, B., Logan, A., Costa, A. S. H., Varma, M., Bryant, C. E., Tourlomousis, P., Dabritz, J. H. M., Gottlieb, E., Latorre, I., Corr, S. C., McManus, G., Ryan, D., Jacobs, H. T., Szibor, M., Xavier, R. J., Braun, T., Frezza, C., Murphy, M. P., & O'Neill, L. A. (2016). Succinate Dehydrogenase Supports Metabolic Repurposing of Mitochondria to Drive Inflammatory Macrophages. *Cell*, *167*(2), 457-470 e413. https://doi.org/10.1016/j.cell.2016.08.064

Mori, M. P., Penjweini, R., Ma, J., Alspaugh, G., Andreoni, A., Kim, Y. C., Wang, P. Y., Knutson, J. R., & Hwang, P. M. (2023). Mitochondrial respiration reduces exposure of the nucleus to oxygen. *J Biol Chem*, *299*(3), 103018. https://doi.org/10.1016/j.jbc.2023.103018

Nabi, I. R., Shankar, J., & Dennis, J. W. (2015). The galectin lattice at a glance. *J Cell Sci*, *128*(13), 2213-2219. https://doi.org/10.1242/jcs.151159

Nagashima, S., Tabara, L. C., Tilokani, L., Paupe, V., Anand, H., Pogson, J. H., Zunino, R., McBride, H. M., & Prudent, J. (2020). Golgi-derived PI(4)P-containing vesicles drive late steps of mitochondrial division. *Science*, *367*(6484), 1366-1371. https://doi.org/10.1126/science.aax6089

Naik, P. P., Praharaj, P. P., Bhol, C. S., Panigrahi, D. P., Mahapatra, K. K., Patra, S., Saha, S., & Bhutia, S. K. (2019). Mitochondrial Heterogeneity in Stem Cells. *Adv Exp Med Biol*, *1123*, 179-194. https://doi.org/10.1007/978-3-030-11096-3_11

Nemani, N., Carvalho, E., Tomar, D., Dong, Z., Ketschek, A., Breves, S. L., Jana, F., Worth, A. M., Heffler, J., Palaniappan, P., Tripathi, A., Subbiah, R., Riitano, M. F., Seelam, A., Manfred, T., Itoh, K., Meng, S., Sesaki, H., Craigen, W. J., . . . Madesh, M. (2018). MIRO-1 Determines Mitochondrial Shape Transition upon GPCR Activation and Ca(2+) Stress. *Cell Rep*, *23*(4), 1005-1019. https://doi.org/10.1016/j.celrep.2018.03.098

Obino, D., Fetler, L., Soza, A., Malbec, O., Saez, J. J., Labarca, M., Oyanadel, C., Del Valle Batalla, F., Goles, N., Chikina, A., Lankar, D., Segovia-Miranda, F., Garcia, C., Leger, T., Gonzalez, A., Espeli, M., Lennon-Dumenil, A. M., & Yuseff, M. I. (2018). Galectin-8 Favors the Presentation of Surface-Tethered Antigens by Stabilizing the B Cell Immune Synapse. *Cell Rep*, *25*(11), 3110-3122 e3116. https://doi.org/10.1016/j.celrep.2018.11.052

Oh, A., Pardo, M., Rodriguez, A., Yu, C., Nguyen, L., Liang, O., Chorzalska, A., & Dubielecka, P. M. (2023). NF-kappaB signaling in neoplastic transition from epithelial to mesenchymal phenotype. *Cell Commun Signal*, *21*(1), 291. https://doi.org/10.1186/s12964-023-01207-z

Ohtsubo, K., & Marth, J. D. (2006). Glycosylation in cellular mechanisms of health and disease. *Cell*, *126*(5), 855-867. https://doi.org/10.1016/j.cell.2006.08.019

Olichon, A., Baricault, L., Gas, N., Guillou, E., Valette, A., Belenguer, P., & Lenaers, G. (2003). Loss of OPA1 perturbates the mitochondrial inner membrane structure and integrity, leading to cytochrome c release and apoptosis. *J Biol Chem*, *278*(10), 7743-7746. https://doi.org/10.1074/jbc.C200677200

Oyanadel, C., Holmes, C., Pardo, E., Retamal, C., Shaughnessy, R., Smith, P., Cortes, P., Bravo-Zehnder, M., Metz, C., Feuerhake, T., Romero, D. t., Roa, J. C., Montecinos, V., Soza, A., & Gonzalez, A. (2018). Galectin-8 induces partial epithelial-mesenchymal transition with invasive tumorigenic capabilities involving a FAK/EGFR/proteasome pathway in Madin-Darby canine kidney cells. *Mol Biol Cell*, *29*(5), 557-574. https://doi.org/10.1091/mbc.E16-05-0301

Palmer, C. S., Osellame, L. D., Laine, D., Koutsopoulos, O. S., Frazier, A. E., & Ryan, M. T. (2011). MiD49 and MiD51, new components of the mitochondrial fission machinery. *EMBO Rep*, *12*(6), 565-573. https://doi.org/10.1038/embor.2011.54

Pangou, E., & Sumara, I. (2021). The Multifaceted Regulation of Mitochondrial Dynamics During Mitosis. *Front Cell Dev Biol*, *9*, 767221. https://doi.org/10.3389/fcell.2021.767221

Pardo, E., Carcamo, C., Uribe-San Martin, R., Ciampi, E., Segovia-Miranda, F., Curkovic-Pena, C., Montecino, F., Holmes, C., Tichauer, J. E., Acuna, E., Osorio-Barrios, F., Castro, M., Cortes, P., Oyanadel, C., Valenzuela, D. M., Pacheco, R., Naves, R., Soza, A., & Gonzalez, A. (2017). Galectin-8 as an immunosuppressor in experimental autoimmune encephalomyelitis and a

target of human early prognostic antibodies in multiple sclerosis. *PLoS One*, *12*(6), e0177472. https://doi.org/10.1371/journal.pone.0177472

Park, M. K., Ashby, M. C., Erdemli, G., Petersen, O. H., & Tepikin, A. V. (2001). Perinuclear, perigranular and sub-plasmalemmal mitochondria have distinct functions in the regulation of cellular calcium transport. *EMBO J*, *20*(8), 1863-1874. https://doi.org/10.1093/emboj/20.8.1863

Parone, P. A., Da Cruz, S., Tondera, D., Mattenberger, Y., James, D. I., Maechler, P., Barja, F., & Martinou, J. C. (2008). Preventing mitochondrial fission impairs mitochondrial function and leads to loss of mitochondrial DNA. *PLoS One*, *3*(9), e3257. https://doi.org/10.1371/journal.pone.0003257

Patnaik, S. K., & Stanley, P. (2006). Lectin-resistant CHO glycosylation mutants. *Methods Enzymol*, *416*, 159-182. https://doi.org/10.1016/S0076-6879(06)16011-5

Picard, M., & Shirihai, O. S. (2022). Mitochondrial signal transduction. *Cell Metab*, *34*(11), 1620-1653. https://doi.org/10.1016/j.cmet.2022.10.008

Pickles, S., Vigie, P., & Youle, R. J. (2018). Mitophagy and Quality Control Mechanisms in Mitochondrial Maintenance. *Curr Biol*, *28*(4), R170-R185. https://doi.org/10.1016/j.cub.2018.01.004

Porporato, P. E., Filigheddu, N., Pedro, J. M. B., Kroemer, G., & Galluzzi, L. (2018). Mitochondrial metabolism and cancer. *Cell Res*, *28*(3), 265-280. https://doi.org/10.1038/cr.2017.155

Prachar, J. (2003). Intimate contacts of mitochondria with nuclear envelope as a potential energy gateway for nucleo-cytoplasmic mRNA transport. *Gen Physiol Biophys*, *22*(4), 525-534. https://www.ncbi.nlm.nih.gov/pubmed/15113124

Prato, C. A., Carabelli, J., Campetella, O., & Tribulatti, M. V. (2020). Galectin-8 Enhances T cell Response by Promotion of Antigen Internalization and Processing. *iScience*, *23*(7), 101278. https://doi.org/10.1016/j.isci.2020.101278

Prieto, J., Leon, M., Ponsoda, X., Sendra, R., Bort, R., Ferrer-Lorente, R., Raya, A., Lopez-Garcia, C., & Torres, J. (2016). Early ERK1/2 activation promotes DRP1-dependent mitochondrial fission necessary for cell reprogramming. *Nat Commun*, *7*, 11124. https://doi.org/10.1038/ncomms11124

Pyakurel, A., Savoia, C., Hess, D., & Scorrano, L. (2015). Extracellular regulated kinase phosphorylates mitofusin 1 to control mitochondrial morphology and apoptosis. *Mol Cell*, *58*(2), 244-254. https://doi.org/10.1016/j.molcel.2015.02.021

Qin, X., Li, H., Zhao, H., Fang, L., & Wang, X. (2024). Enhancing healthy aging with small molecules: A mitochondrial perspective. *Med Res Rev*. https://doi.org/10.1002/med.22034

Qing, Y., Gao, L., Han, L., Su, R., & Chen, J. (2021). Evaluation of glycolytic rates in human hematopoietic stem/progenitor cells after target gene depletion. *STAR Protoc*, *2*(2), 100603. https://doi.org/10.1016/j.xpro.2021.100603

Rabinovich, G. A., & Croci, D. O. (2012). Regulatory circuits mediated by lectin-glycan interactions in autoimmunity and cancer. *Immunity*, *36*(3), 322-335. https://doi.org/10.1016/j.immuni.2012.03.004

Rajasekaran, S. A., Huynh, T. P., Wolle, D. G., Espineda, C. E., Inge, L. J., Skay, A., Lassman, C., Nicholas, S. B., Harper, J. F., Reeves, A. E., Ahmed, M. M., Leatherman, J. M., Mullin, J. M., & Rajasekaran, A. K. (2010). Na,K-ATPase subunits as markers for epithelial-mesenchymal transition in cancer and fibrosis. *Mol Cancer Ther*, *9*(6), 1515-1524. https://doi.org/10.1158/1535-7163.MCT-09-0832

Rapoport, E. M., & Bovin, N. V. (2015). Specificity of human galectins on cell surfaces. *Biochemistry (Mosc)*, *80*(7), 846-856. https://doi.org/10.1134/S0006297915070056

Ravenhill, B. J., Boyle, K. B., von Muhlinen, N., Ellison, C. J., Masson, G. R., Otten, E. G., Foeglein, A., Williams, R., & Randow, F. (2019). The Cargo Receptor NDP52 Initiates Selective Autophagy by Recruiting the ULK Complex to Cytosol-Invading Bacteria. *Mol Cell*, *74*(2), 320-329 e326. https://doi.org/10.1016/j.molcel.2019.01.041

Reily, C., Stewart, T. J., Renfrow, M. B., & Novak, J. (2019). Glycosylation in health and disease. *Nat Rev Nephrol*, *15*(6), 346-366. https://doi.org/10.1038/s41581-019-0129-4

Reticker-Flynn, N. E., Malta, D. F., Winslow, M. M., Lamar, J. M., Xu, M. J., Underhill, G. H., Hynes, R. O., Jacks, T. E., & Bhatia, S. N. (2012). A combinatorial extracellular matrix platform identifies cell-extracellular matrix interactions that

correlate with metastasis. *Nat Commun*, *3*, 1122. https://doi.org/10.1038/ncomms2128

Rolland, S. G., Motori, E., Memar, N., Hench, J., Frank, S., Winklhofer, K. F., & Conradt, B. (2013). Impaired complex IV activity in response to loss of LRPPRC function can be compensated by mitochondrial hyperfusion. *Proc Natl Acad Sci U S A*, *110*(32), E2967-2976. https://doi.org/10.1073/pnas.1303872110

Romaniuk, M. A., Tribulatti, M. V., Cattaneo, V., Lapponi, M. J., Molinas, F. C., Campetella, O., & Schattner, M. (2010). Human platelets express and are activated by galectin-8. *Biochem J*, *432*(3), 535-547. https://doi.org/10.1042/BJ20100538

Schmidt, C. A., Fisher-Wellman, K. H., & Neufer, P. D. (2021). From OCR and ECAR to energy: Perspectives on the design and interpretation of bioenergetics studies. *J Biol Chem*, *297*(4), 101140. https://doi.org/10.1016/j.jbc.2021.101140

Sciacovelli, M., & Frezza, C. (2017). Metabolic reprogramming and epithelial-to-mesenchymal transition in cancer. *FEBS J*, *284*(19), 3132-3144. https://doi.org/10.1111/febs.14090

Sharma, L. K., Fang, H., Liu, J., Vartak, R., Deng, J., & Bai, Y. (2011). Mitochondrial respiratory complex I dysfunction promotes tumorigenesis through ROS alteration and AKT activation. *Hum Mol Genet*, *20*(23), 4605-4616. https://doi.org/10.1093/hmg/ddr395

Shatz-Azoulay, H., Vinik, Y., Isaac, R., Kohler, U., Lev, S., & Zick, Y. (2020). The Animal Lectin Galectin-8 Promotes Cytokine Expression and Metastatic Tumor Growth in Mice. *Sci Rep*, *10*(1), 7375. https://doi.org/10.1038/s41598-020-64371-z

Shi, L., & Tu, B. P. (2015). Acetyl-CoA and the regulation of metabolism: mechanisms and consequences. *Curr Opin Cell Biol*, *33*, 125-131. https://doi.org/10.1016/j.ceb.2015.02.003

Smith, P. C., Metz, C., de la Pena, A., Oyanadel, C., Avila, P., Arancibia, R., Vicuna, L., Retamal, C., Barake, F., Gonzalez, A., & Soza, A. (2020). Galectin-8 mediates fibrogenesis induced by cyclosporine in human gingival fibroblasts. *J Periodontal Res*, *55*(5), 724-733. https://doi.org/10.1111/jre.12761

Stanley, P. (1989). Chinese hamster ovary cell mutants with multiple glycosylation defects for production of glycoproteins with minimal carbohydrate heterogeneity. *Mol Cell Biol*, *9*(2), 377-383. https://doi.org/10.1128/mcb.9.2.377-383.1989

Sun, N., Malide, D., Liu, J., Rovira, II, Combs, C. A., & Finkel, T. (2017). A fluorescence-based imaging method to measure in vitro and in vivo mitophagy using mt-Keima. *Nat Protoc*, *12*(8), 1576-1587. https://doi.org/10.1038/nprot.2017.060

Tang, Y., He, Y., Zhang, P., Wang, J., Fan, C., Yang, L., Xiong, F., Zhang, S., Gong, Z., Nie, S., Liao, Q., Li, X., Li, X., Li, Y., Li, G., Zeng, Z., Xiong, W., & Guo, C. (2018). LncRNAs regulate the cytoskeleton and related Rho/ROCK signaling in cancer metastasis. *Mol Cancer*, *17*(1), 77. https://doi.org/10.1186/s12943-018-0825-x

Taparra, K., Tran, P. T., & Zachara, N. E. (2016). Hijacking the Hexosamine Biosynthetic Pathway to Promote EMT-Mediated Neoplastic Phenotypes. *Front Oncol*, *6*, 85. https://doi.org/10.3389/fonc.2016.00085

Teresak, P., Lapao, A., Subic, N., Boya, P., Elazar, Z., & Simonsen, A. (2022). Regulation of PRKN-independent mitophagy. *Autophagy*, *18*(1), 24-39. https://doi.org/10.1080/15548627.2021.1888244

Thurston, T. L., Boyle, K. B., Allen, M., Ravenhill, B. J., Karpiyevich, M., Bloor, S., Kaul, A., Noad, J., Foeglein, A., Matthews, S. A., Komander, D., Bycroft, M., & Randow, F. (2016). Recruitment of TBK1 to cytosol-invading Salmonella induces WIPI2-dependent antibacterial autophagy. *EMBO J*, *35*(16), 1779-1792. https://doi.org/10.15252/embj.201694491

Thurston, T. L., Wandel, M. P., von Muhlinen, N., Foeglein, A., & Randow, F. (2012). Galectin 8 targets damaged vesicles for autophagy to defend cells against bacterial invasion. *Nature*, *482*(7385), 414-418. https://doi.org/10.1038/nature10744

Tilokani, L., Nagashima, S., Paupe, V., & Prudent, J. (2018). Mitochondrial dynamics: overview of molecular mechanisms. *Essays Biochem*, *62*(3), 341-360. https://doi.org/10.1042/EBC20170104

Trinchese, G., Cimmino, F., Catapano, A., Cavaliere, G., & Mollica, M. P. (2024). Mitochondria: the gatekeepers between metabolism and immunity. *Front Immunol*, *15*, 1334006. https://doi.org/10.3389/fimmu.2024.1334006

Villa, E., Proics, E., Rubio-Patino, C., Obba, S., Zunino, B., Bossowski, J. P., Rozier, R. M., Chiche, J., Mondragon, L., Riley, J. S., Marchetti, S., Verhoeyen, E., Tait, S. W. G., & Ricci, J. E. (2017). Parkin-Independent Mitophagy Controls Chemotherapeutic Response in Cancer Cells. *Cell Rep*, *20*(12), 2846-2859. https://doi.org/10.1016/j.celrep.2017.08.087

Villeneuve, C., Baricault, L., Canelle, L., Barboule, N., Racca, C., Monsarrat, B., Magnaldo, T., & Larminat, F. (2011). Mitochondrial proteomic approach reveals galectin-7 as a novel BCL-2 binding protein in human cells. *Mol Biol Cell*, *22*(7), 999-1013. https://doi.org/10.1091/mbc.E10-06-0534

Vinik, Y., Shatz-Azoulay, H., Vivanti, A., Hever, N., Levy, Y., Karmona, R., Brumfeld, V., Baraghithy, S., Attar-Lamdar, M., Boura-Halfon, S., Bab, I., & Zick, Y. (2015). The mammalian lectin galectin-8 induces RANKL expression, osteoclastogenesis, and bone mass reduction in mice. *Elife*, *4*, e05914. https://doi.org/10.7554/eLife.05914

Vladoiu, M. C., Labrie, M., & St-Pierre, Y. (2014). Intracellular galectins in cancer cells: potential new targets for therapy (Review). *Int J Oncol*, *44*(4), 1001-1014. https://doi.org/10.3892/ijo.2014.2267

Wakabayashi, J., Zhang, Z., Wakabayashi, N., Tamura, Y., Fukaya, M., Kensler, T. W., Iijima, M., & Sesaki, H. (2009). The dynamin-related GTPase Drp1 is required for embryonic and brain development in mice. *J Cell Biol*, *186*(6), 805-816. https://doi.org/10.1083/jcb.200903065

Walker, B. R., & Moraes, C. T. (2022). Nuclear-Mitochondrial Interactions. *Biomolecules*, *12*(3). https://doi.org/10.3390/biom12030427

Wang, Y., Yang, C., Wang, Z., Wang, Y., Yan, Q., Feng, Y., Liu, Y., Huang, J., & Zhou, J. (2023). Epithelial Galectin-3 Induced the Mitochondrial Complex Inhibition and Cell Cycle Arrest of CD8(+) T Cells in Severe/Critical COVID-19. *Int J Mol Sci*, *24*(16). https://doi.org/10.3390/ijms241612780

Wong, Y. C., Ysselstein, D., & Krainc, D. (2018). Mitochondria-lysosome contacts regulate mitochondrial fission via RAB7 GTP hydrolysis. *Nature*, *554*(7692), 382-386. https://doi.org/10.1038/nature25486

Wu, Y., Deng, J., Rychahou, P. G., Qiu, S., Evers, B. M., & Zhou, B. P. (2009). Stabilization of snail by NF-kappaB is required for inflammation-induced cell migration and invasion. *Cancer Cell*, *15*(5), 416-428. https://doi.org/10.1016/j.ccr.2009.03.016

Xia, M., Zhang, Y., Jin, K., Lu, Z., Zeng, Z., & Xiong, W. (2019). Communication between mitochondria and other organelles: a brand-new perspective on mitochondria in cancer. *Cell Biosci*, *9*, 27. https://doi.org/10.1186/s13578-019-0289-8

Xiao, J. J., Liu, Q., Li, Y., Peng, F. F., Wang, S., Zhang, Z., Liu, H., Yu, H., Tao, S., & Zhang, B. F. (2022). Regulator of calcineurin 1 deletion attenuates mitochondrial dysfunction and apoptosis in acute kidney injury through JNK/Mff signaling pathway. *Cell Death Dis*, *13*(9), 774. https://doi.org/10.1038/s41419-022-05220-x

Xue, D., Zhou, X., & Qiu, J. (2020). Emerging role of NRF2 in ROS-mediated tumor chemoresistance. *Biomed Pharmacother*, *131*, 110676. https://doi.org/10.1016/j.biopha.2020.110676

Yan, C., Luo, L., Guo, C. Y., Goto, S., Urata, Y., Shao, J. H., & Li, T. S. (2017). Doxorubicin-induced mitophagy contributes to drug resistance in cancer stem cells from HCT8 human colorectal cancer cells. *Cancer Lett*, *388*, 34-42. https://doi.org/10.1016/j.canlet.2016.11.018

Yang, J. Y., & Yang, W. Y. (2013). Bit-by-bit autophagic removal of parkin-labelled mitochondria. *Nat Commun*, *4*, 2428. https://doi.org/10.1038/ncomms3428

Yapa, N. M. B., Lisnyak, V., Reljic, B., & Ryan, M. T. (2021). Mitochondrial dynamics in health and disease. *FEBS Lett*, *595*(8), 1184-1204. https://doi.org/10.1002/1873-3468.14077

Yu, F., Finley, R. L., Jr., Raz, A., & Kim, H. R. (2002). Galectin-3 translocates to the perinuclear membranes and inhibits cytochrome c release from the mitochondria. A role for synexin in galectin-3 translocation. *J Biol Chem*, *277*(18), 15819-15827. https://doi.org/10.1074/jbc.M200154200

Zaman, M., & Shutt, T. E. (2022). The Role of Impaired Mitochondrial Dynamics in MFN2-Mediated Pathology. *Front Cell Dev Biol*, *10*, 858286. https://doi.org/10.3389/fcell.2022.858286

Zerihun, M., Sukumaran, S., & Qvit, N. (2023). The Drp1-Mediated Mitochondrial Fission Protein Interactome as an Emerging Core Player in Mitochondrial Dynamics and Cardiovascular Disease Therapy. *Int J Mol Sci*, *24*(6). https://doi.org/10.3390/ijms24065785

Zervopoulos, S. D., Boukouris, A. E., Saleme, B., Haromy, A., Tejay, S., Sutendra, G., & Michelakis, E. D. (2022). MFN2-driven mitochondria-to-nucleus tethering allows a non-canonical nuclear entry pathway of the mitochondrial pyruvate dehydrogenase complex. *Mol Cell*, *82*(5), 1066-1077 e1067. https://doi.org/10.1016/j.molcel.2022.02.003

Zhan, L., Cao, H., Wang, G., Lyu, Y., Sun, X., An, J., Wu, Z., Huang, Q., Liu, B., & Xing, J. (2016). Drp1-mediated mitochondrial fission promotes cell proliferation through crosstalk of p53 and NF-kappaB pathways in hepatocellular carcinoma. *Oncotarget*, *7*(40), 65001-65011. https://doi.org/10.18632/oncotarget.11339

Zhang, C., Lin, M., Wu, R., Wang, X., Yang, B., Levine, A. J., Hu, W., & Feng, Z. (2011). Parkin, a p53 target gene, mediates the role of p53 in glucose metabolism and the Warburg effect. *Proc Natl Acad Sci U S A*, *108*(39), 16259-16264. https://doi.org/10.1073/pnas.1113884108

Zhao, R. Z., Jiang, S., Zhang, L., & Yu, Z. B. (2019). Mitochondrial electron transport chain, ROS generation and uncoupling (Review). *Int J Mol Med*, *44*(1), 3-15. https://doi.org/10.3892/ijmm.2019.4188